Title: Modelling waveforms from binary neutron stars

Date: Jun 25, 2010 10:30 AM

URL: http://pirsa.org/10060072

Abstract: The familiar post-Newtonian inspiral description of a binary neutron star system is sufficient for detection in current instruments. However, as we consider making astrophysical measurements using advanced detectors, the effects of matter and strong gravity on gravitational wave signals may become significant. I will review recent work modelling the waveforms produced by the inspiral and coalescence of binary neutron stars. In the mid-to-late inspiral this includes modifications to the post-Newtonian waveform models from tidal deformations. In the late inspiral and coalescence, numerical simulations are exploring a range of masses, mass ratios, equations of state, and magnetic fields. In some circumstances a hypermassive remnant produces significant additional signal after the merger. Numerical simulation results also link neutron-star merger to potential counterpart signals.

Waveforms from binary neutron stars

Jocelyn Read

Max Planck Institute for Gravitational Physics

26 June 2010

Gravitational waves from merging binary neutron stars

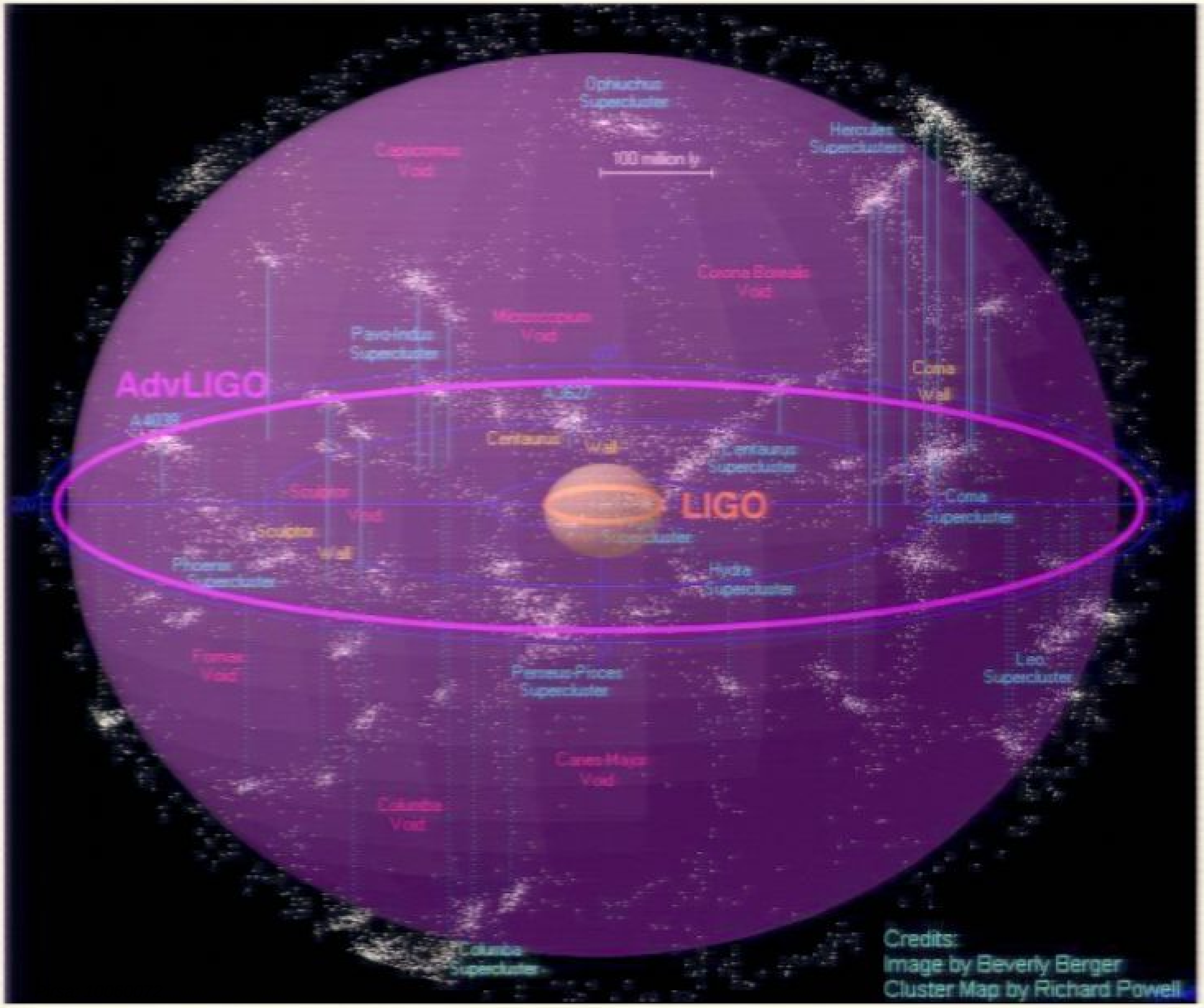

Expect $\sim$1-60 NS-NS / year with SNR > 8 in single 2nd generation detector

10% within 100 Mpc @ SNR $\sim$ 2

$\sim$ 1% within 50 Mpc @ SNR $\sim$ 4

O'Shaughnessy 2009

Signal in binary neutron star waveforms

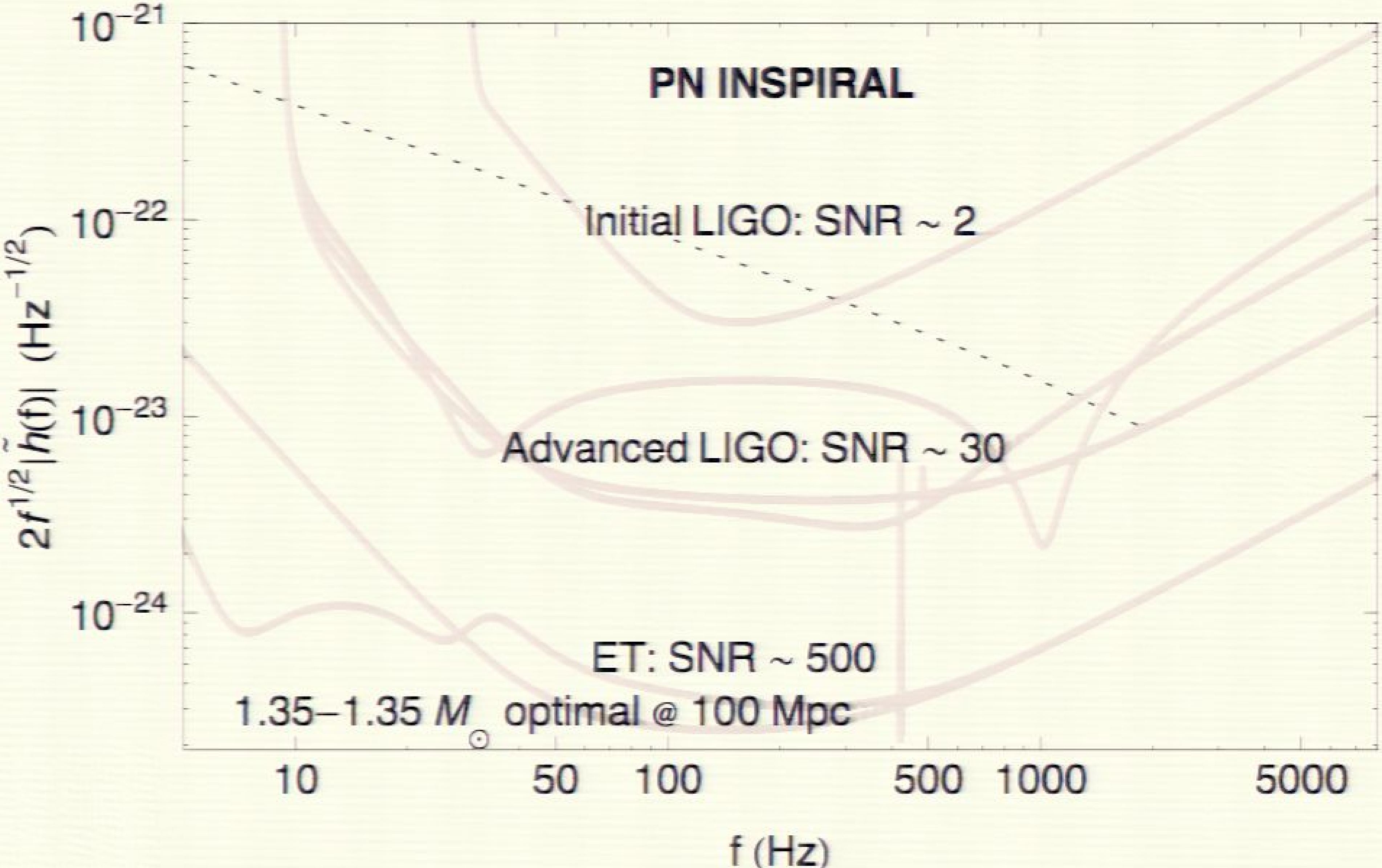

Signal in binary neutron star waveforms

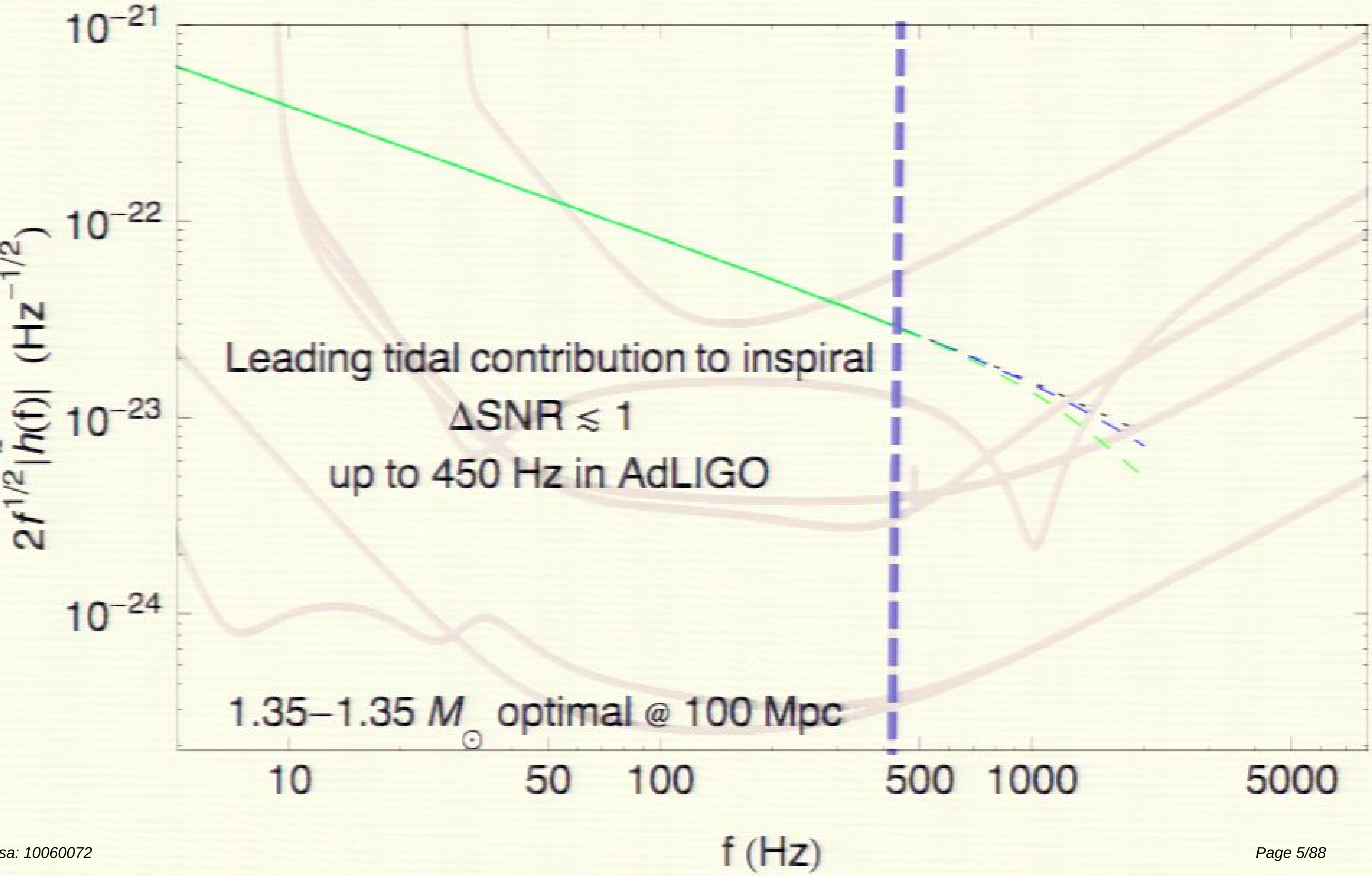

Signal in binary neutron star waveforms

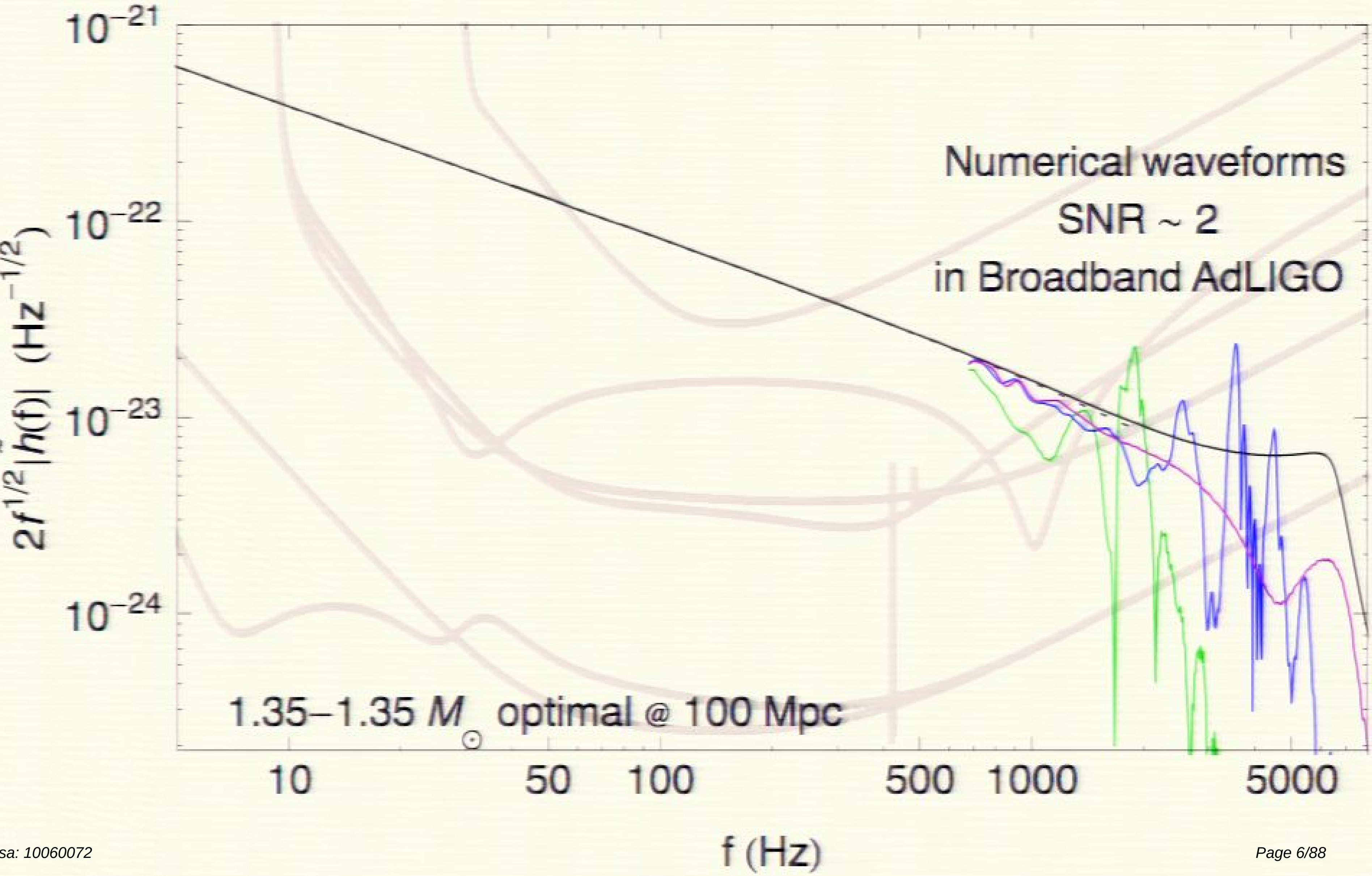

Outline: Recent and in-progress work

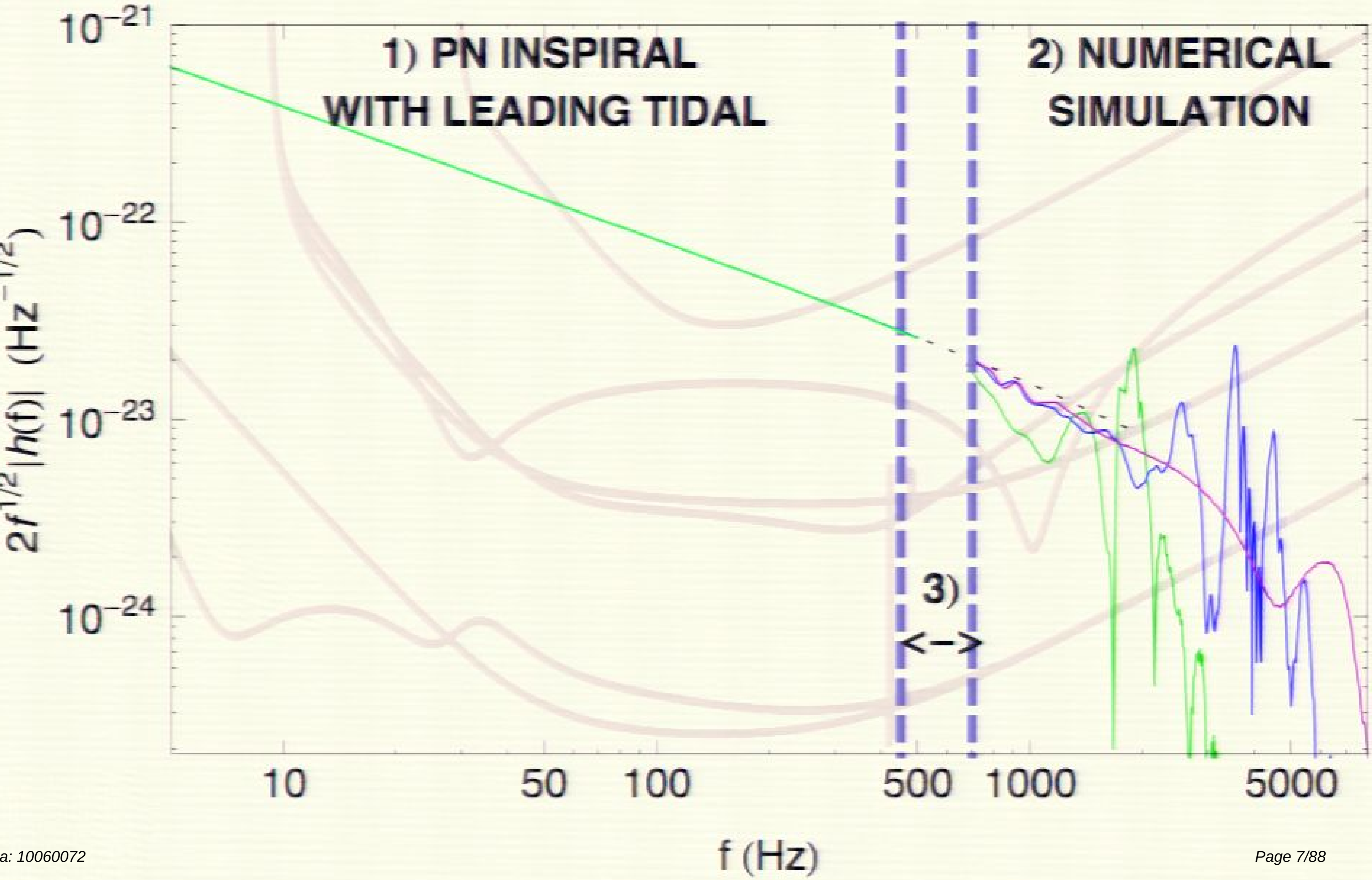

Preliminary: Equations of state for neutron star cores

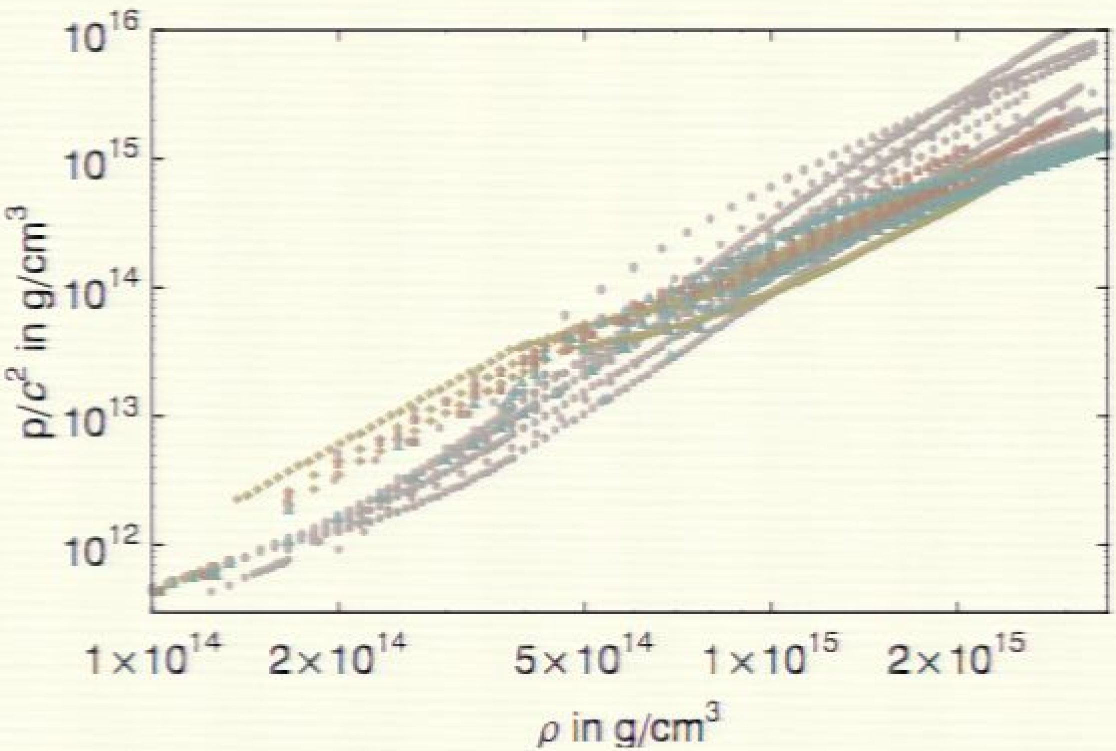

Matter in neutron stars compressed to $\sim$ 1-10 times nuclear density

($\sim$ 2-20 $\times$ 10^{14} g/cm^3)

Different microphysics gives different ground state pressures

EOS determines structure of neutron star

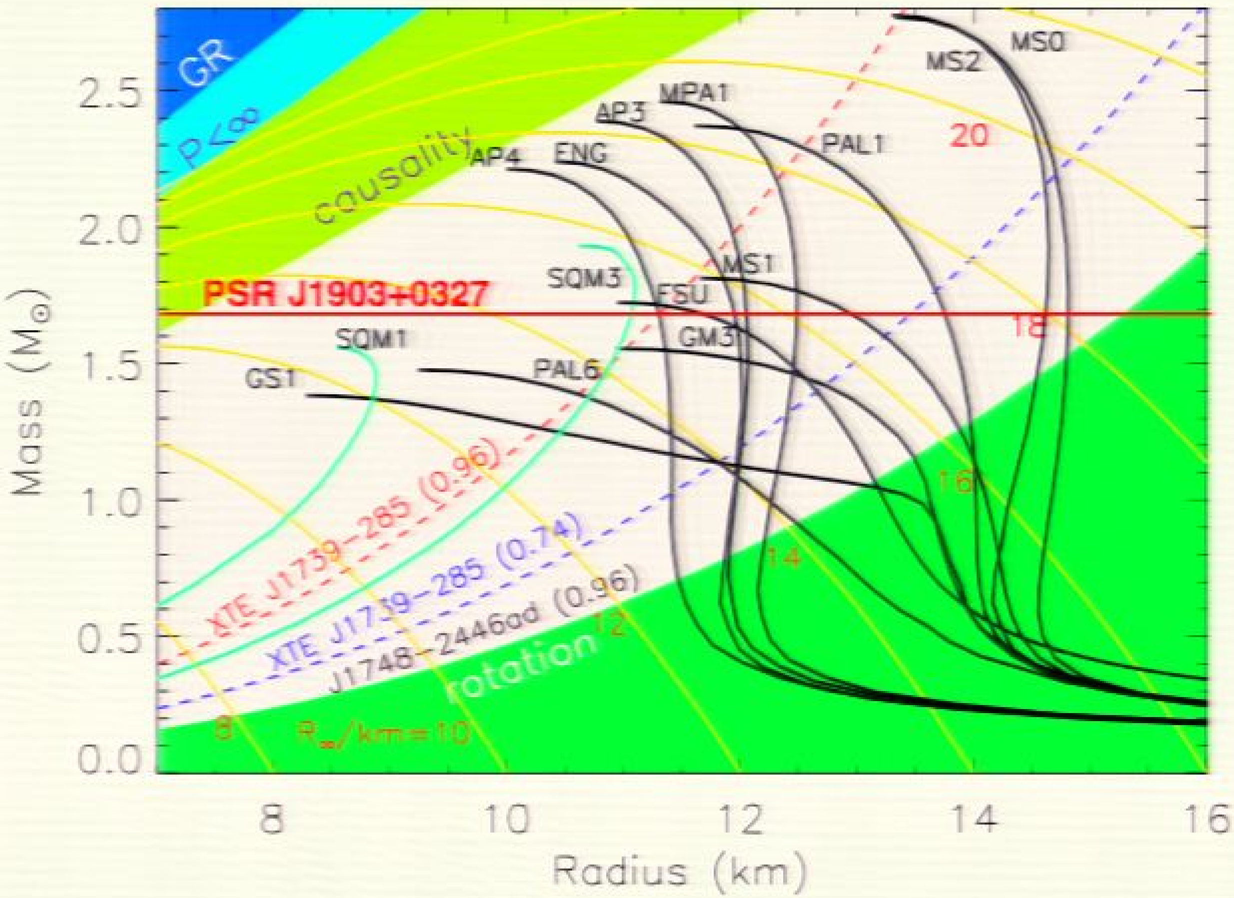

e.g. different pressure-density relationships
give different mass-radius relationships

from Lattimer and Prakash 2007

Preliminary: Equations of state for neutron star cores

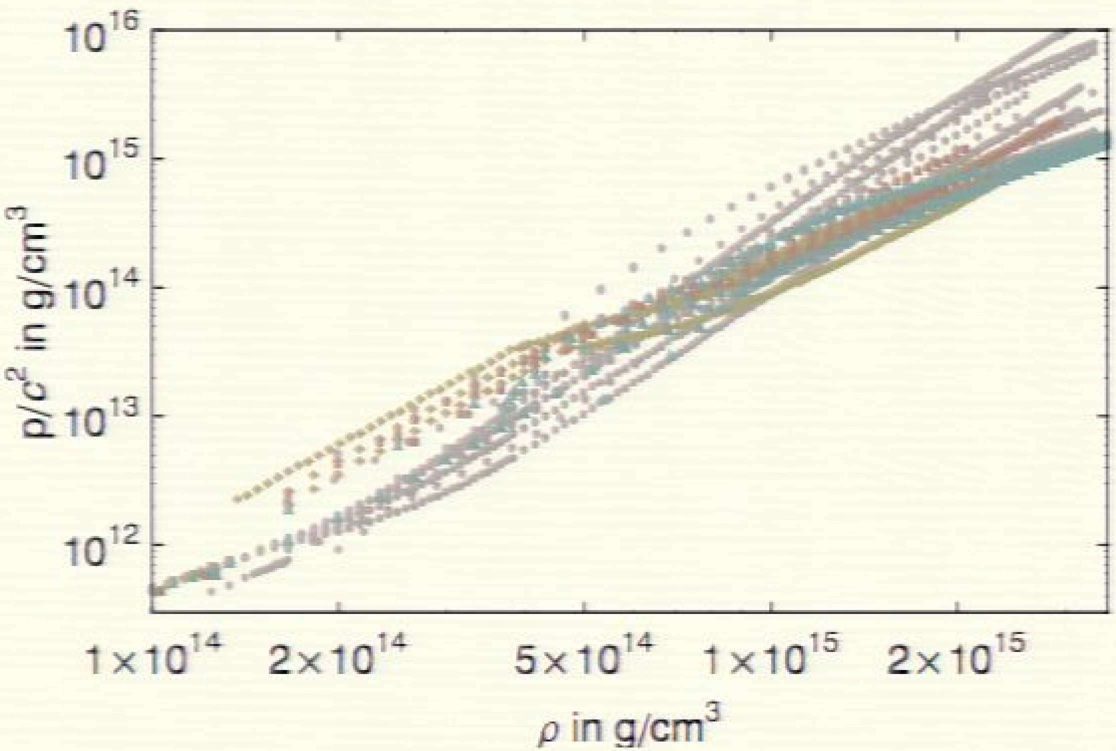

Matter in neutron stars compressed to $\sim$ 1-10 times nuclear density

($\sim$ 2-20 $\times\ 10^{14}$ g/cm^3)

Different microphysics gives different ground state pressures

EOS determines structure of neutron star

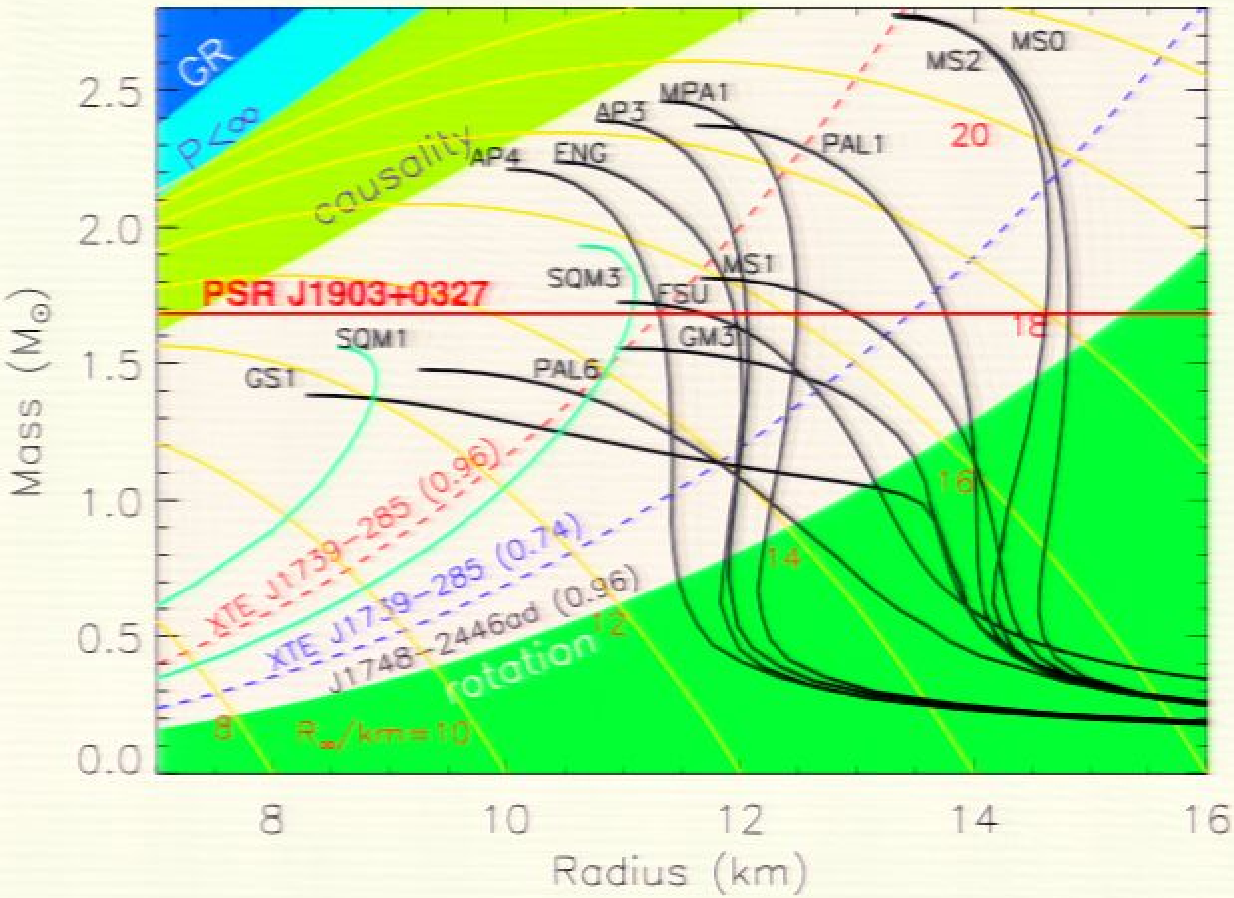

e.g. different pressure-density relationships
give different mass-radius relationships

from Lattimer and Prakash 2007

Constraint of EOS

Observations of neutron star properties can constrain EOS:

Constraint of EOS

Observations of neutron star properties can constrain EOS:

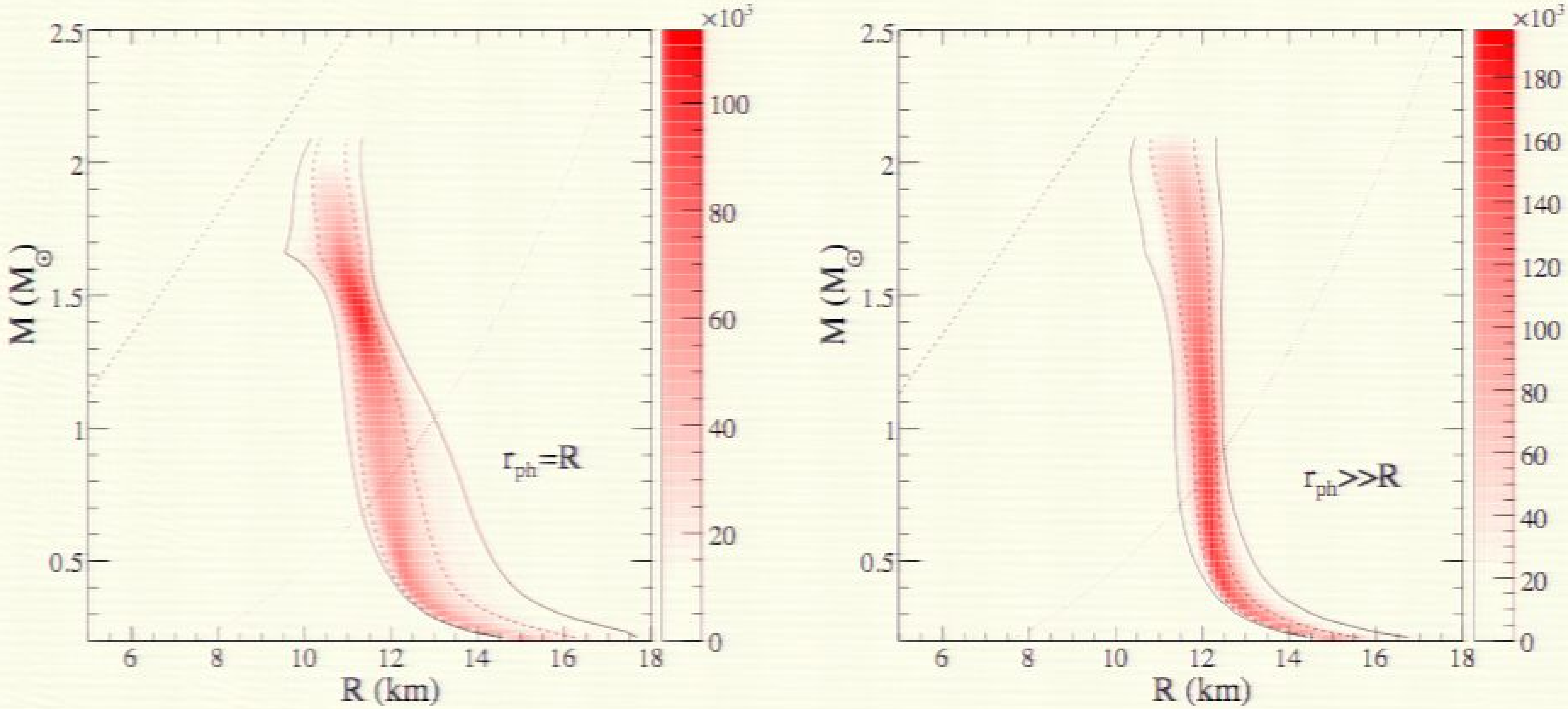

Three X-ray bursters + thermal emission from transiant LMXBs + cooling of an isolated neutron star. (Steiner et. al. 2010, 1005.0811)

Matter effects on binary neutron star inspiral

Initial estimates for LIGO

Kochanek 1992, Bildsten and Cutler 1992, Lai and Wiseman 1996

- Tidal effects change phase evolution only at end of inspiral
- Point particle waveforms can be used for template-based detection

Matter effects on binary neutron star inspiral

Initial estimates for LIGO

Kochanek 1992, Bildsten and Cutler 1992, Lai and Wiseman 1996

- Tidal effects change phase evolution only at end of inspiral
- Point particle waveforms can be used for template-based detection

Results are still valid.

For advanced detectors and parameter estimation matter can play a role.

1) Modified inspiral: tidal deformation

Consider two extended bodies in orbit or free-fall:

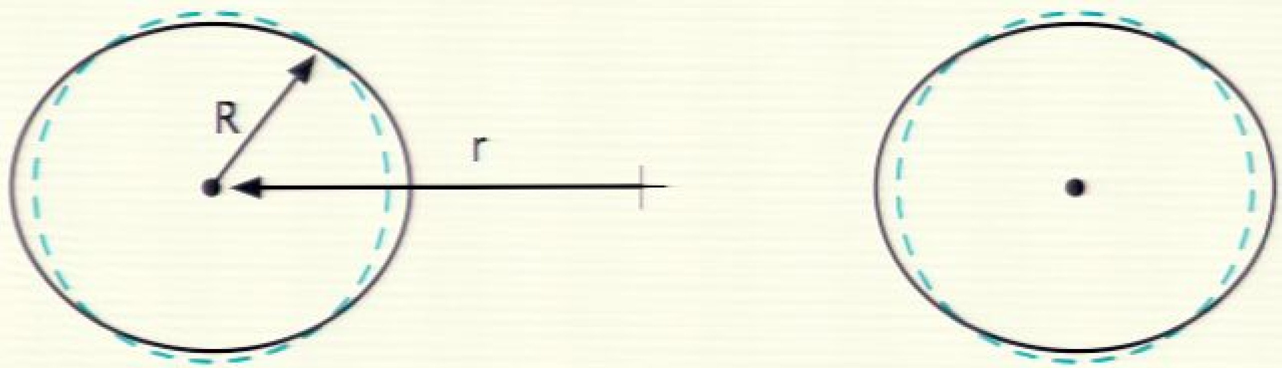

Residual gravitational effect is tidal deformation.

Amount of deformation depends on size and matter properties.

Deformations induce changes in the gravitational potential.

Effect on waveform

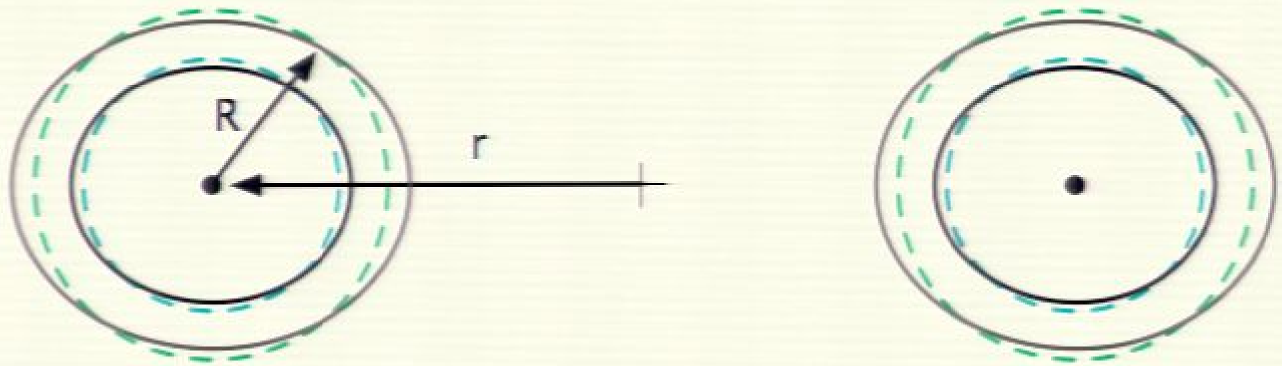

Add perturbative estimate of tidal deformation
for given mass, mass ratio, and EOS
to energy balance waveform

Flanagan and Hinderer 2008 0709.1915, Hinderer 2008 0711.2420

Damour and Nagar 2009 0906.0096,
Binnington and Poisson 2009 0906.1366

Hinderer et. al. 2010 0911.3535, Damour and Nagar 2010 0911.5041

1) Modified inspiral: tidal deformation

Consider two extended bodies in orbit or free-fall:

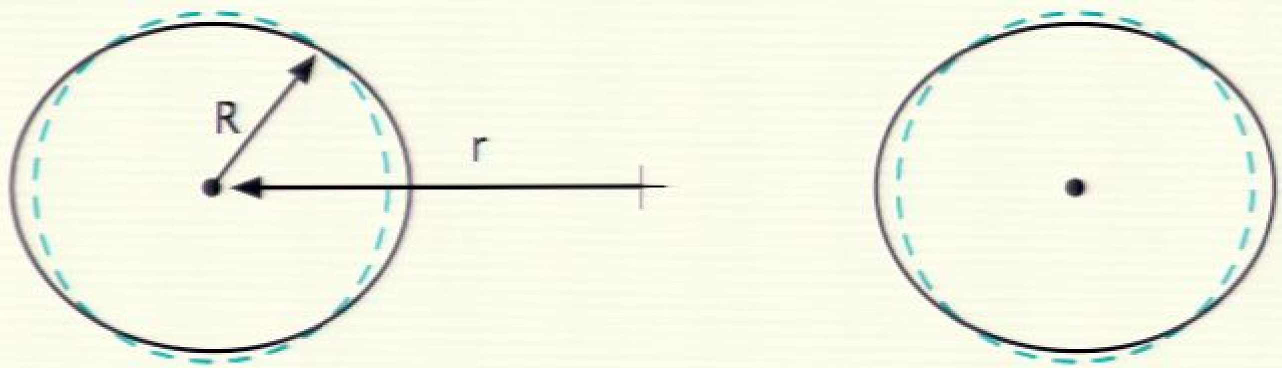

Residual gravitational effect is tidal deformation.

Amount of deformation depends on size and matter properties.

Deformations induce changes in the gravitational potential.

Effect on waveform

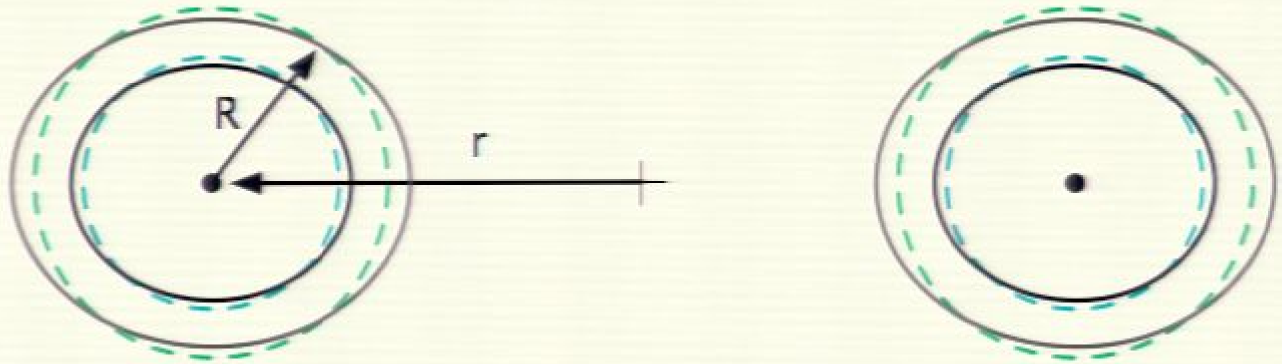

Add perturbative estimate of tidal deformation
for given mass, mass ratio, and EOS
to energy balance waveform

Flanagan and Hinderer 2008 0709.1915, Hinderer 2008 0711.2420

Damour and Nagar 2009 0906.0096,
Binnington and Poisson 2009 0906.1366

Hinderer et. al. 2010 0911.3535, Damour and Nagar 2010 0911.5041

Tidal deformability λ for realistic EOS

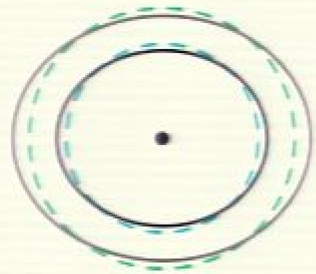

$$\lambda = \frac{Q}{\mathcal{E}} = \frac{\text{size of quadrupole deformation}}{\text{strength of external tidal field}}$$

$$\lambda = \frac{2}{3} k_2 R^5$$

Calculate via linear Y_{20} perturbation of spherical neutron star
Q and $\mathcal{E}$ defined by external field of perturbed star
leading terms $\sim r^2$ and $\sim r^{-3}$ when far from star

For given realistic EOS, λ is function of M
(similar to radius or moment of inertia)

Measuring tidal deformability λ

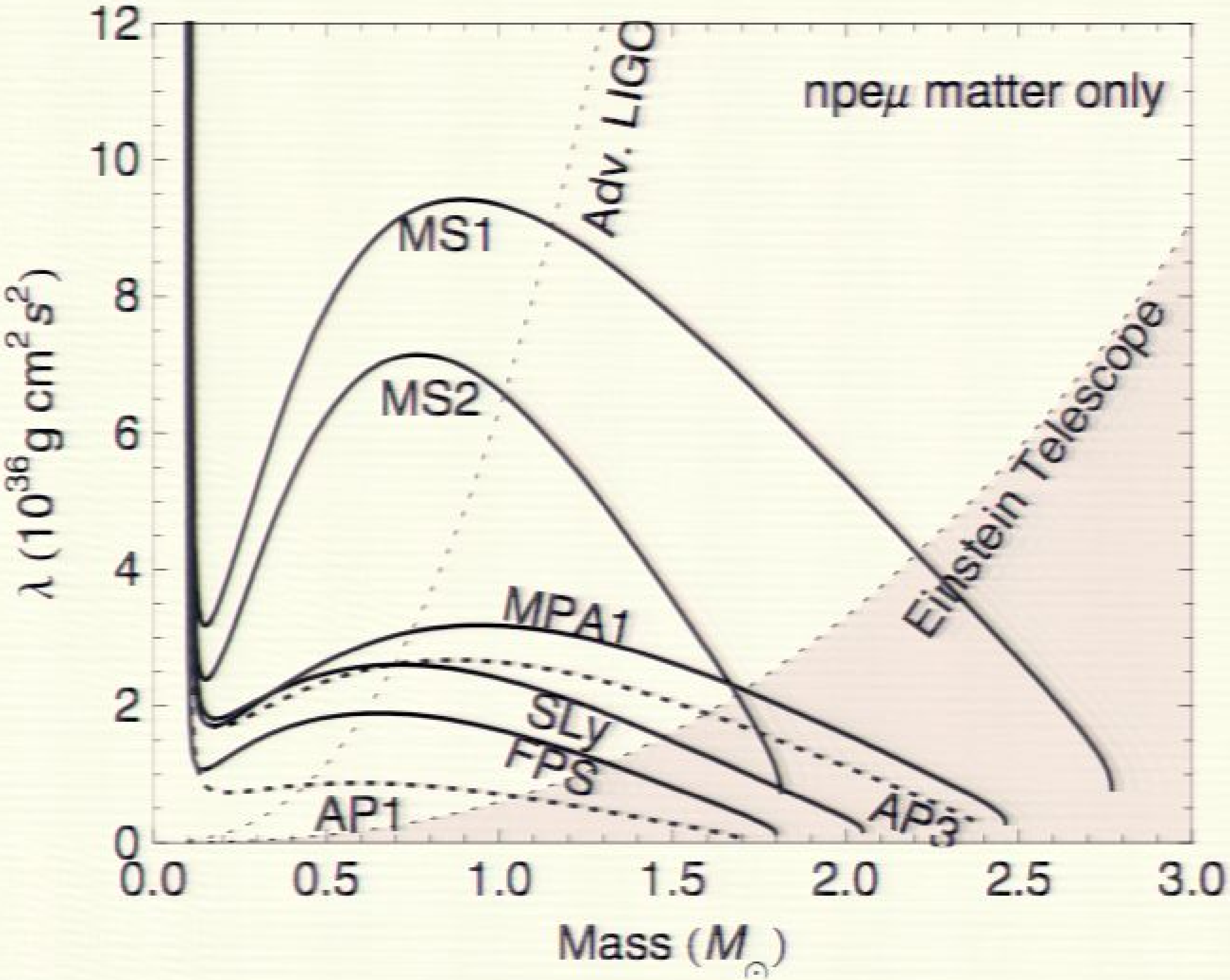

Each thick line: a candidate neutron star equation of state gives λ as function of mass.

$\lambda = 0$ for black holes [Damour and Nagar 2009, Binnington and Poisson 2009]

Measuring tidal deformability λ

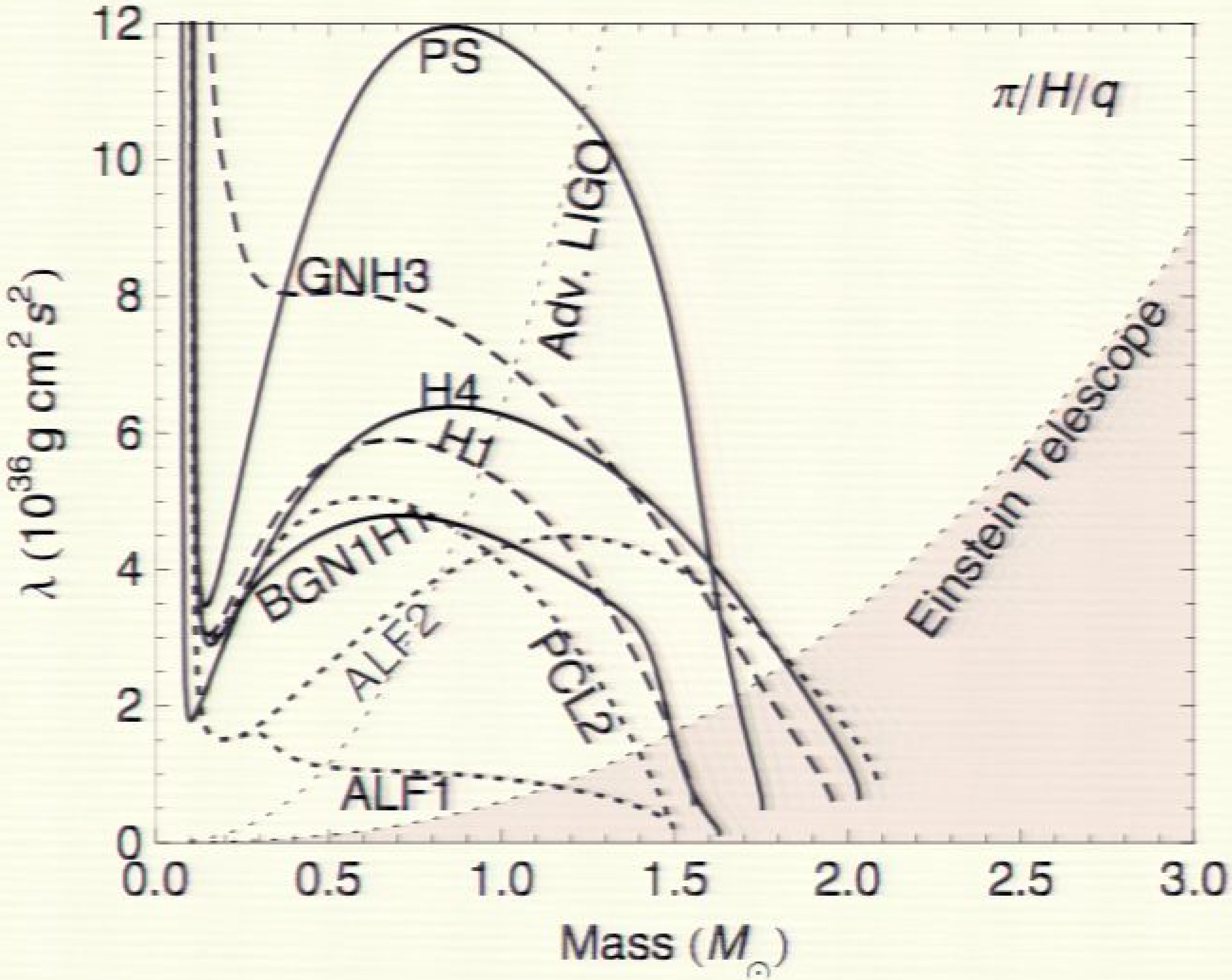

Each thick line: a candidate neutron star equation of state gives λ as function of mass.

$\lambda = 0$ for black holes [Damour and Nagar 2009, Binnington and Poisson 2009]

Measuring tidal deformability λ

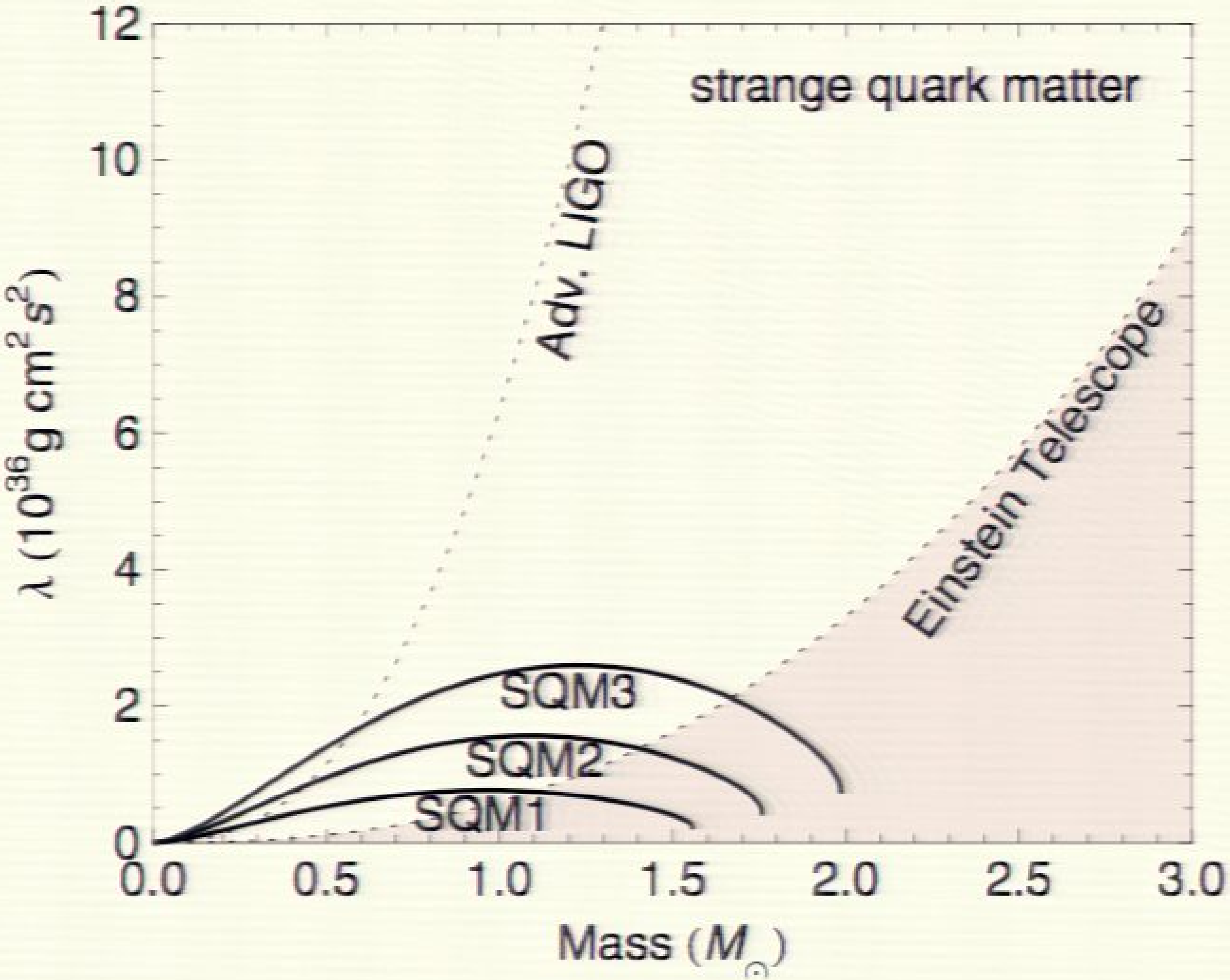

Each thick line: a candidate neutron star equation of state gives λ as function of mass.

$\lambda = 0$ for black holes [Damour and Nagar 2009, Binnington and Poisson 2009]

Tidal deformability λ for realistic EOS

Incorporate first order tidal correction to post-Newtonian waveform

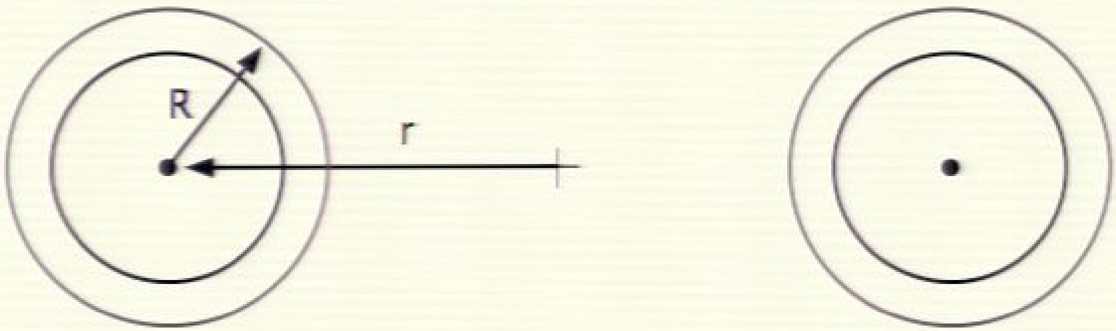

$$E = \text{Energy of system} = -\frac{1}{2}Mc^2\eta x\,(1 + [\text{PN}])$$

$$\dot{E}\ (\text{from GW}) = \frac{32}{5}\frac{c^5}{G}\eta^2 x^5\,(1 + [\ \text{PN}])$$

$x \sim M/r$
$M = m_1 + m_2$
$\eta = m_1 m_2/M^2$

Evolve orbit using balance of luminosity and orbital energy

Measuring tidal deformability λ

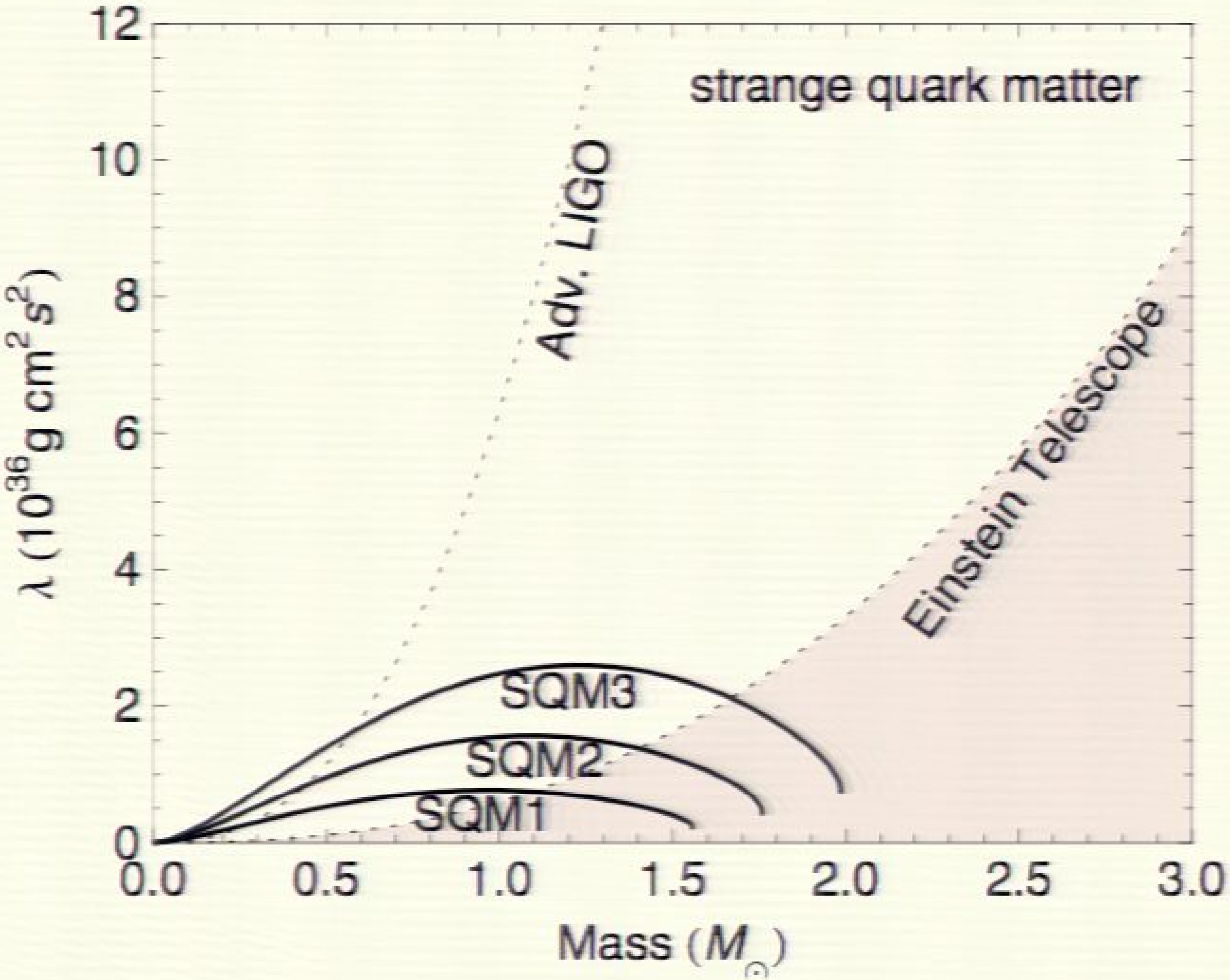

Each thick line: a candidate neutron star equation of state gives λ as function of mass.

$\lambda = 0$ for black holes [Damour and Nagar 2009, Binnington and Poisson 2009]

Measuring tidal deformability λ

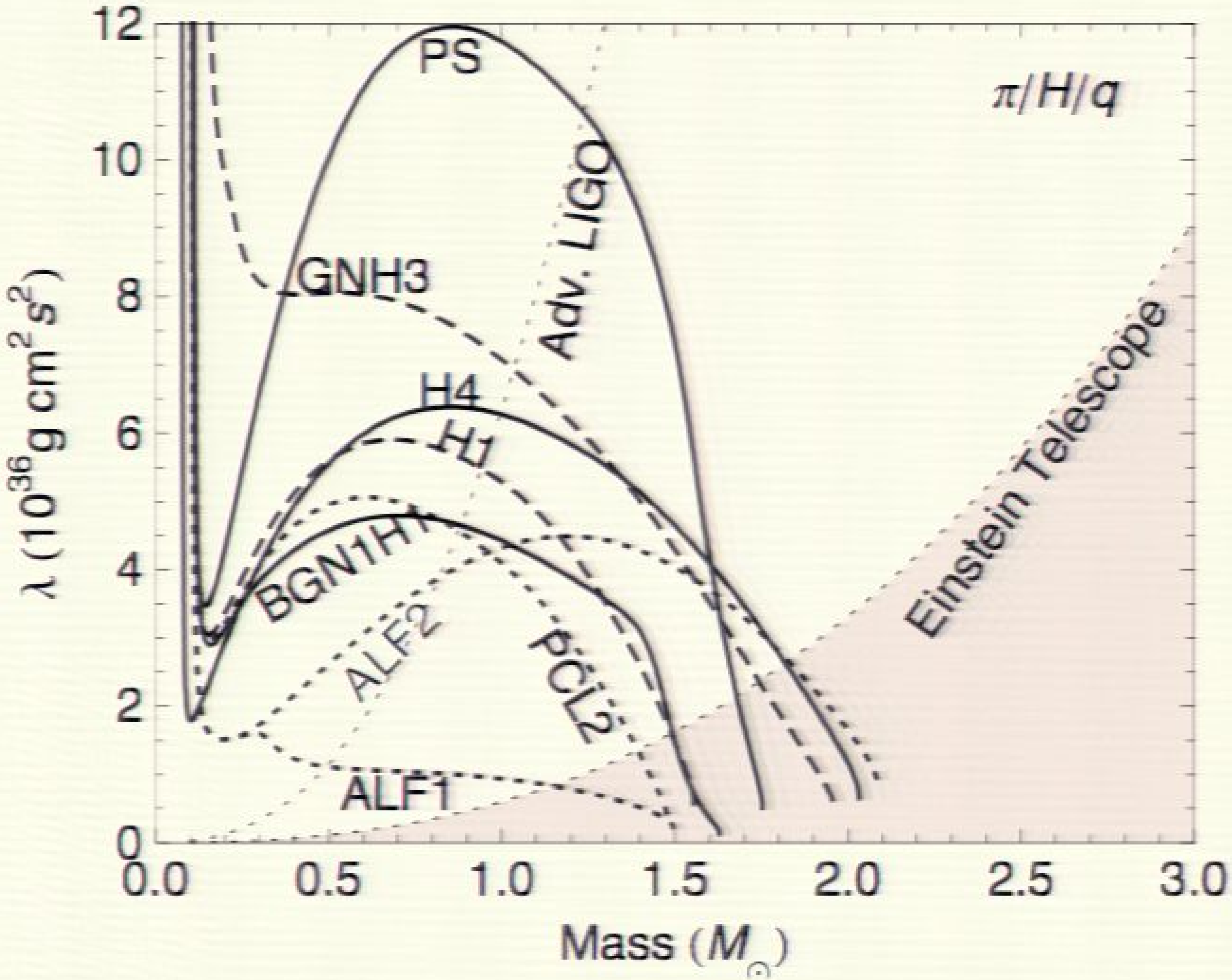

Each thick line: a candidate neutron star equation of state gives λ as function of mass.

$\lambda = 0$ for black holes [Damour and Nagar 2009, Binnington and Poisson 2009]

Measuring tidal deformability λ

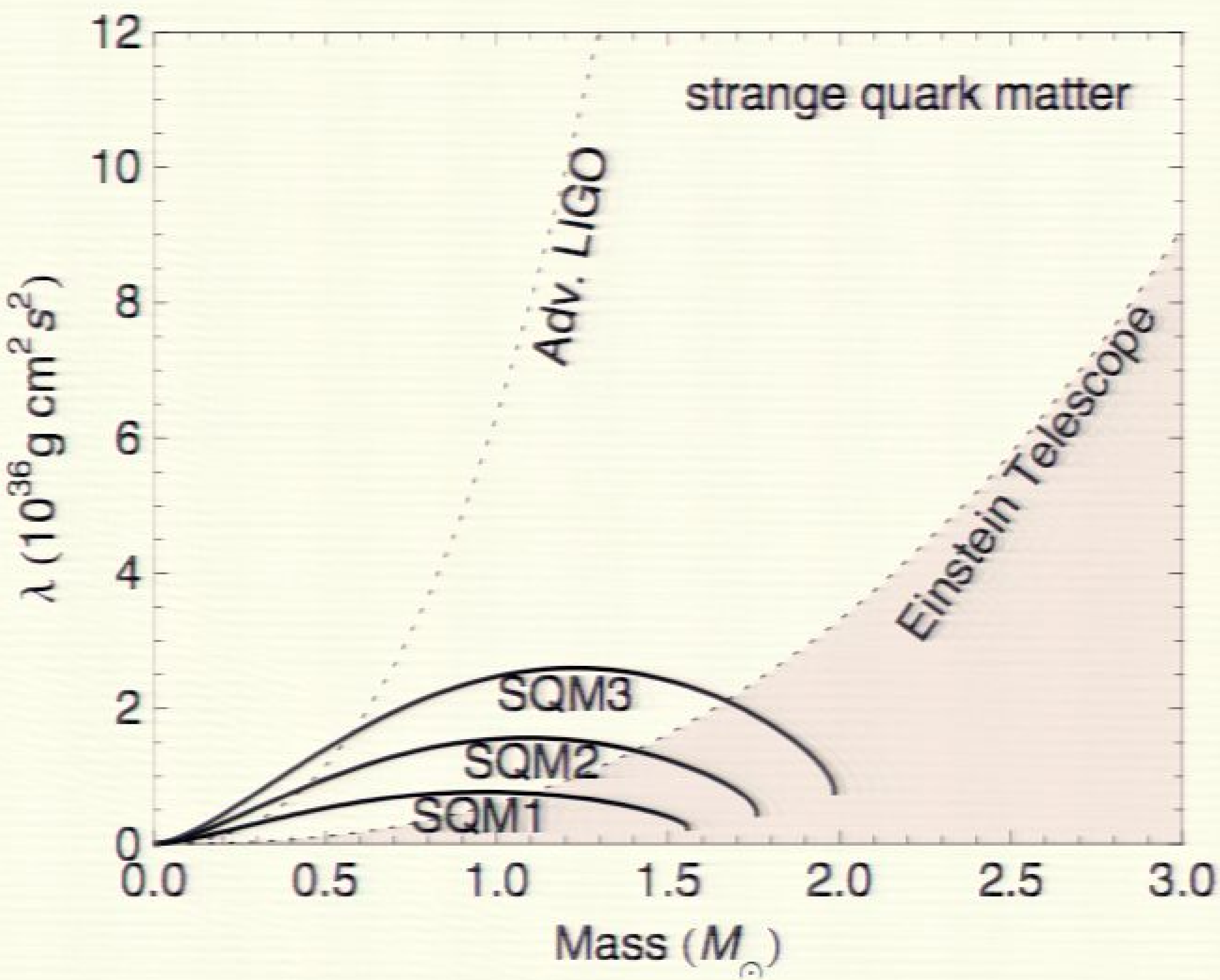

Each thick line: a candidate neutron star equation of state gives λ as function of mass.

$\lambda = 0$ for black holes [Damour and Nagar 2009, Binnington and Poisson 2009]

Tidal deformability λ for realistic EOS

Incorporate first order tidal correction to post-Newtonian waveform

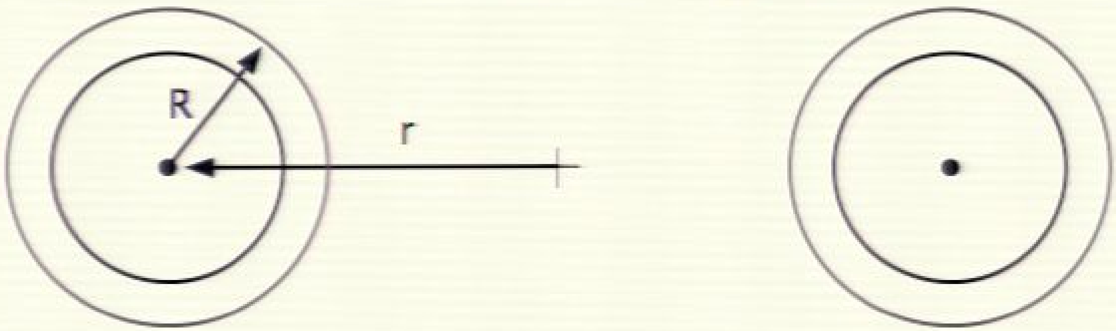

$$E = \text{Energy of system} = -\frac{1}{2}Mc^2\eta x\,(1+[\text{PN}])$$

$$\dot{E}\ (\text{from GW}) = \frac{32}{5}\frac{c^5}{G}\eta^2 x^5\,(1+[\ \text{PN}])$$

$x \sim M/r$
$M = m_1 + m_2$
$\eta = m_1 m_2/M^2$

Evolve orbit using balance of luminosity and orbital energy

Tidal deformability λ for realistic EOS

Incorporate first order tidal correction to post-Newtonian waveform

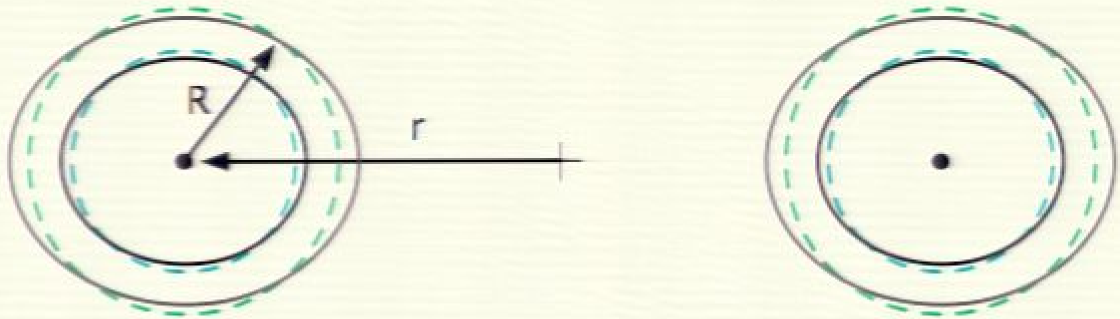

$$E = \text{Energy of system} = -\frac{1}{2}Mc^2\eta x\left(1 + [\text{PN}] - \frac{1}{2}Q^1_{ij}\mathcal{E}^2_{ij} + 2 \leftrightarrow 1\right)$$

$$\dot{E}\ (\text{from GW}) = \frac{32}{5}\frac{c^5}{G}\eta^2 x^5\left(1 + [\ \text{PN}] - \frac{1}{5}\langle \dddot{Q}^1_{ij}\dddot{Q}^1_{ij}\rangle + 2 \leftrightarrow 1\right)$$

$x \sim M/r$
$M = m_1 + m_2$
$\eta = m_1 m_2/M^2$

Evolve orbit using balance of luminosity and orbital energy

Tidal deformability λ for realistic EOS

Incorporate first order tidal correction to post-Newtonian waveform

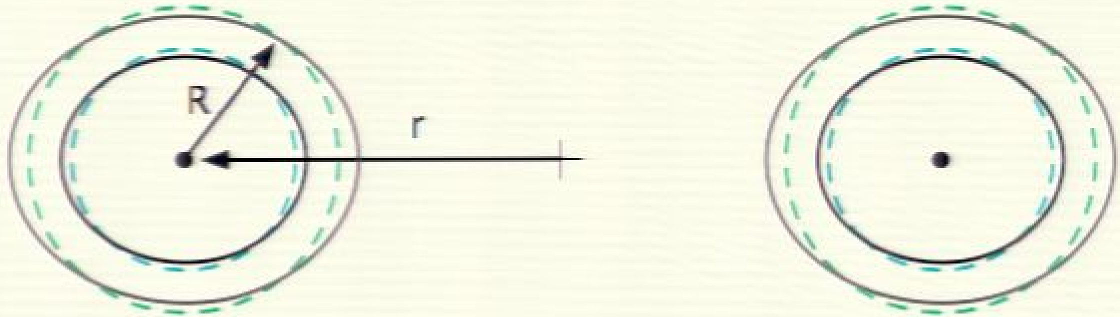

$$E = \text{Energy of system} = -\frac{1}{2}Mc^2\eta x\left(1 + [\text{PN}] - 9\frac{m_2}{m_1}\lambda_1\frac{x^5}{M^5} + 2 \leftrightarrow 1\right)$$

$$\dot{E}\ (\text{from GW}) = \frac{32}{5}\frac{c^5}{G}\eta^2 x^5\left(1 + [\ \text{PN}] + 6\left(\frac{M}{m_1} + 2\frac{m_2}{m_1}\right)\lambda_1\frac{x^5}{M^5} + 2 \leftrightarrow 1\right)$$

$x \sim M/r$
$M = m_1 + m_2$
$\eta = m_1 m_2/M^2$

Evolve orbit using balance of luminosity and orbital energy

Measuring tidal deformability λ

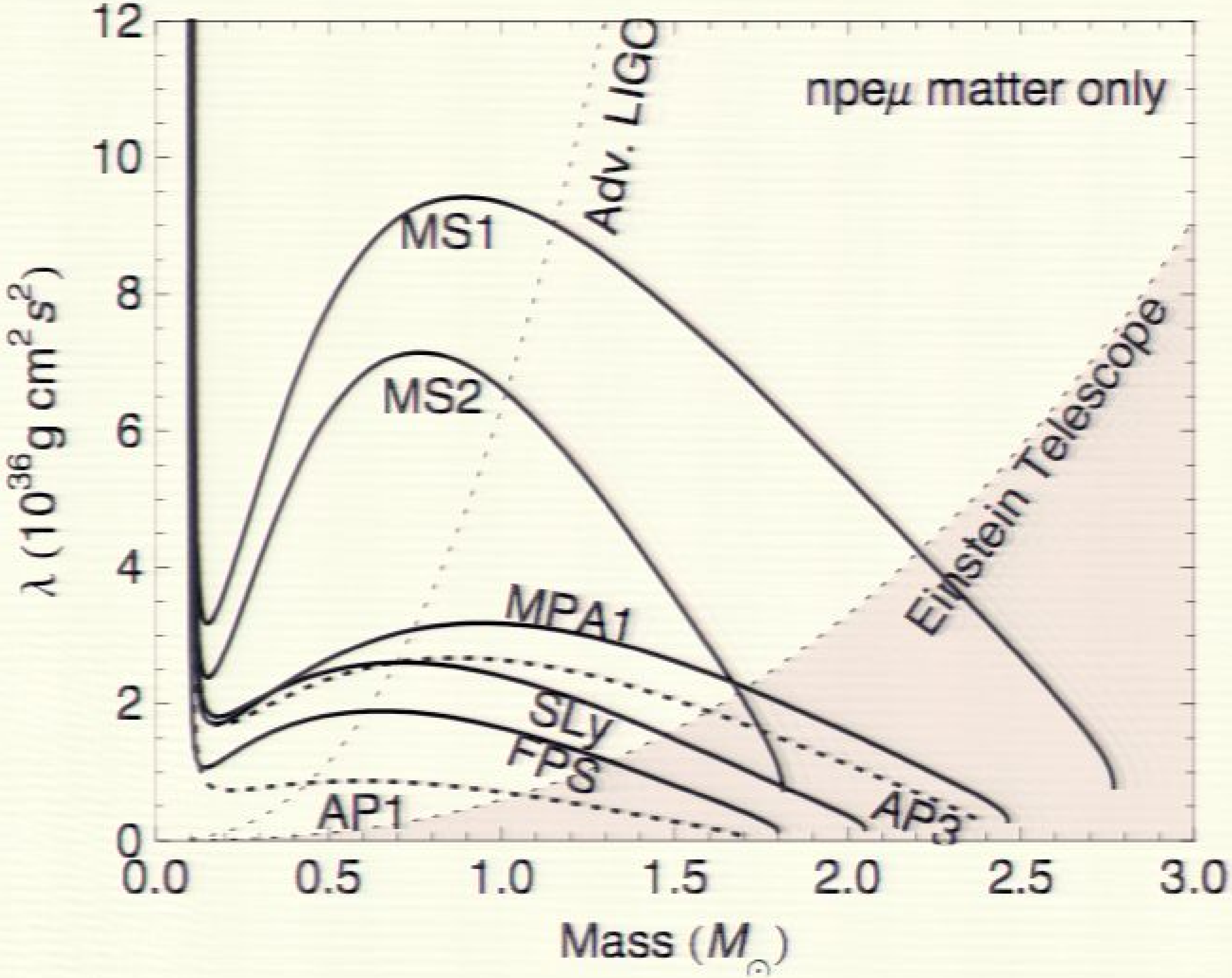

Each thick line: a candidate equation of state gives λ as function of mass.

shaded: Uncertainty in estimating λ for Advanced LIGO and ET using "clean" waveform: below 450 Hz only

Measuring tidal deformability λ

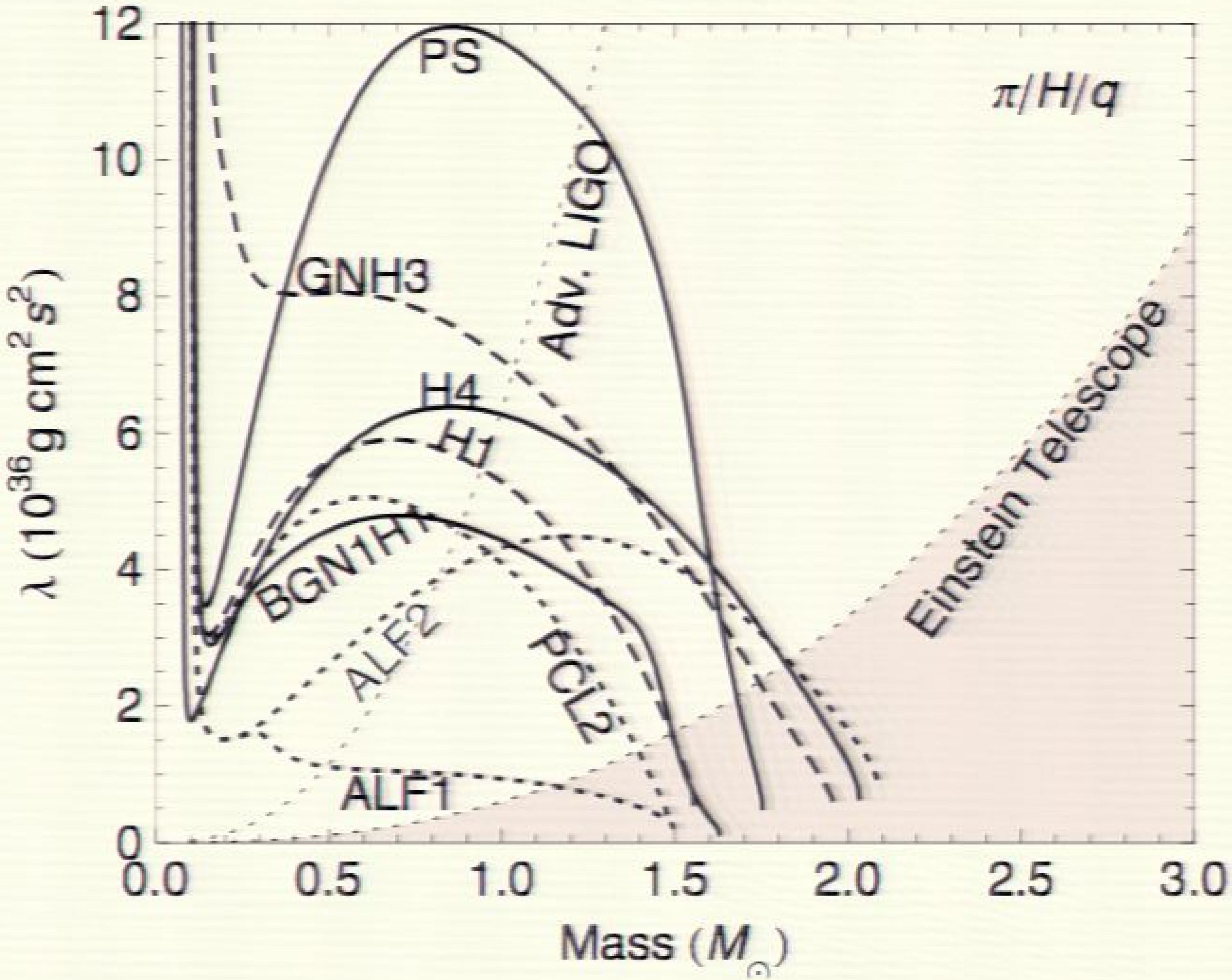

Each thick line: a candidate equation of state gives λ as function of mass.

shaded: Uncertainty in estimating λ for Advanced LIGO and ET using "clean" waveform: below 450 Hz only

Measuring tidal deformability λ

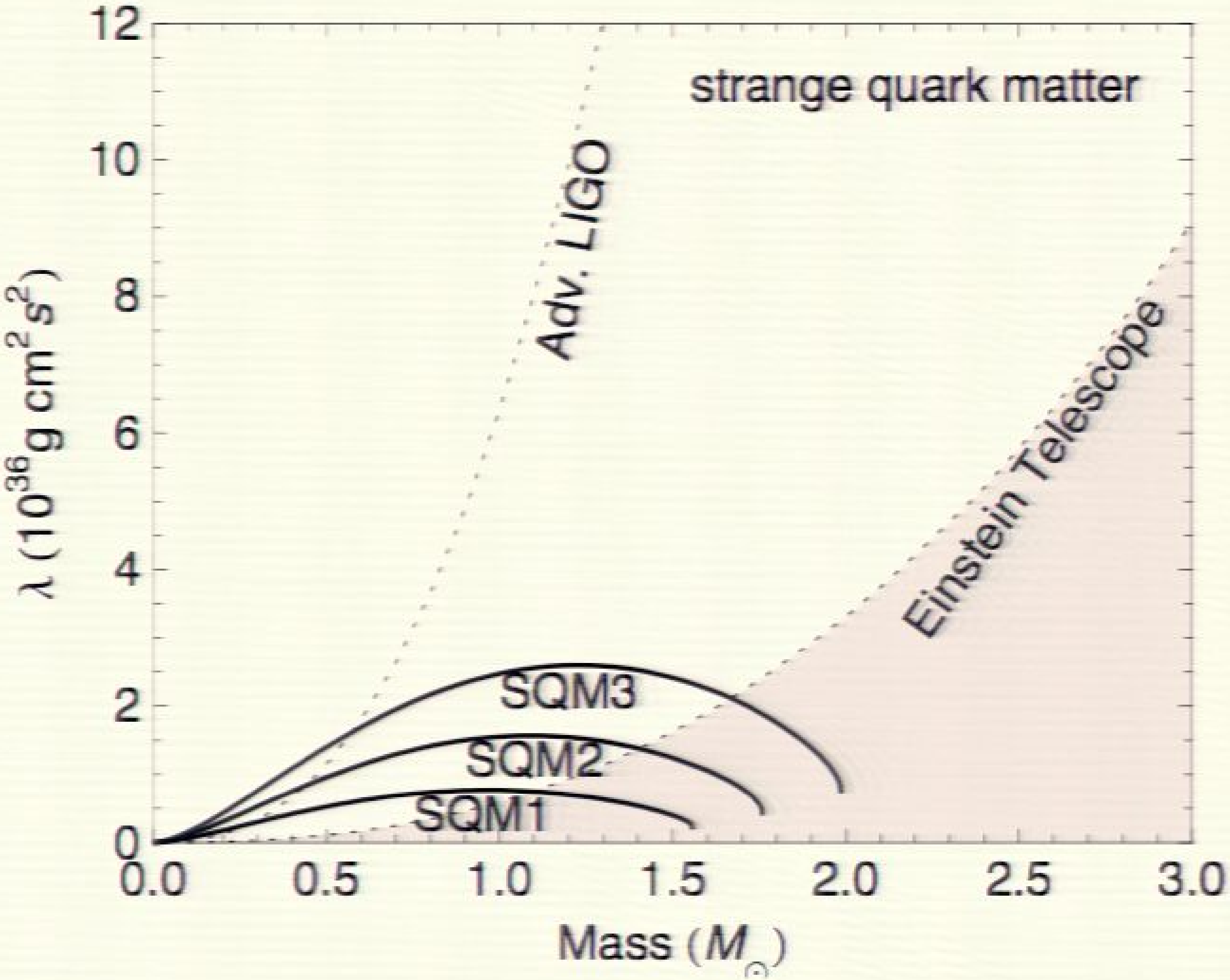

Each thick line: a candidate equation of state gives λ as function of mass.

shaded: Uncertainty in estimating λ for Advanced LIGO and ET using "clean" waveform: below 450 Hz only

Unequal mass binaries

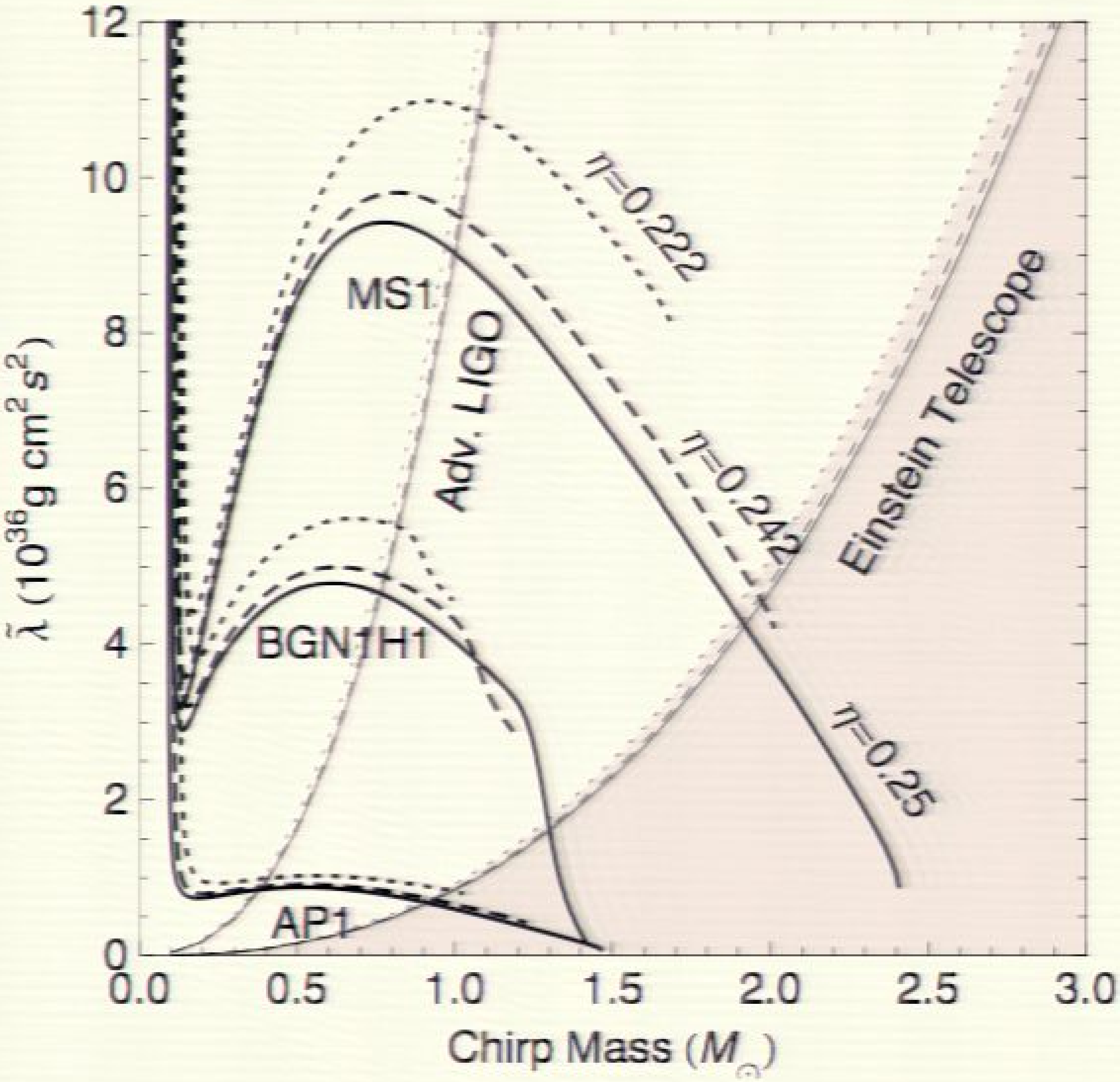

Tidal effects on gravitational wave phase depend on a weighted average

$\tilde{\lambda}(m, \eta)$

combining

λ_1 for m_1

and

λ_2 for m_2

Spin and η considered

Advanced LIGO

M ($M_\odot$)	m_2/m_1	$\Delta\mathcal{M}/\mathcal{M}$	$\Delta\eta/\eta$	$\Delta\tilde{\lambda}(10^{36}\,\mathrm{g\,cm^2\,s^2})$	ρ
2.0	1.0	0.00028	0.073	8.4	27
2.8	1.0	0.00037	0.055	19.3	35
3.4	1.0	0.00046	0.047	31.3	41
2.0	0.7	0.00026	0.058	8.2	26
2.8	0.7	0.00027	0.058	18.9	35
3.4	0.7	0.00028	0.055	30.5	41
2.8	0.5	0.00037	0.06	17.8	33

2) Numerical simulations

Current Status

Waveforms: up to 20 cycles inspiral, realistic mass ratios, GR, shock-capturing hydrodynamics, "realistic" cold EOS, thermal EOS, ideal MHD

Sample of recent results:

- Longer waveforms, increased accuracy, unequal massses, torus formation
  - Kiuchi et al 0904.4551 & 1002.2689, SACRA
  - Rezzolla et al 1001.3074, WHISKY
- Improvements to quasiequilibrium sequences and initial data:
  - Uryu et al 2009 0908.0579
  - Taniguchi and Shibata 2010 1005.0958
- Effect of magnetic field on waveform
  - Giacomazzo et al 2009 0901.2722, WHISKY
- Measurability of EOS in late inspiral
  - JR et al 0901.3258
- Effect of fully thermal EOS on waveform
  - Bauswein et al 2010 1006.3315 CF-SPH

Sampling of results

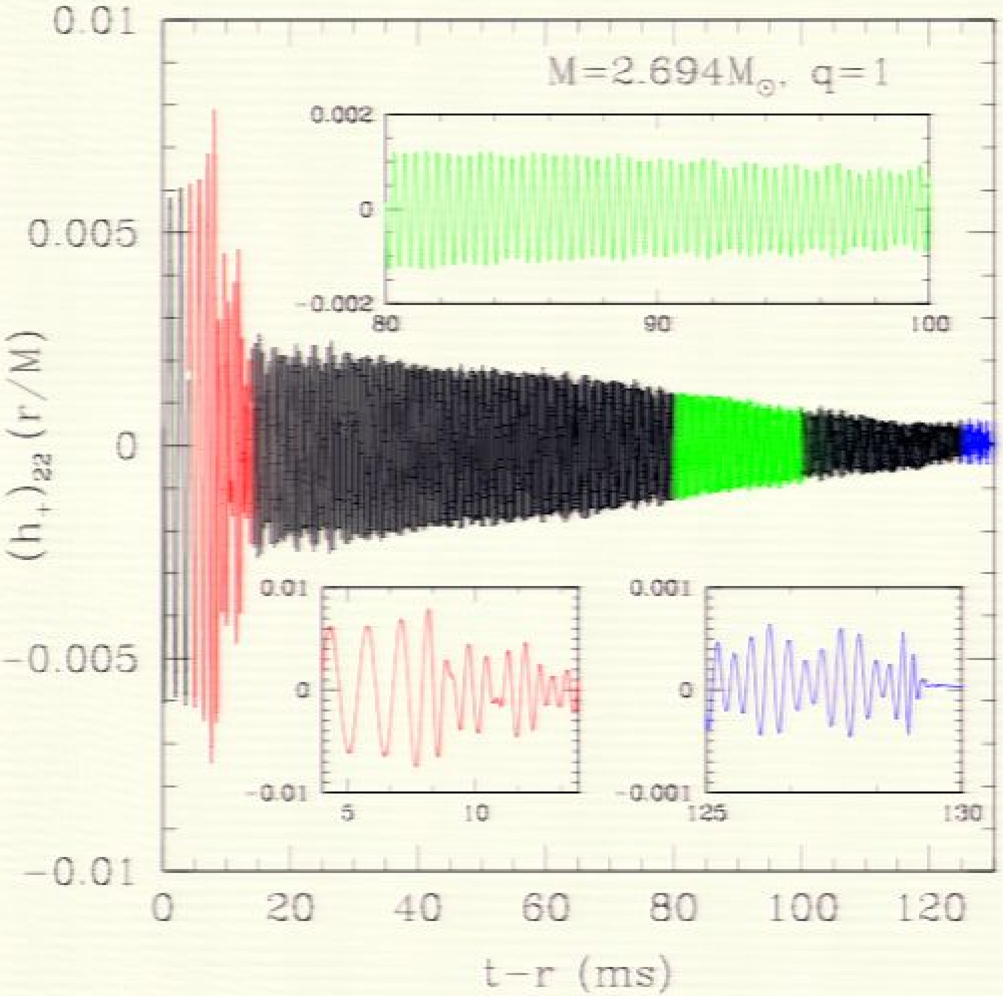

Rezzolla et al 1001.3074

2) Numerical simulations

Current Status

Waveforms: up to 20 cycles inspiral, realistic mass ratios, GR, shock-capturing hydrodynamics, "realistic" cold EOS, thermal EOS, ideal MHD

Sample of recent results:

- Longer waveforms, increased accuracy, unequal massses, torus formation
  - Kiuchi et al 0904.4551 & 1002.2689, SACRA
  - Rezzolla et al 1001.3074, WHISKY
- Improvements to quasiequilibrium sequences and initial data:
  - Uryu et al 2009 0908.0579
  - Taniguchi and Shibata 2010 1005.0958
- Effect of magnetic field on waveform
  - Giacomazzo et al 2009 0901.2722, WHISKY
- Measurability of EOS in late inspiral
  - JR et al 0901.3258
- Effect of fully thermal EOS on waveform
  - Bauswein et al 2010 1006.3315 CF-SPH

Sampling of results

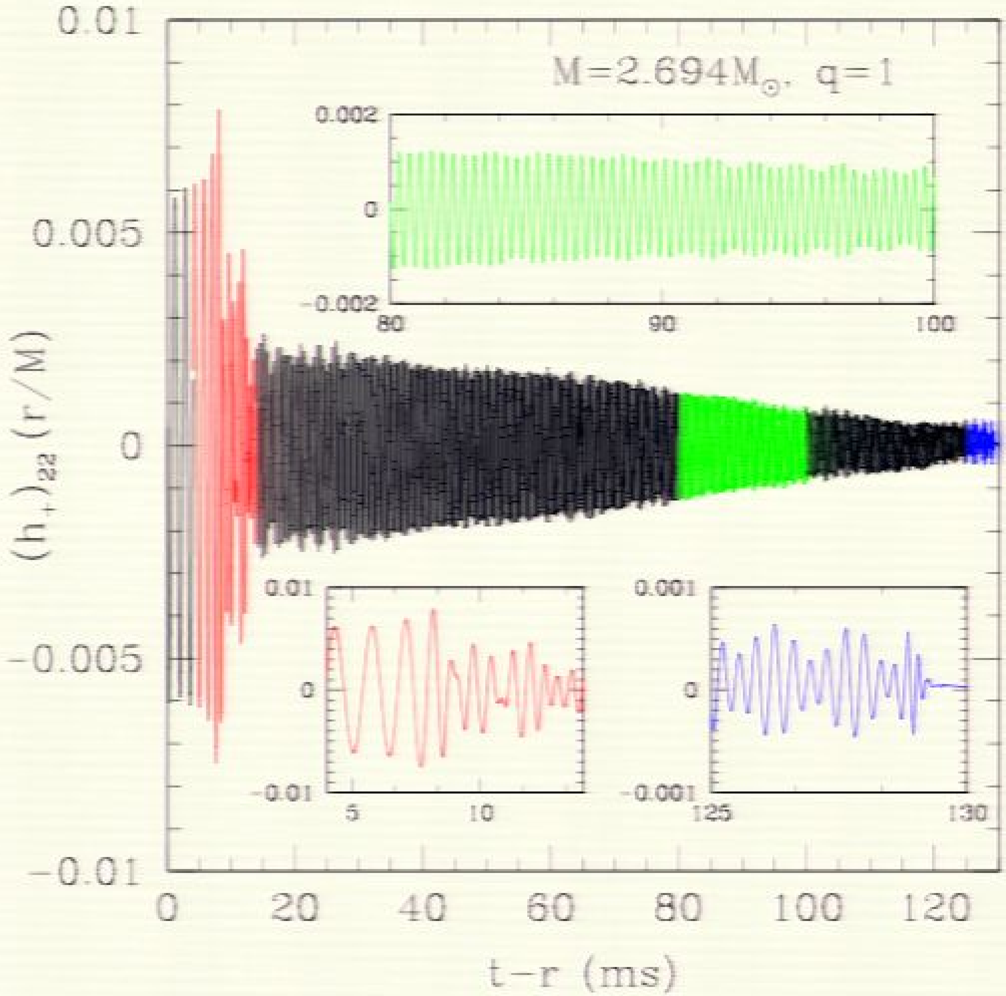

Rezzolla et al 1001.3074

Sampling of results

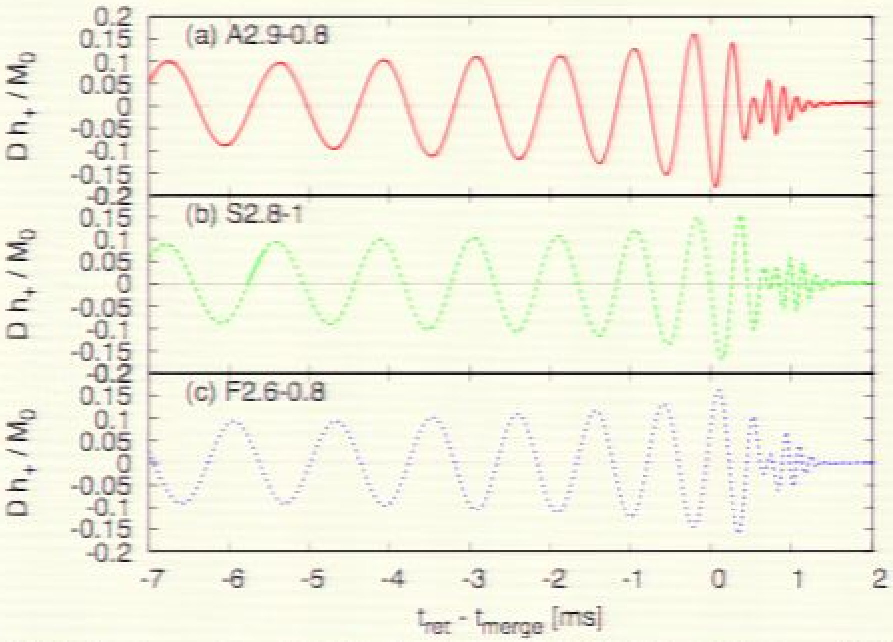

FIG. 1: + modes of GWs for (a) A2.9-0.8, (b) S2.8-1, and (c) F2.6-0.8. D is the distance from the source to the observer, who is located along the axis perpendicular to the orbital plane. $t_{\rm merge}$ denotes approximate time at the onset of the merger.

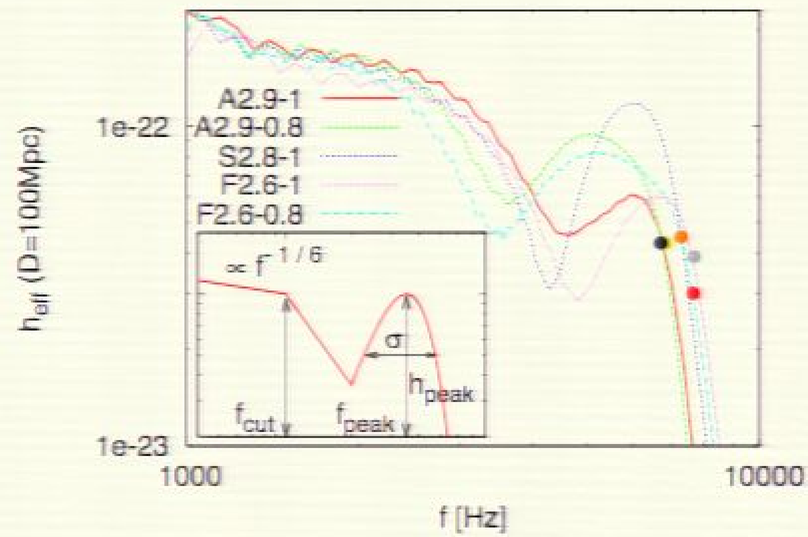

FIG. 2: Effective amplitude for models A2.9-1, A2.9-0.8, S2.8-1, F2.6-1, and F2.6-0.8. The filled circles denote the QNM frequency of the formed BHs. The small panel shows a schematic figure of the GW spectrum.

Kiuchi et al 1002.2689

Sampling of results

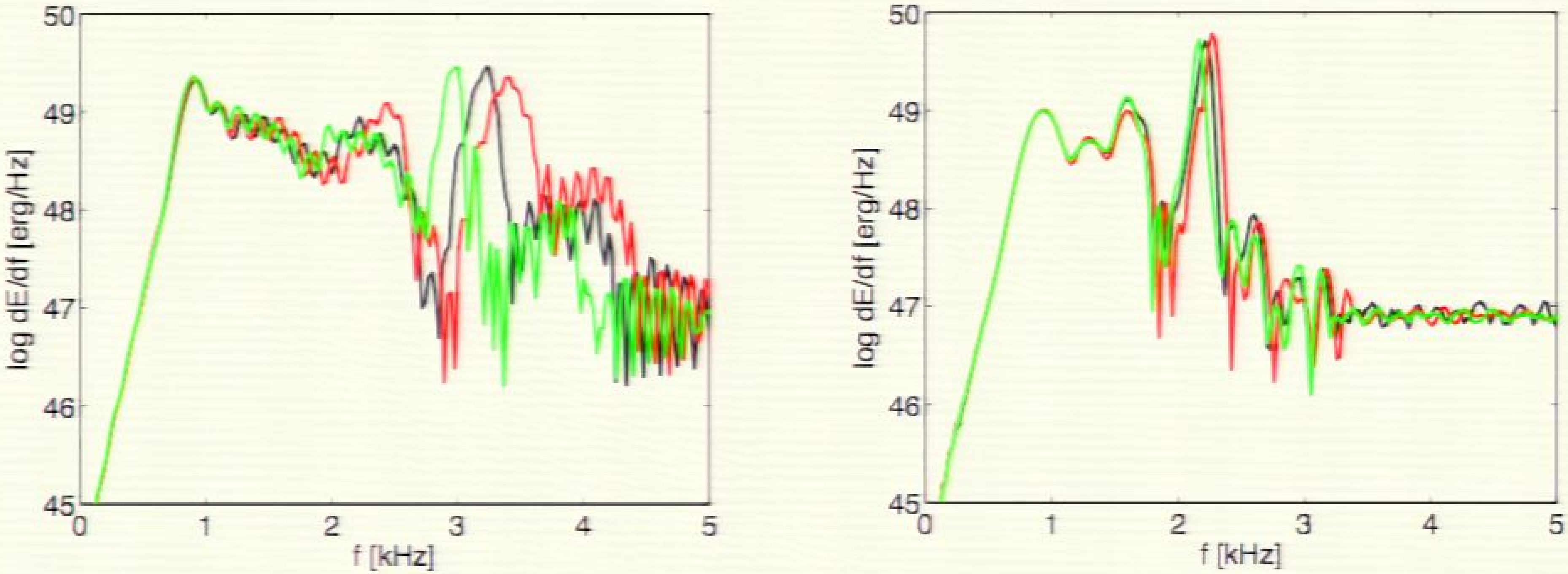

Cold+thermal approximations vs. full thermal (black line) for two EOS.
Bauswein et al 1006.3315

My current picture

Inspiral physics under control; full understanding of numerical resolution and error estimates in progress.

Qualitative understanding of merger is robust.

Shibata and Taniguchi 2006:

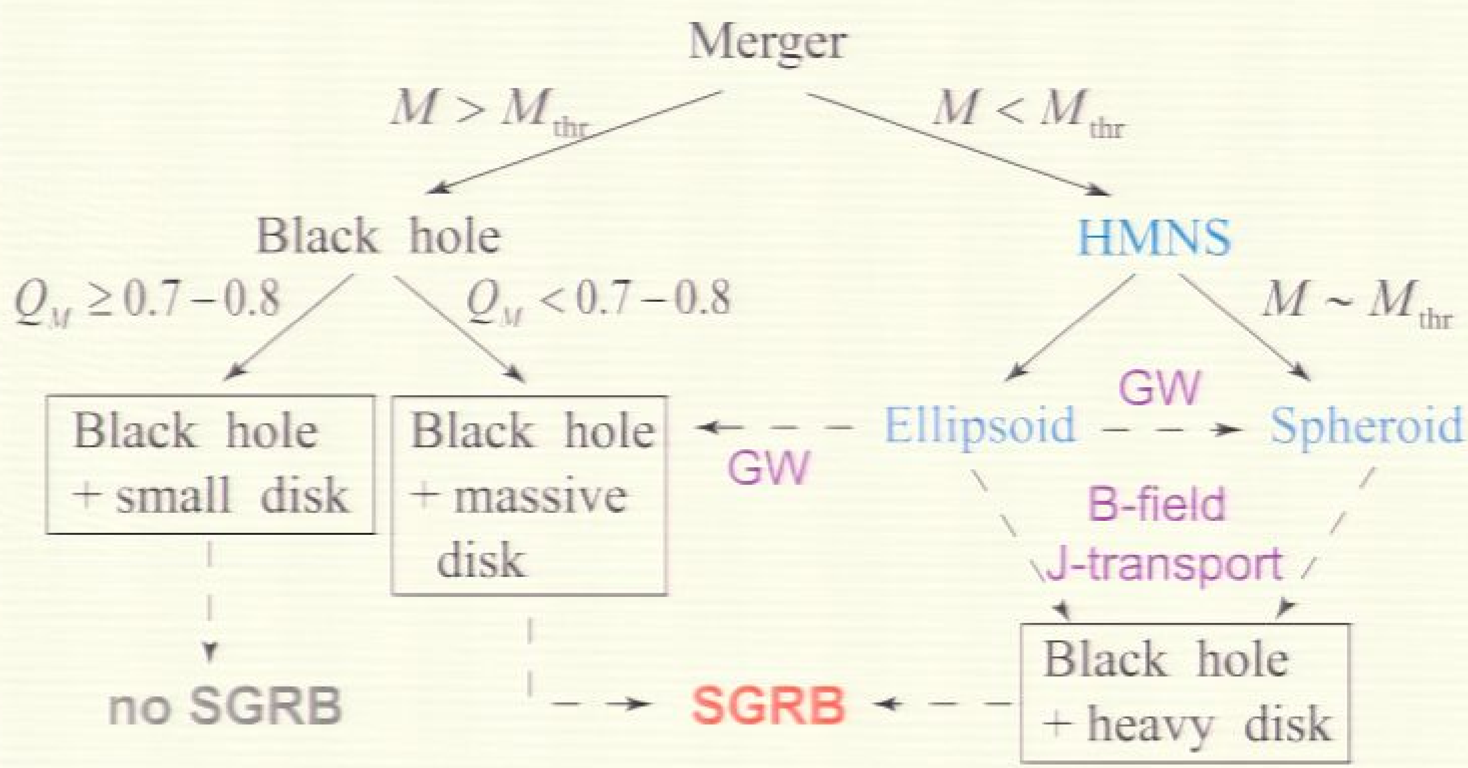

Waveform characteristics: freq of maximum amplitude at end of inspiral, peak freq of post-merger, amplitude/duration of post-merger oscillations

Sampling of results

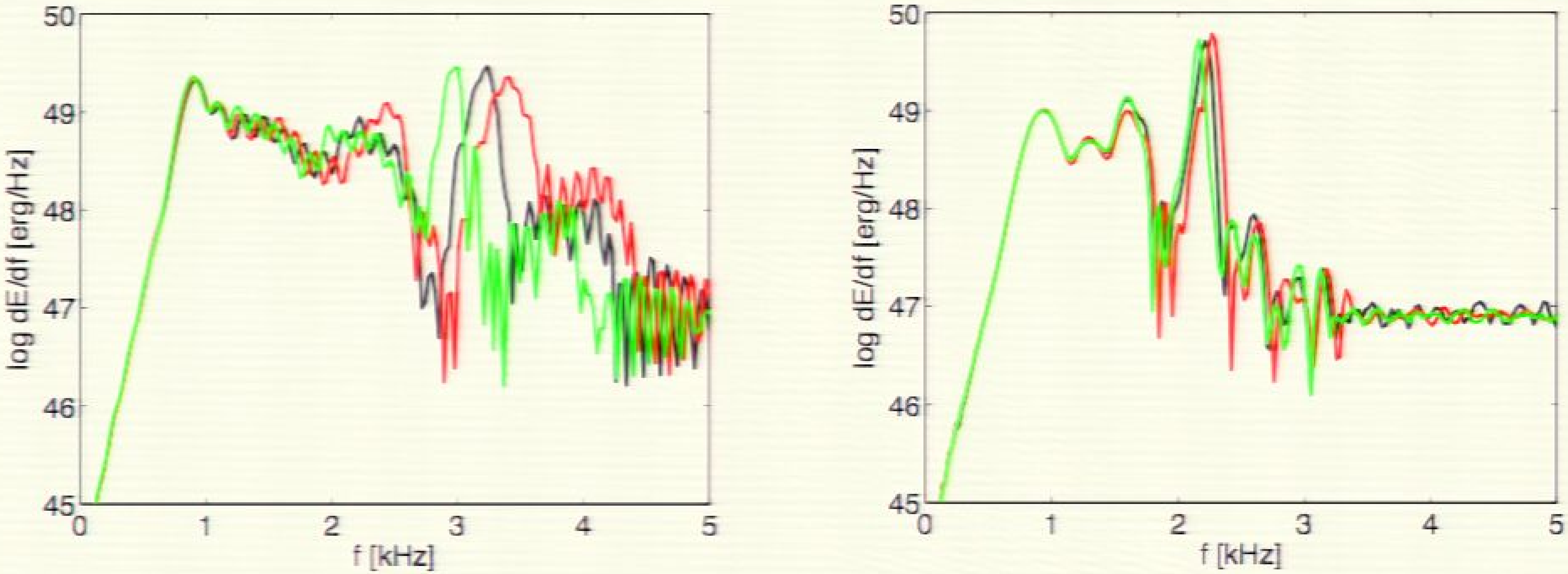

Cold+thermal approximations vs. full thermal (black line) for two EOS.
Bauswein et al 1006.3315

My current picture

Inspiral physics under control; full understanding of numerical resolution and error estimates in progress.

Qualitative understanding of merger is robust.

Shibata and Taniguchi 2006:

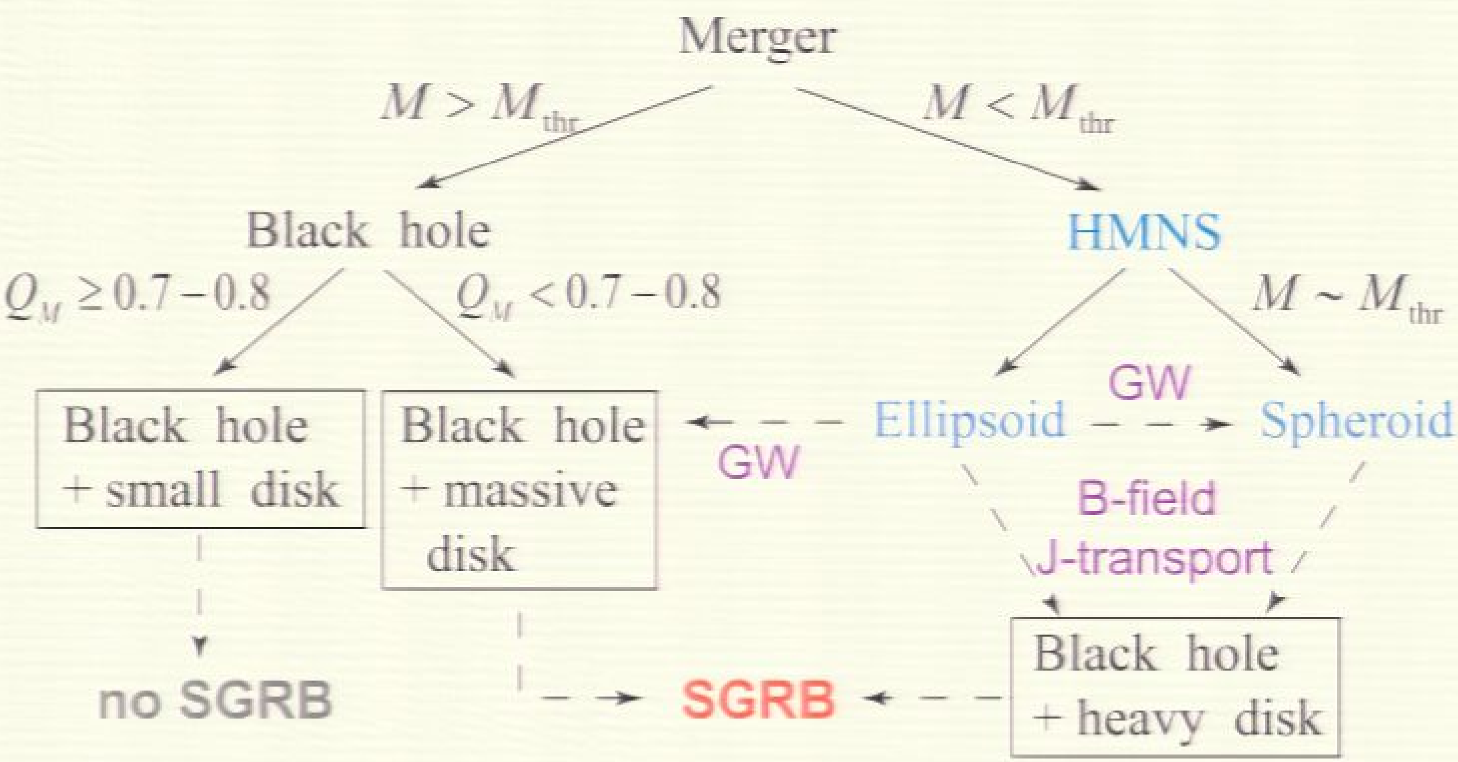

Waveform characteristics: freq of maximum amplitude at end of inspiral, peak freq of post-merger, amplitude/duration of post-merger oscillations

Neutron star Samurai: WHISKY and SACRA (so far)

- Same initial data (Taniguchi quasiequilibrium code)
- Range of EOS
- 1.35-1.35 $M_\odot$ equal mass binary
  - Observed NS masses 1.2-1.5 $M_\odot$ in DNS, "average" 1.35 $M_\odot$, mass ratio > 0.8

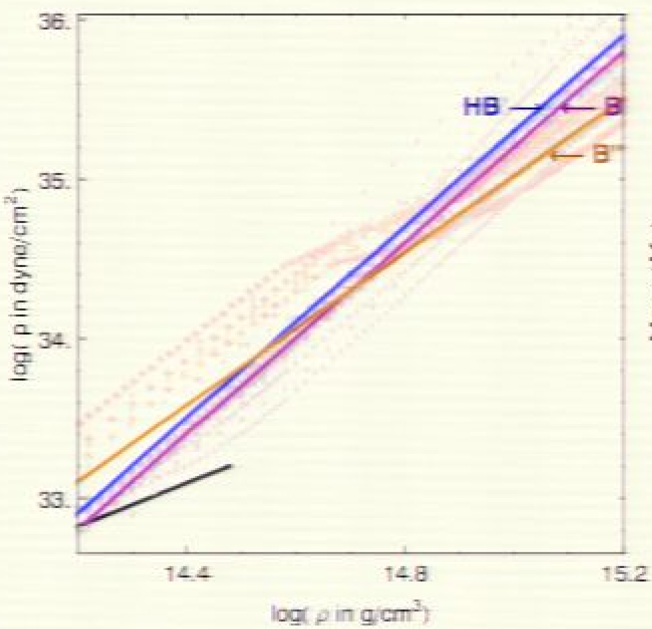

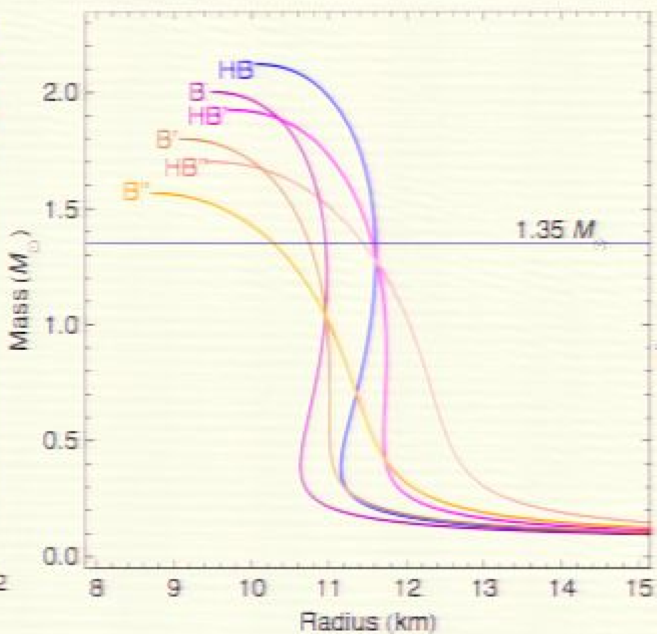

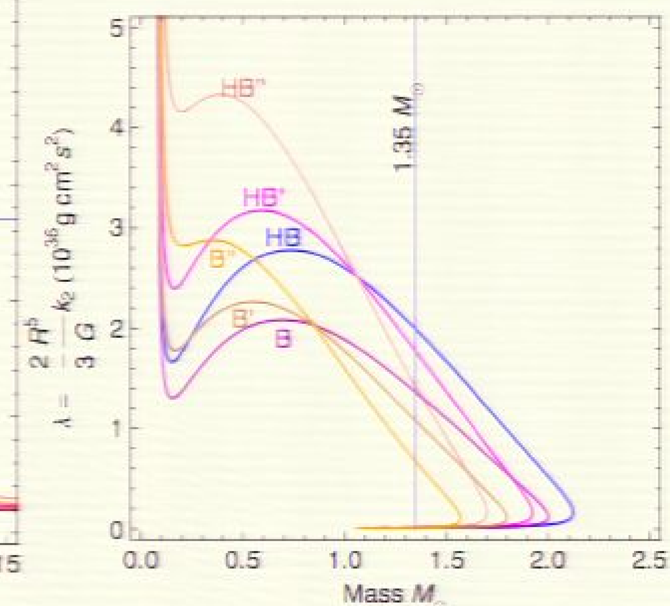

Inspiral agreement

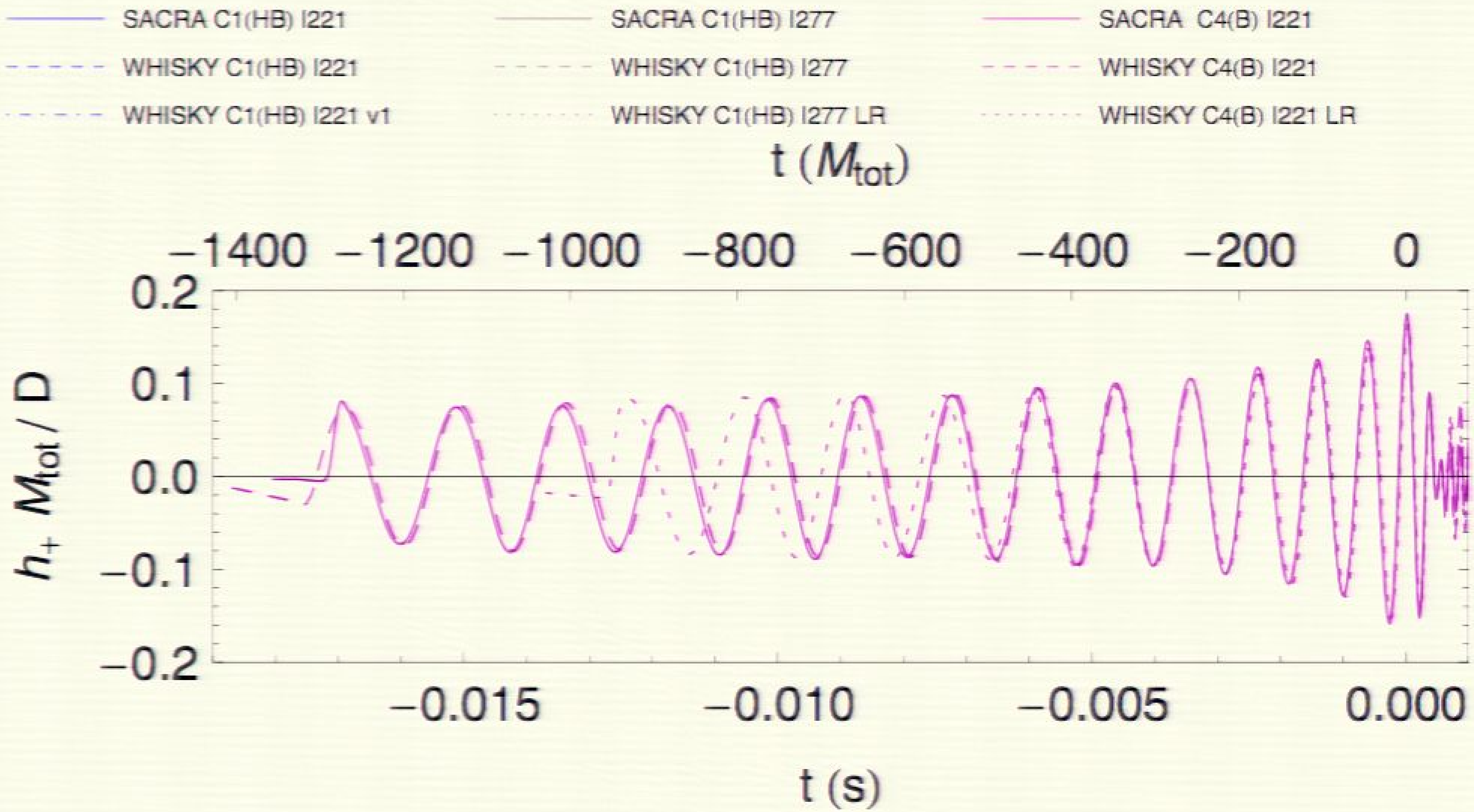

Inspiral agreement

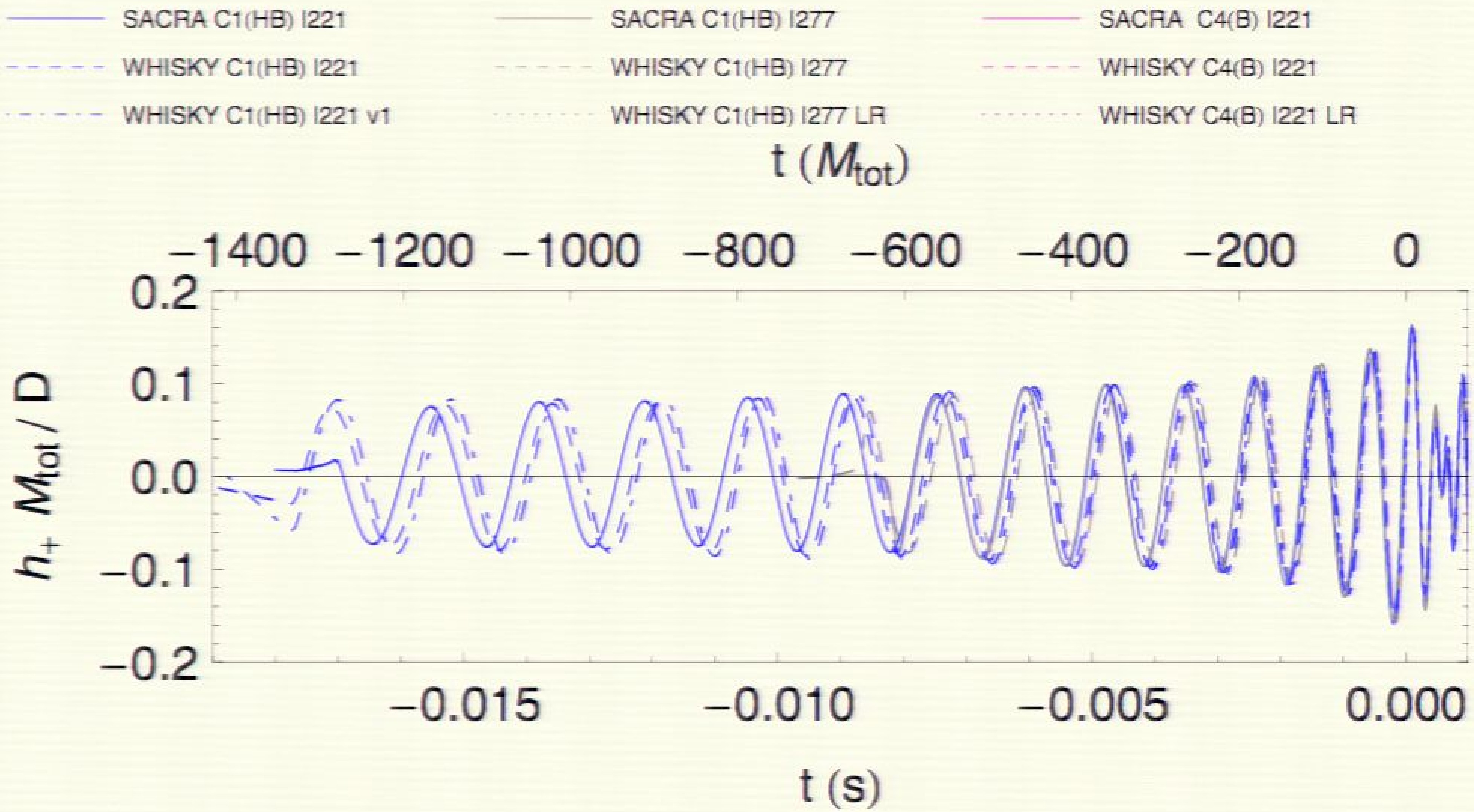

Merger agreement

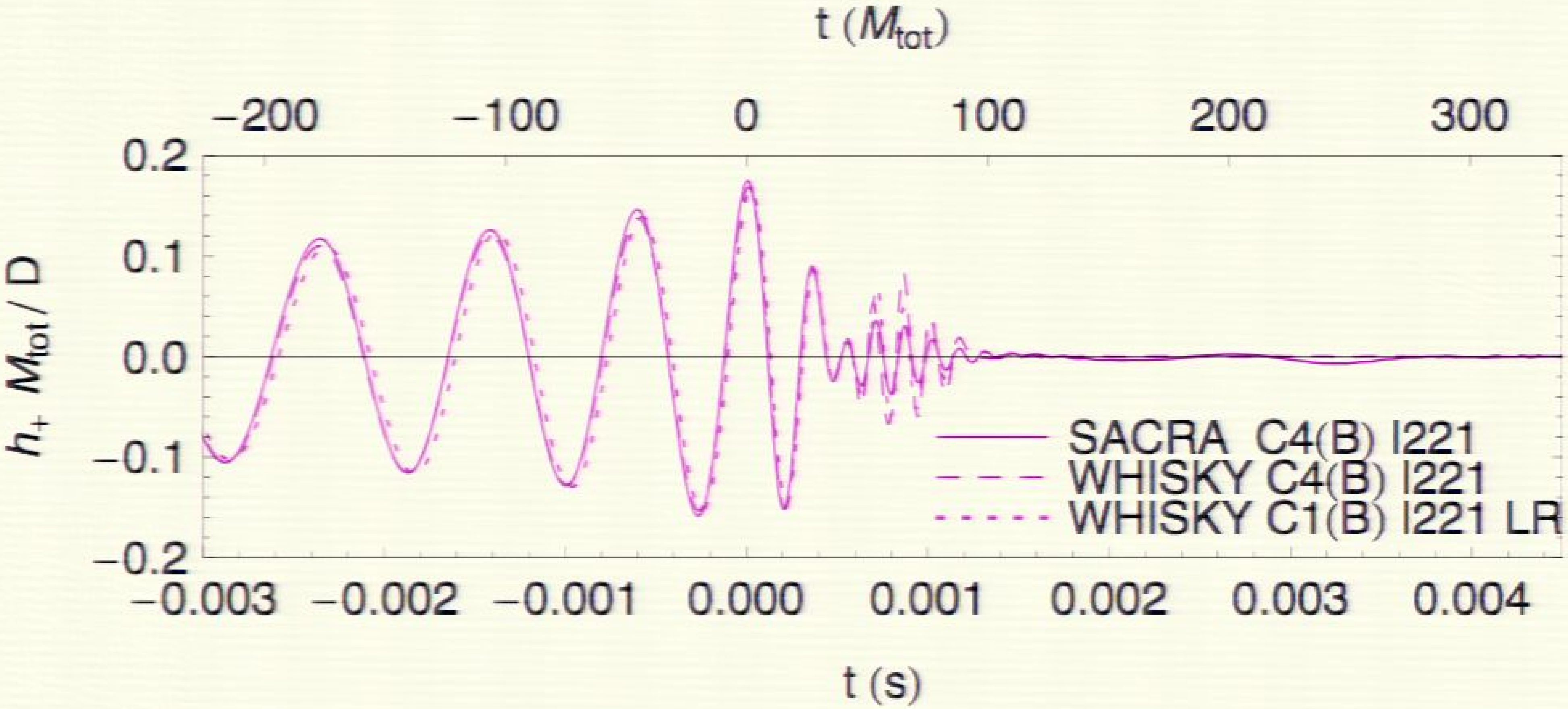

Merger agreement

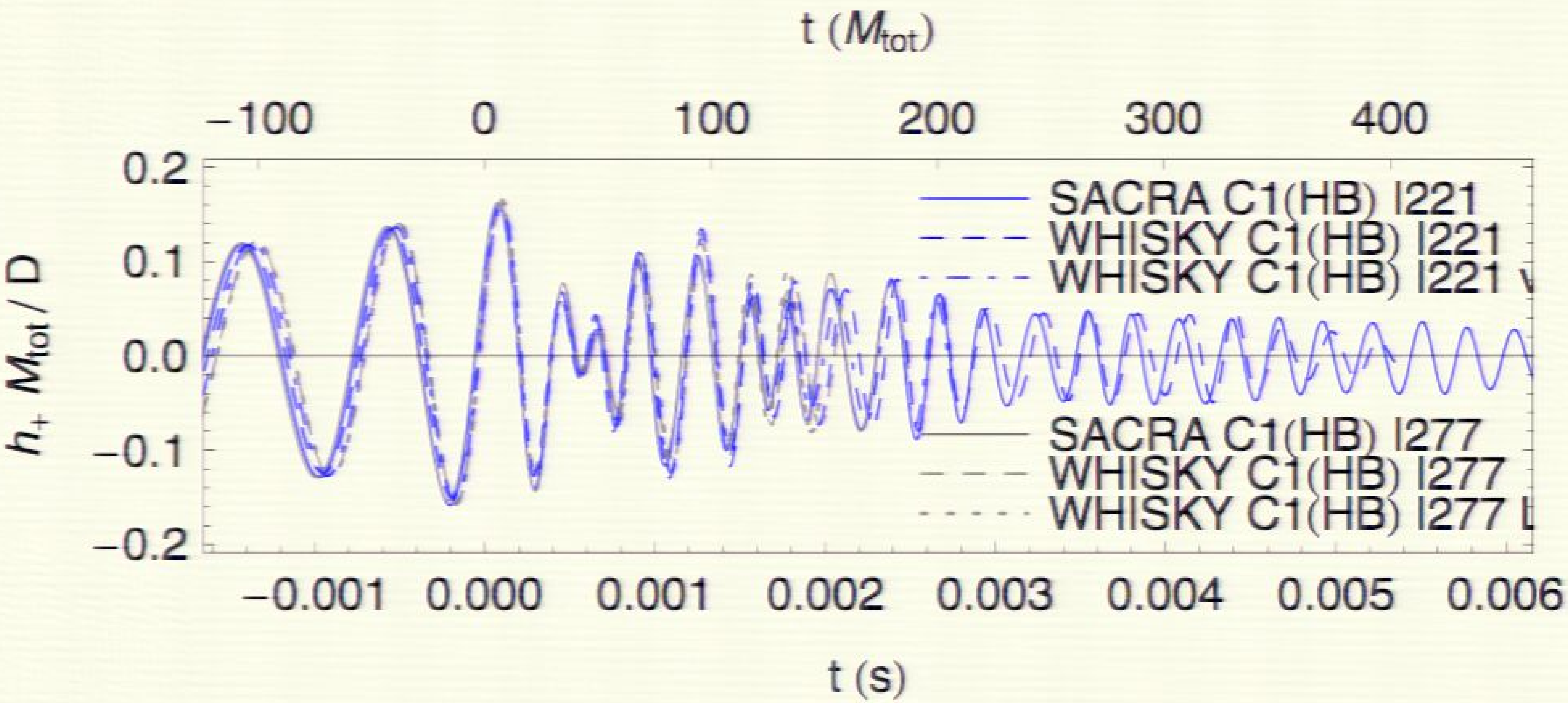

Spectra

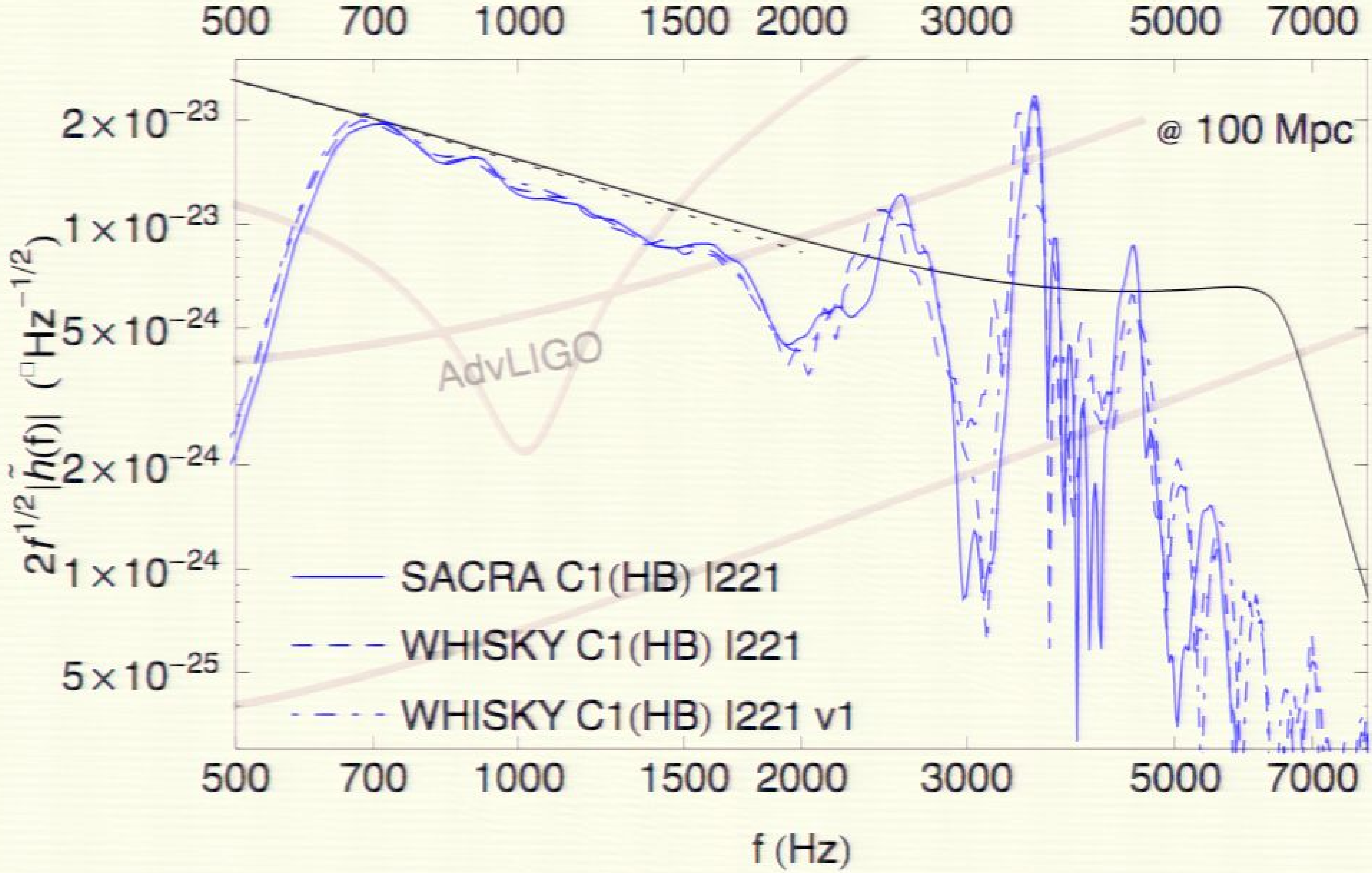

500 700 1000 1500 2000 3000 5000 7000
@ 100 Mpc
2×10^{-23}
1×10^{-23}
5×10^{-24}
2×10^{-24}
1×10^{-24}
5×10^{-25}
$2f^{1/2}|\tilde{h}(f)|$ (Hz$^{-1/2}$)
AdvLIGO
SACRA C1(HB) I221
WHISKY C1(HB) I221
WHISKY C1(HB) I221 v1
f (Hz)

Spectra

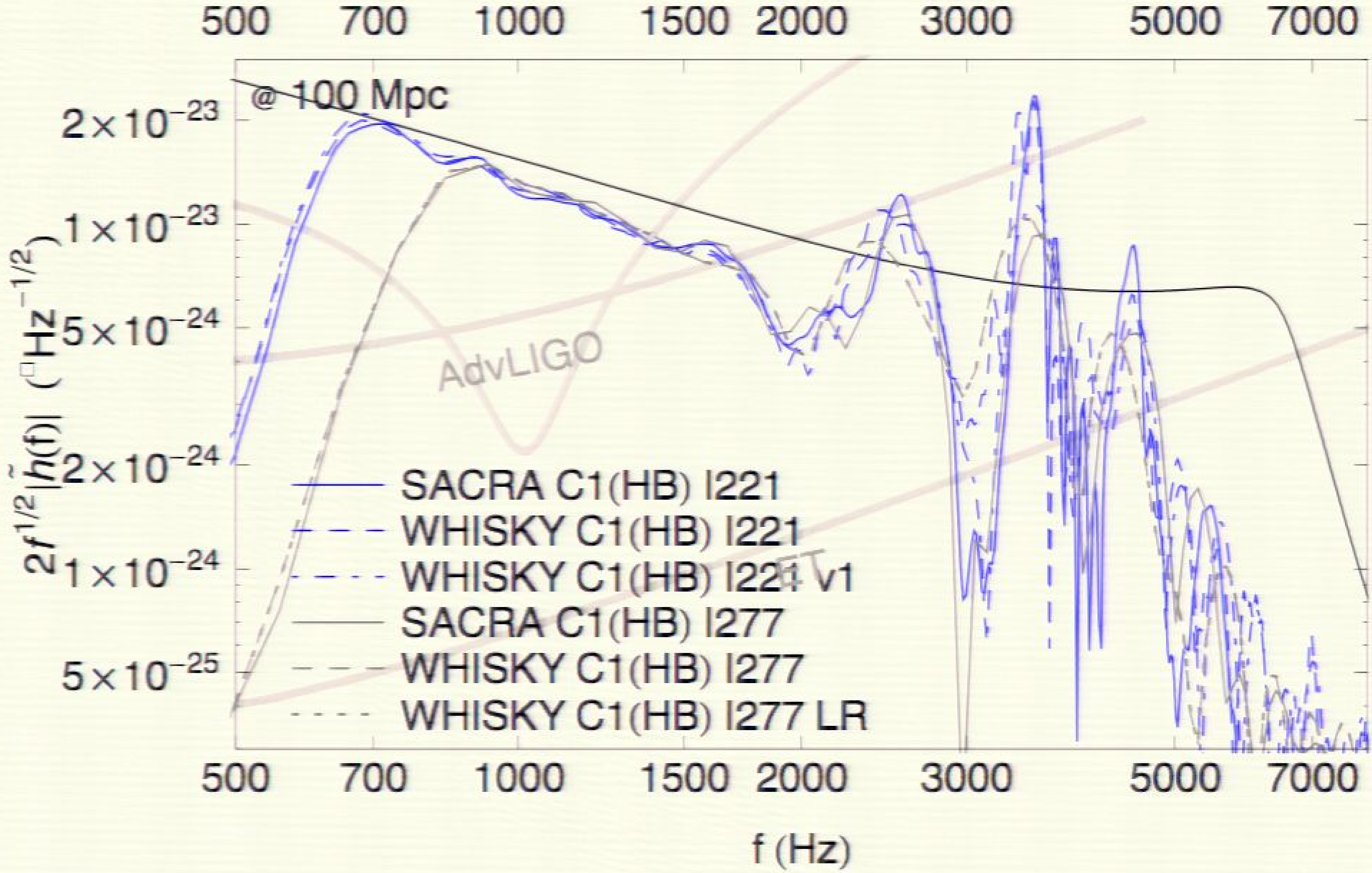

@ 100 Mpc
AdvLIGO
ET
SACRA C1(HB) I221
WHISKY C1(HB) I221
WHISKY C1(HB) I221 v1
SACRA C1(HB) I277
WHISKY C1(HB) I277
WHISKY C1(HB) I277 LR
500
700
1000
1500
2000
3000
5000
7000
f (Hz)
2×10^{-23}
1×10^{-23}
5×10^{-24}
2×10^{-24}
1×10^{-24}
5×10^{-25}
$2f^{1/2}|\tilde{h}(f)|$ (Hz$^{-1/2}$)

Spectra

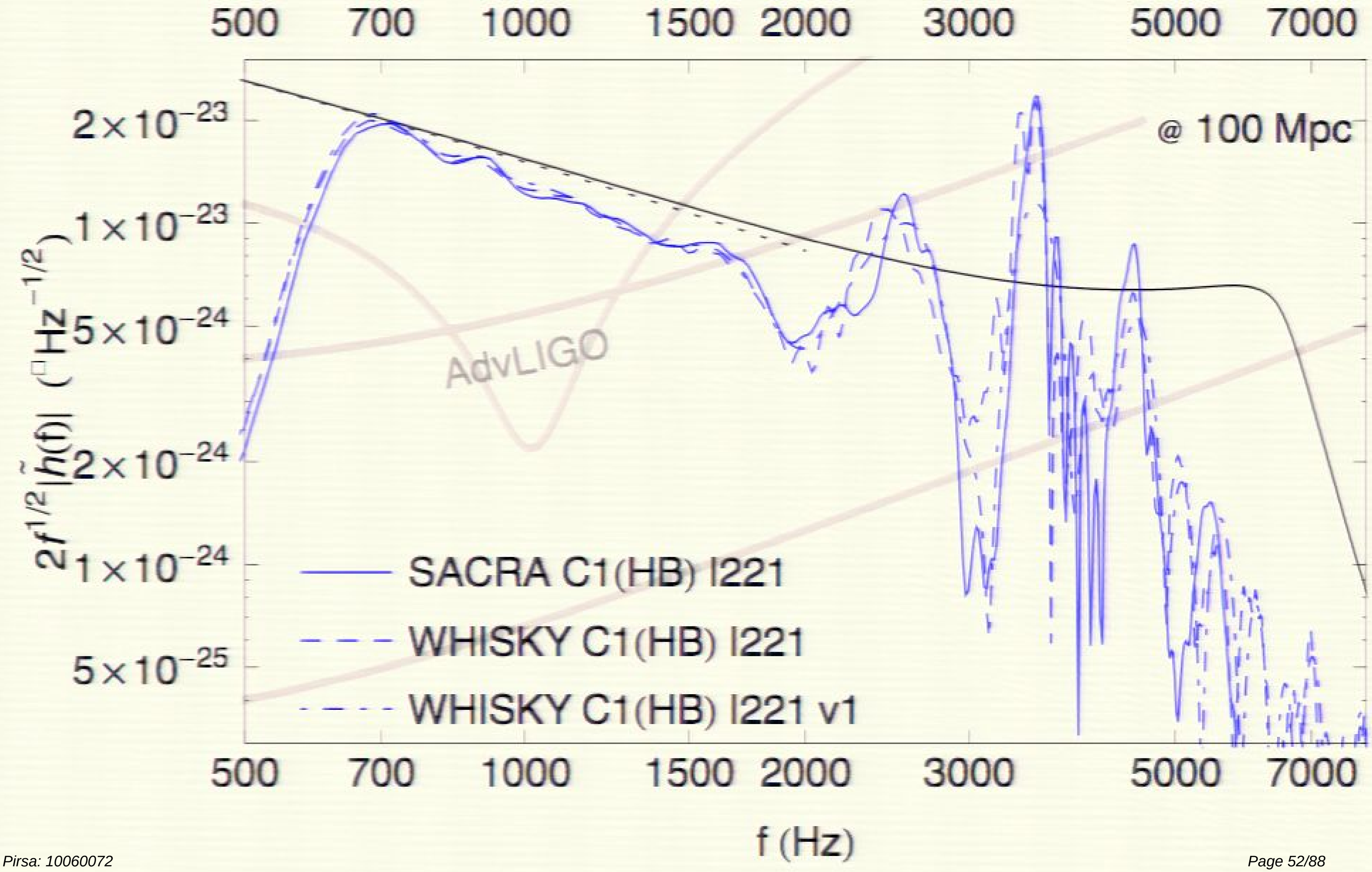
500
700
1000
1500
2000
3000
5000
7000
@ 100 Mpc
2×10^{-23}
1×10^{-23}
5×10^{-24}
2×10^{-24}
1×10^{-24}
5×10^{-25}
$2f^{1/2}|\tilde{h}(f)|$ ($\mathrm{Hz}^{-1/2}$)
AdvLIGO
SACRA C1(HB) I221
WHISKY C1(HB) I221
WHISKY C1(HB) I221 v1
f (Hz)

Spectra

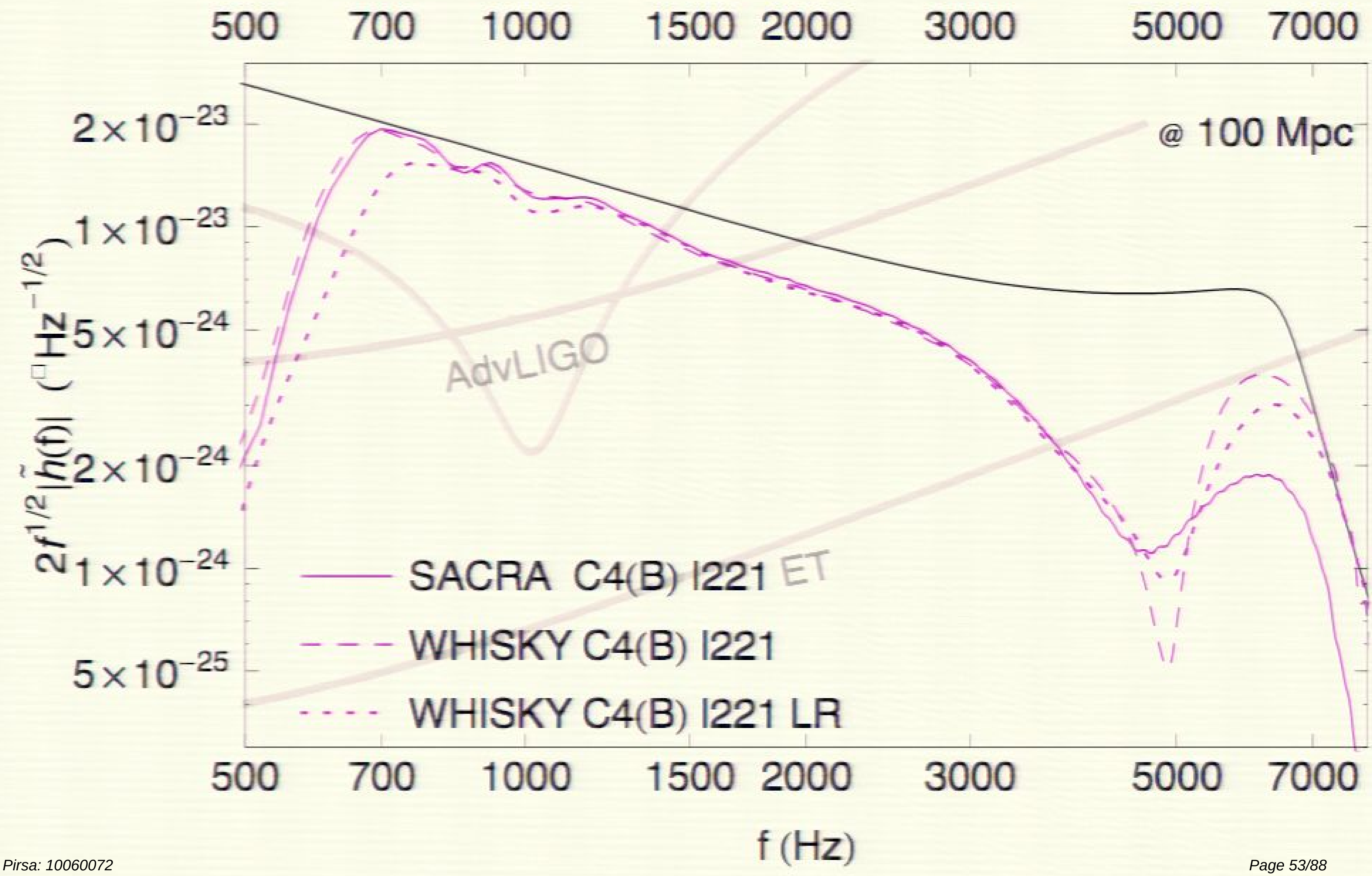

500 700 1000 1500 2000 3000 5000 7000
@ 100 Mpc
2×10^{-23}
1×10^{-23}
5×10^{-24}
2×10^{-24}
1×10^{-24}
5×10^{-25}
$2f^{1/2}|\tilde{h}(f)|$ (Hz$^{-1/2}$)
AdvLIGO
ET
SACRA C4(B) I221
WHISKY C4(B) I221
WHISKY C4(B) I221 LR
f (Hz)

Spectra

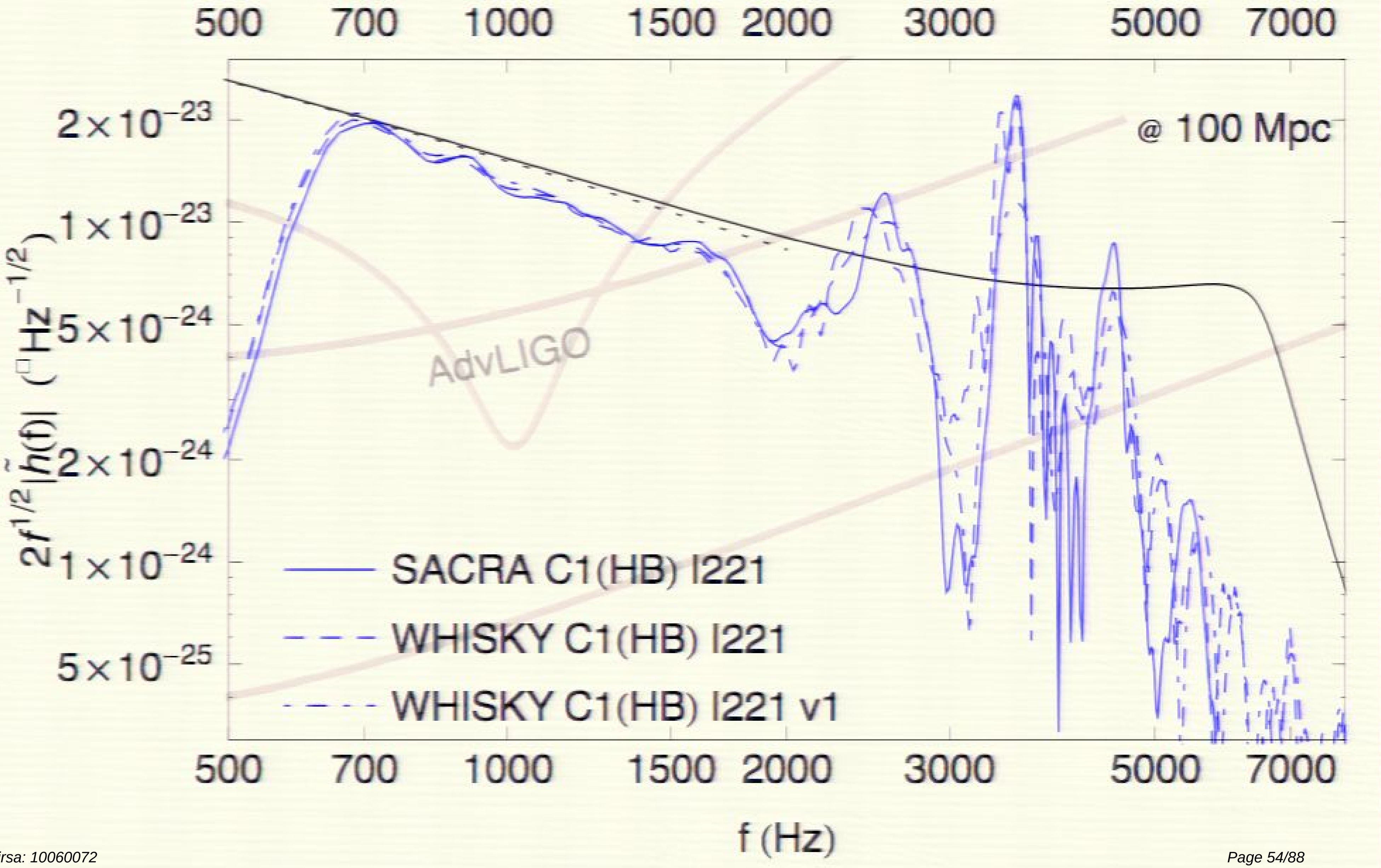

500 700 1000 1500 2000 3000 5000 7000
@ 100 Mpc
2×10^{-23}
1×10^{-23}
5×10^{-24}
2×10^{-24}
1×10^{-24}
5×10^{-25}
$2f^{1/2}|\tilde{h}(f)|$ ($\mathrm{Hz}^{-1/2}$)
AdvLIGO
SACRA C1(HB) I221
WHISKY C1(HB) I221
WHISKY C1(HB) I221 v1
500 700 1000 1500 2000 3000 5000 7000
f (Hz)

Spectra

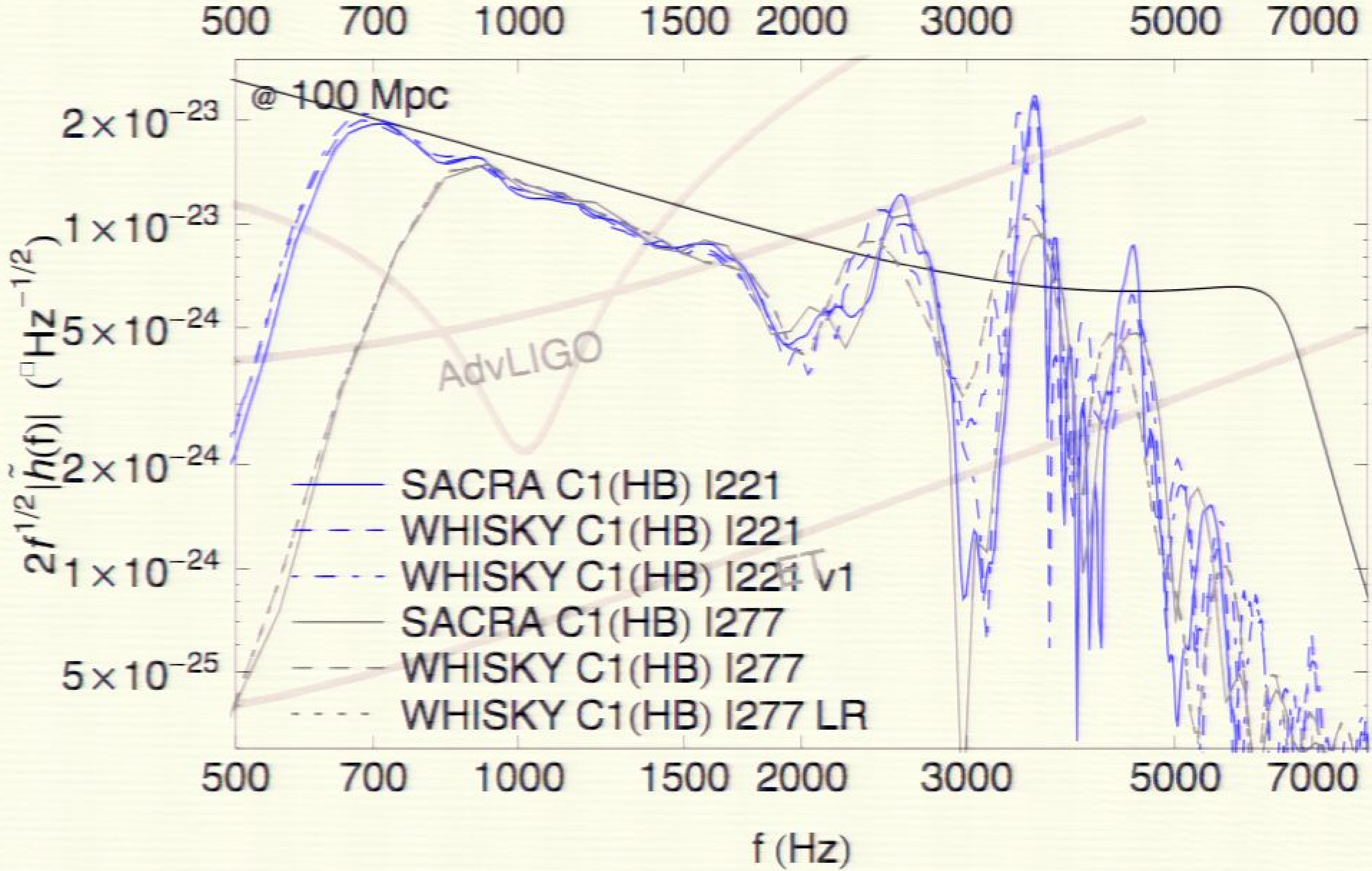

500
700
1000
1500
2000
3000
5000
7000
@ 100 Mpc
2×10^−23
1×10^−23
5×10^−24
2×10^−24
1×10^−24
5×10^−25
AdvLIGO
ET
SACRA C1(HB) l221
WHISKY C1(HB) l221
WHISKY C1(HB) l221 v1
SACRA C1(HB) l277
WHISKY C1(HB) l277
WHISKY C1(HB) l277 LR
f (Hz)

Spectra

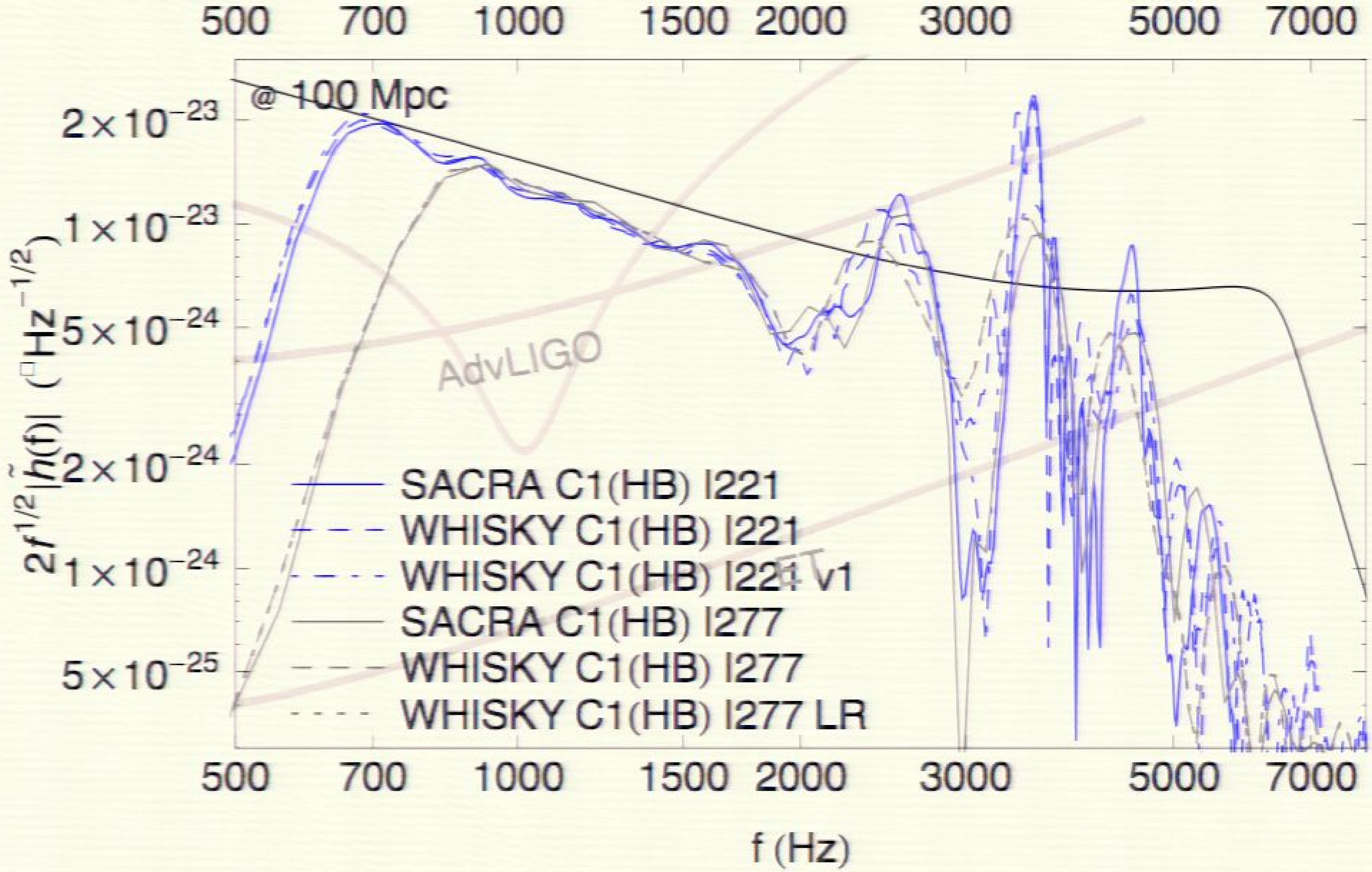

500
700
1000
1500
2000
3000
5000
7000
@ 100 Mpc
2×10^{-23}
1×10^{-23}
5×10^{-24}
2×10^{-24}
1×10^{-24}
5×10^{-25}
$2f^{1/2}|\tilde{h}(f)|$ ($\mathrm{Hz}^{-1/2}$)
AdvLIGO
ET
SACRA C1(HB) I221
WHISKY C1(HB) I221
WHISKY C1(HB) I221 v1
SACRA C1(HB) I277
WHISKY C1(HB) I277
WHISKY C1(HB) I277 LR
f (Hz)

Spectra

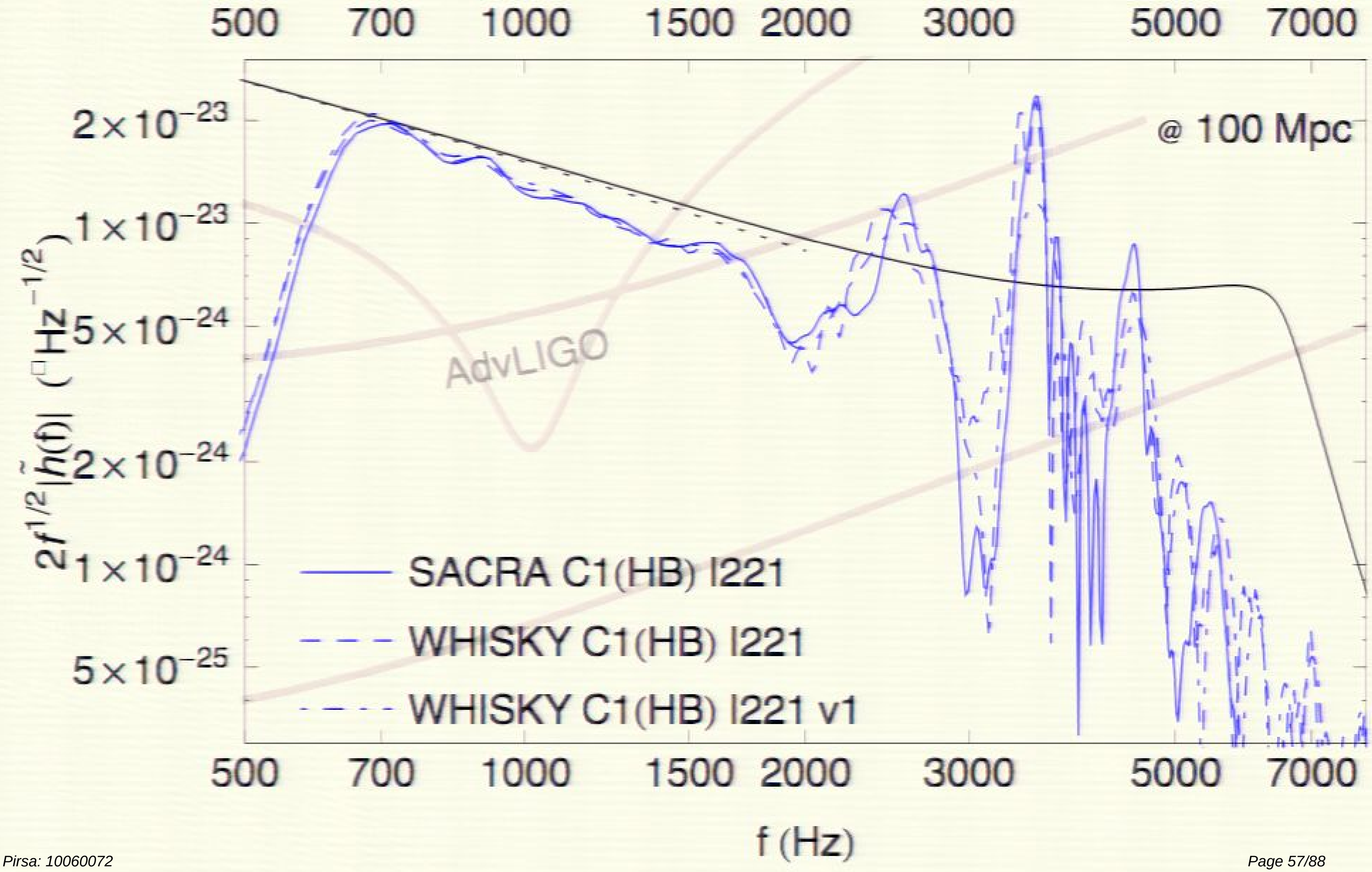

500
700
1000
1500
2000
3000
5000
7000
2×10^{-23}
1×10^{-23}
5×10^{-24}
2×10^{-24}
1×10^{-24}
5×10^{-25}
$2f^{1/2}|\tilde{h}(f)|$ ($\mathrm{Hz}^{-1/2}$)
@ 100 Mpc
AdvLIGO
SACRA C1(HB) l221
WHISKY C1(HB) l221
WHISKY C1(HB) l221 v1
f (Hz)

Spectra

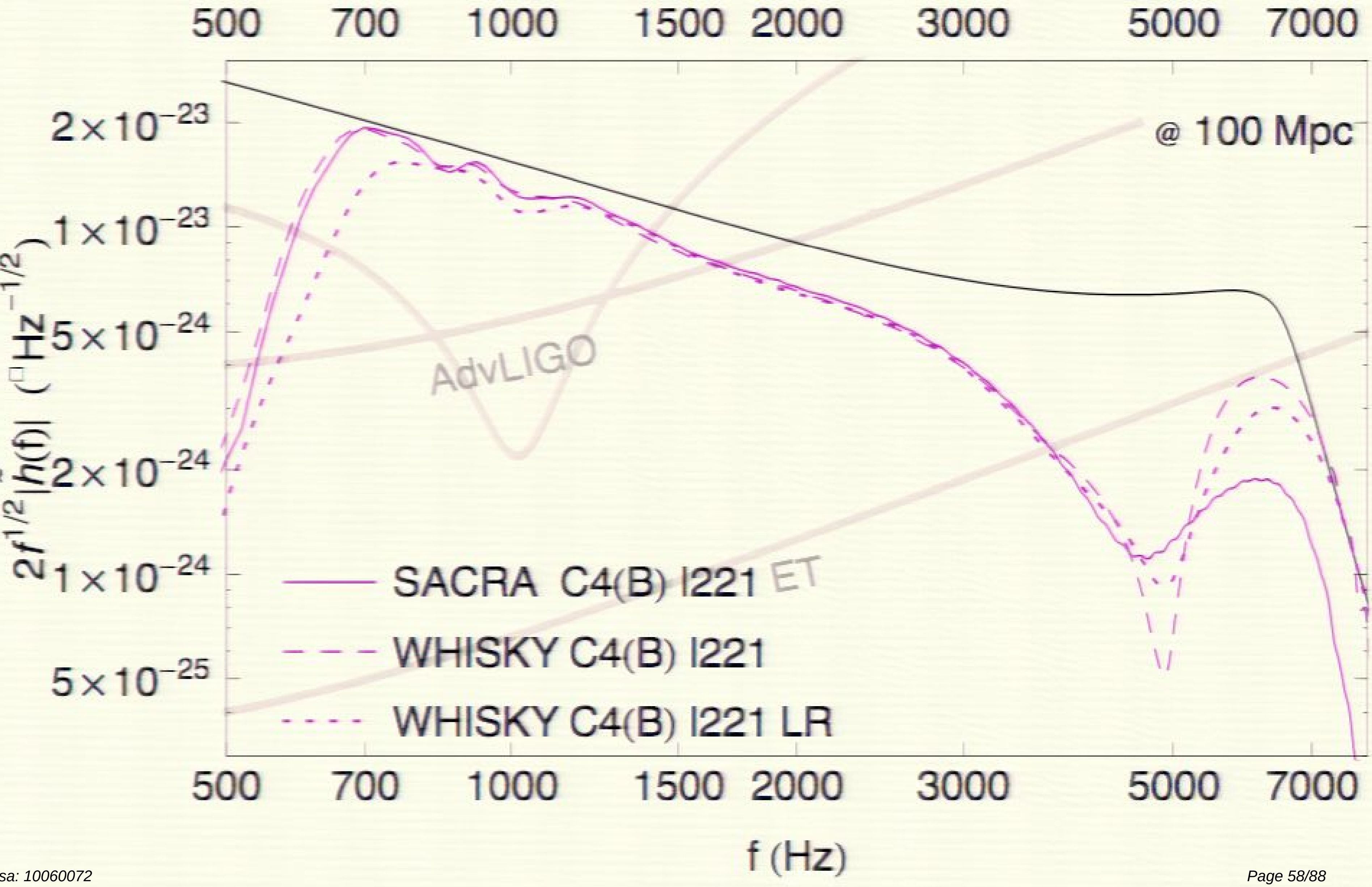

500
700
1000
1500
2000
3000
5000
7000
@ 100 Mpc
2×10^{-23}
1×10^{-23}
5×10^{-24}
2×10^{-24}
1×10^{-24}
5×10^{-25}
$2f^{1/2}|\tilde{h}(f)|$ ($\mathrm{Hz}^{-1/2}$)
AdvLIGO
ET
SACRA C4(B) I221
WHISKY C4(B) I221
WHISKY C4(B) I221 LR
f (Hz)

Measurability estimates: EOS effects on inspiral

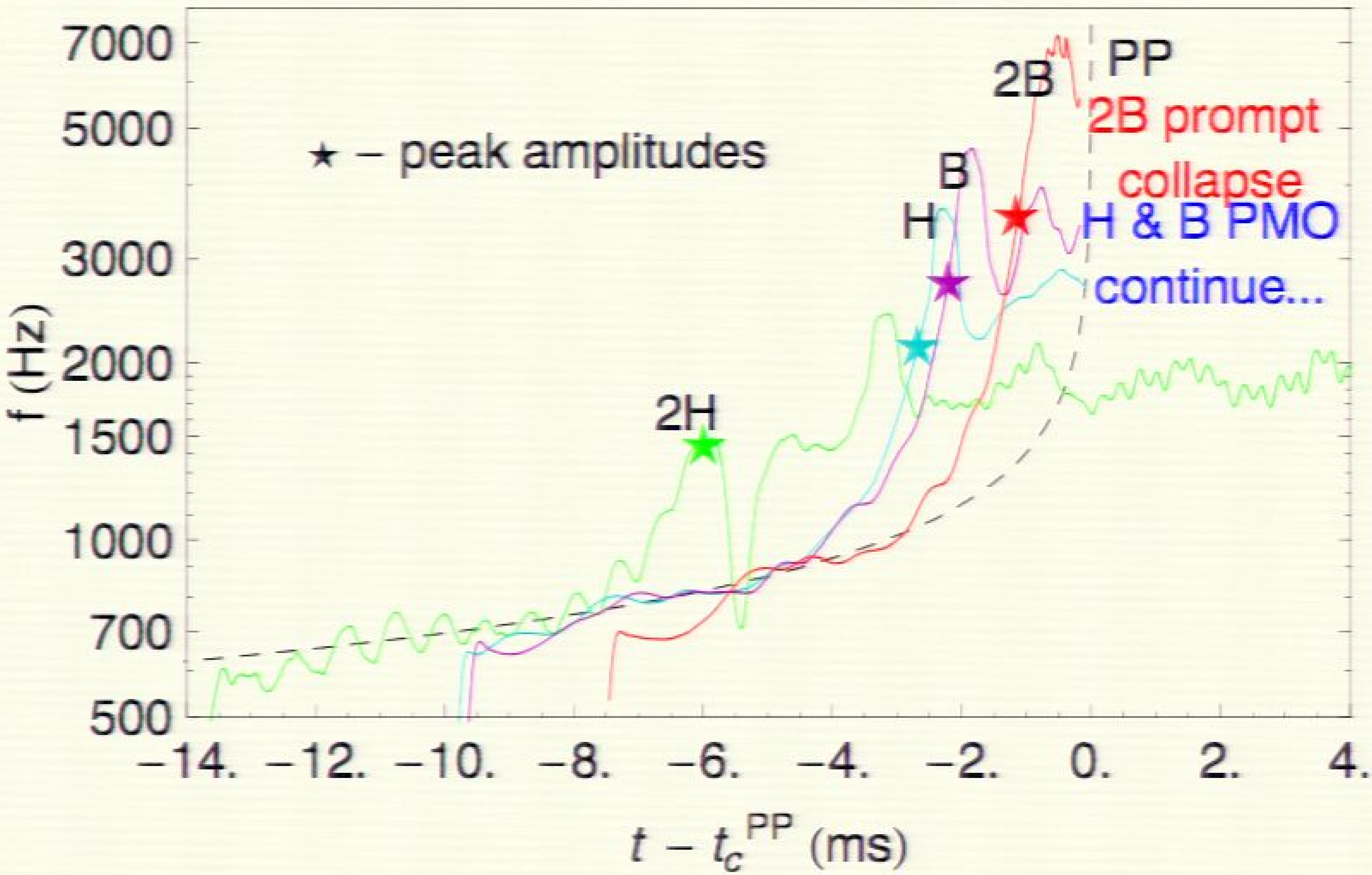

Initial study waveforms 0901.3258: Late inspiral of realistic EOS marginally differentiable in broadband Advanced LIGO; radius measured to $\pm \sim 1$ km

Measurability estimates: EOS effects on inspiral

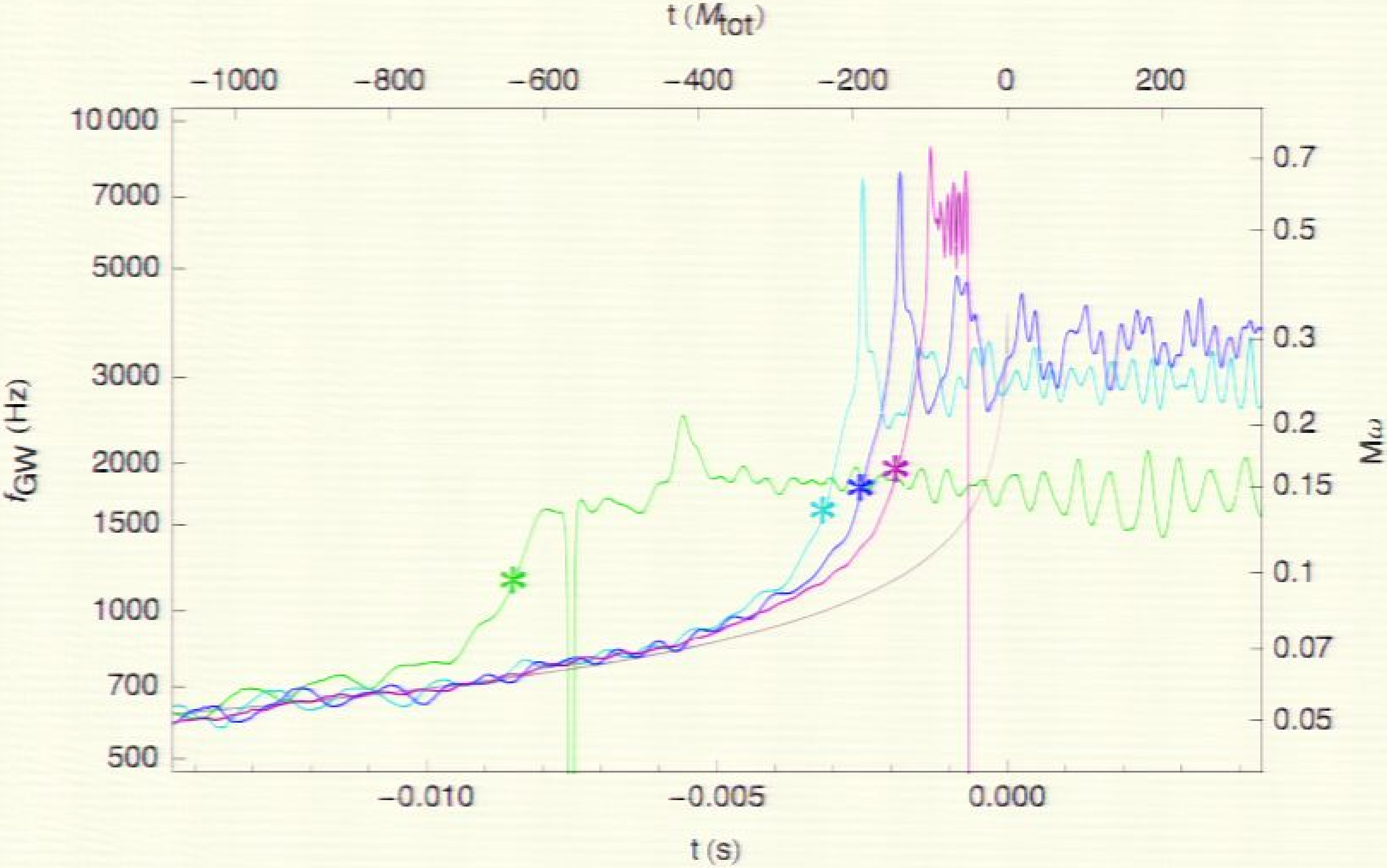

Improved WHISKY/SACRA waveforms now available; looks qualitatively similar; quantitative results in progres...

Measurability estimates: EOS effects on inspiral

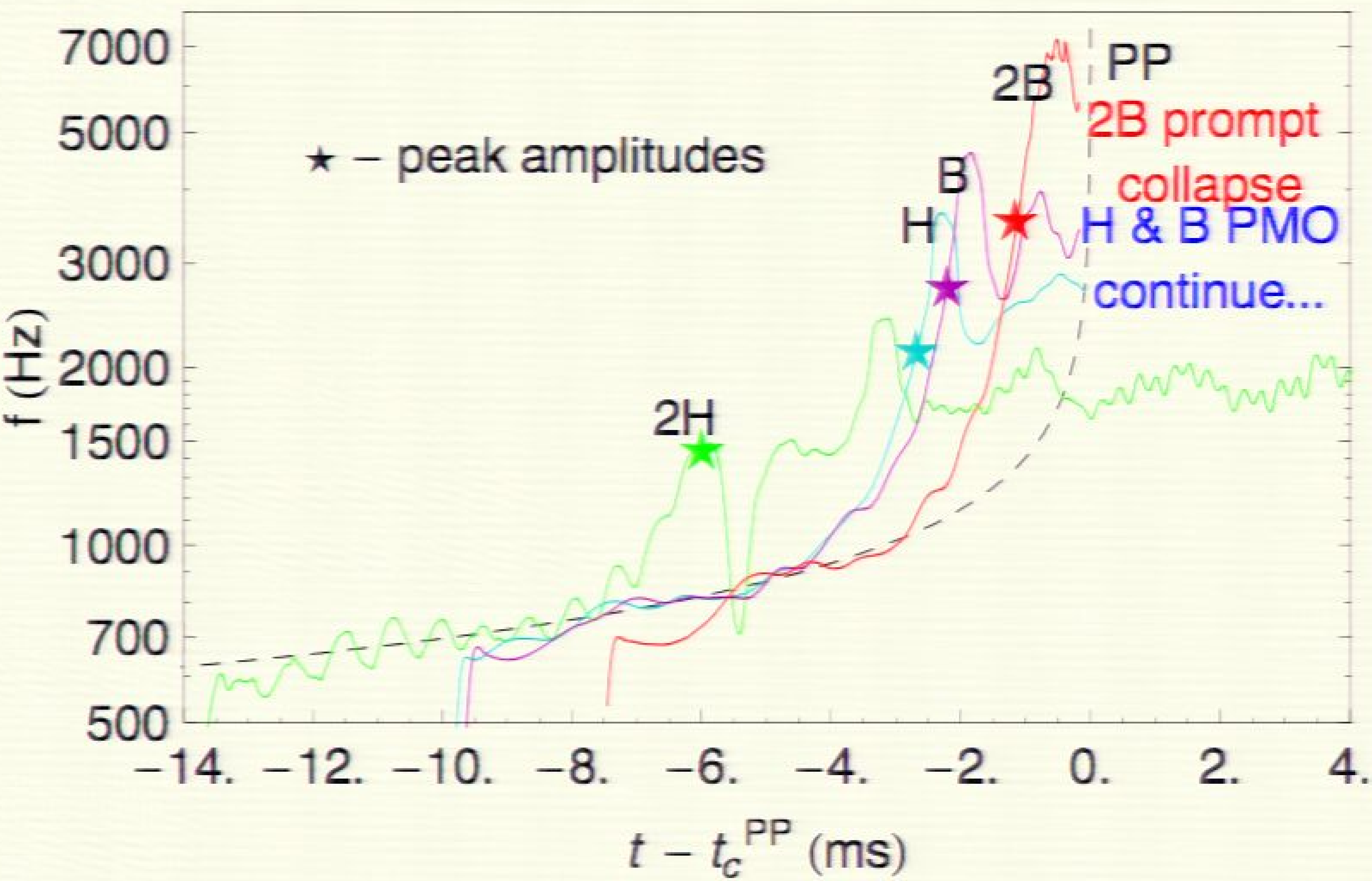

Initial study waveforms 0901.3258: Late inspiral of realistic EOS marginally differentiable in broadband Advanced LIGO; radius measured to $\pm \sim 1$ km

Measurability estimates: EOS effects on inspiral

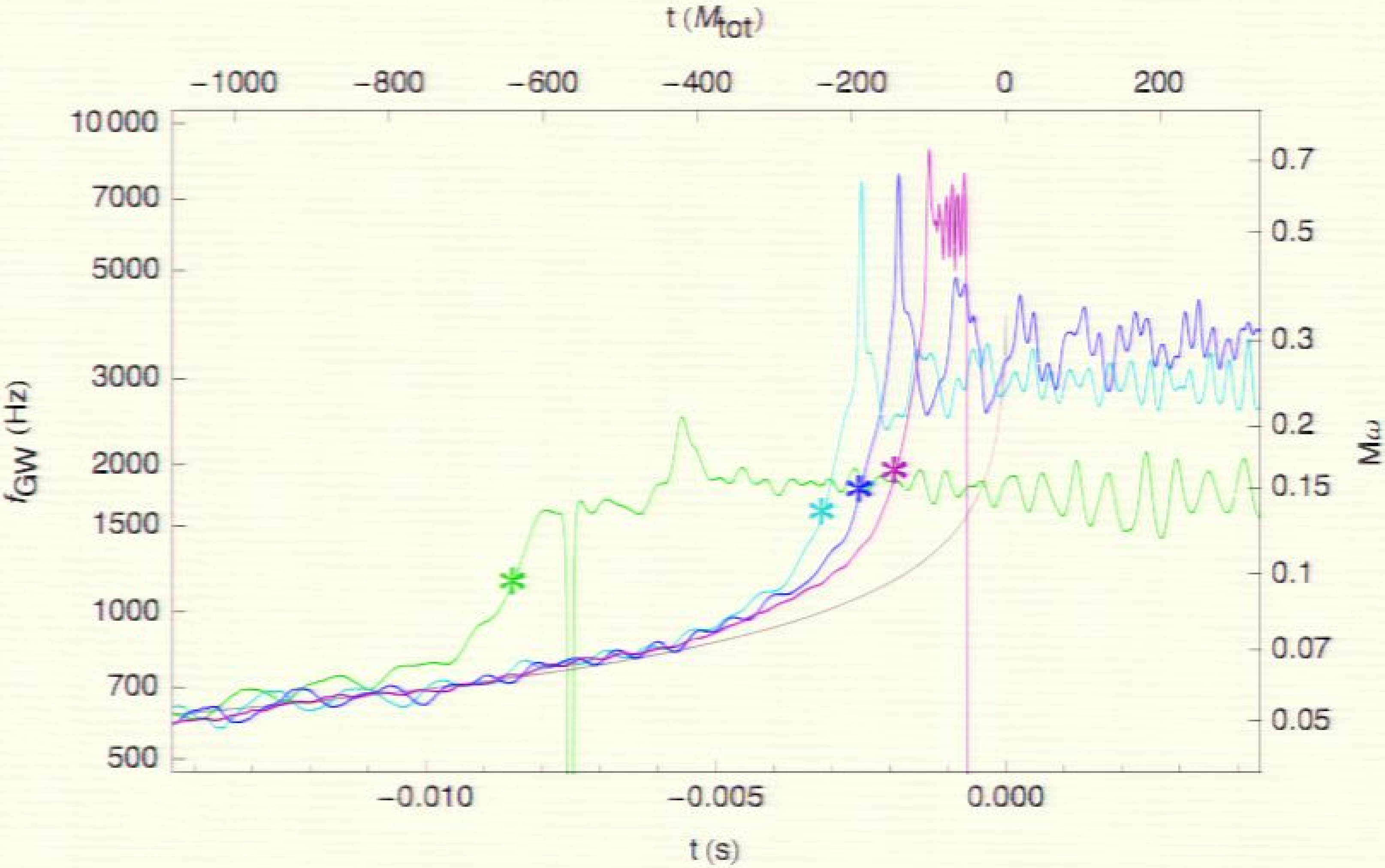

Improved WHISKY/SACRA waveforms now available; looks qualitatively similar; quantitative results in progres...

3) Linking regions

Two measurability estimates

Modified PN waveform	Numerical simulation
realistic EOS indistinguishble at 100 Mpc in AdLIGO	realistic EOS distinguishable at 100 Mpc in AdLIGO

3) Linking regions

Two measurability estimates

Modified PN waveform	Numerical simulation
realistic EOS indistinguishble at 100 Mpc in AdLIGO	realistic EOS distinguishable at 100 Mpc in AdLIGO
valid < 450 Hz	valid > 700 Hz
additional effects at higher frequency	assumes identical (PP) waveforms before numerical simulation

Note: Putting in leading order tidal λ of the largest-radius 2H waveform (green) gives $\Delta\varphi > 2\pi$ between 450 Hz and start of simulations.

3) Linking regions

Two measurability estimates

Modified PN waveform	Numerical simulation
realistic EOS indistinguishble at 100 Mpc in AdLIGO	realistic EOS distinguishable at 100 Mpc in AdLIGO

Measurability estimates: EOS effects on inspiral

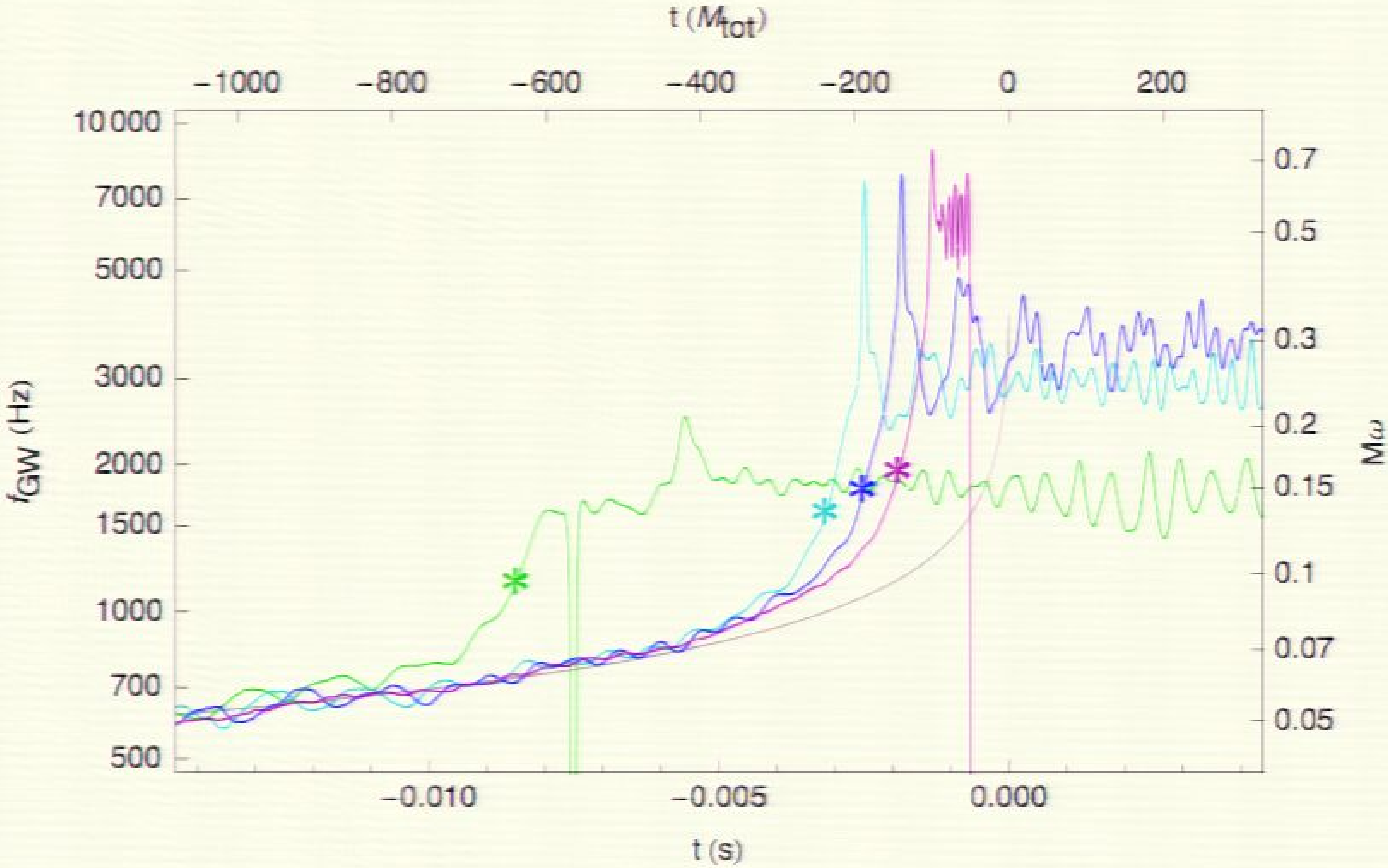

Improved WHISKY/SACRA waveforms now available; looks qualitatively similar; quantitative results in progres...

3) Linking regions

Two measurability estimates

Modified PN waveform	Numerical simulation
realistic EOS indistinguishble at 100 Mpc in AdLIGO	realistic EOS distinguishable at 100 Mpc in AdLIGO
valid $<$ 450 Hz	valid $>$ 700 Hz

Intermediate frequency and hybrids

Imminent improvements: calculation of next leading order piece; longer numerical simulations - still may not give robust overlap of applicability

Can we tune the inspiral model using the numerical results?

Intermediate frequency and hybrids

EOB radial potential [Damour&Nagar 09b]

$$A(r) = A_{3PN}(r) + A^{\rm tidal}(r)$$

where

$$A^{\rm tidal}(u) = \sum_{\ell \geq 2} -\kappa_\ell^T u^{2\ell+2} \hat{A}_\ell^{\rm tidal}(u)$$

Dimensionless relativistic Love numbers (self-gravity of the NS) [FH08, DN09a, BP09, H09]

$$\kappa_\ell^T = 2\frac{M_B M_A^{2\ell}}{(M_A+M_B)^{2\ell+1}}\frac{k_\ell^A}{\mathcal{C}_A^{2\ell+1}} + 2\frac{M_A M_B^{2\ell}}{(M_A+M_B)^{2\ell+1}}\frac{k_\ell^B}{\mathcal{C}_B^{2\ell+1}}$$

With higher (NLO & NNLO) PN corrections

$$\hat{A}_\ell^{\rm tidal} = 1 + \bar{\alpha}_{1PN} u + \bar{\alpha}_{2PN} u^2 \qquad u = 1/r$$

$$\kappa_\ell^{T,eff}(u) = \kappa_\ell^T \hat{A}_\ell^{\rm tidal}(u)$$

Effective *amplification* of tidal effects [DN09b]

where $\bar{\alpha}_{1PN}, \bar{\alpha}_{2PN}$; can be computed analytically (in principle) or estimated by comparing with numerical simulations (in practice).

Intermediate frequency and hybrids

Comparison between longest (20 cycles) BNS (Γ=2 polytropes) simulations and EOB with NLO corrections

$$M_A = M_B = 1.36 M_\odot$$
$$\mathcal{C}_A = \frac{M_A}{R_A} = 0.12$$

$$M_A = M_B = 1.51 M_\odot$$
$$\mathcal{C}_A = \frac{M_A}{R_A} = 0.14$$

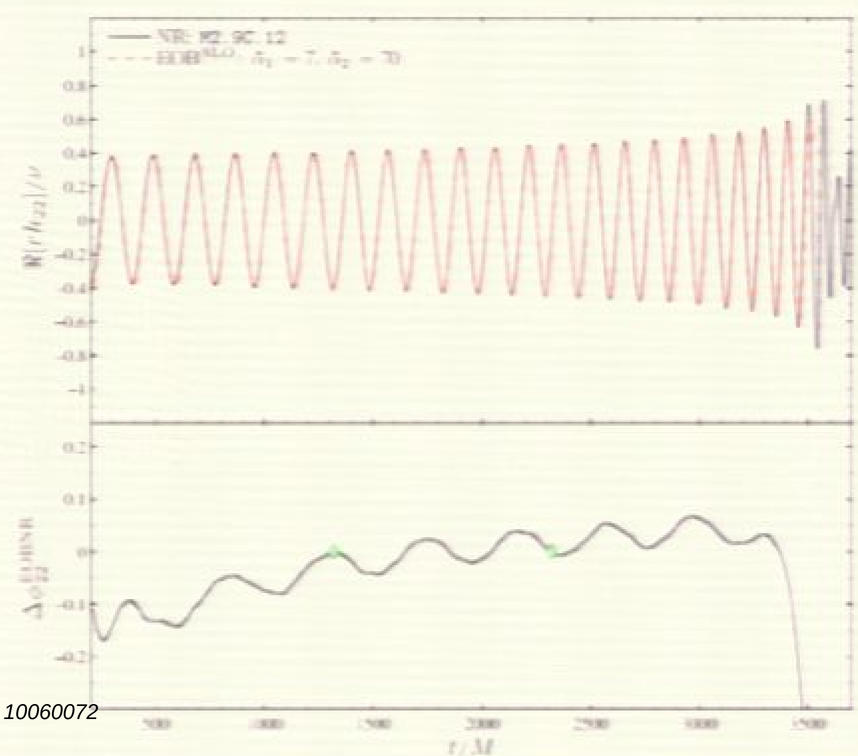

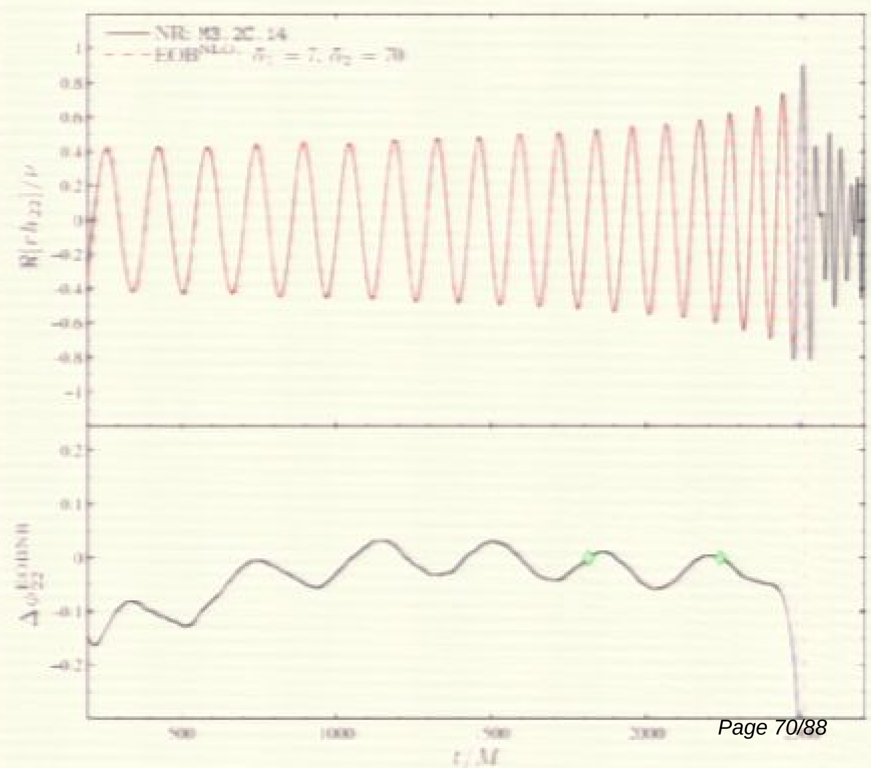

Intermediate frequency and hybrids

Comparison between longest (20 cycles) BNS (Γ=2 polytropes) simulations and EOB with NLO corrections

$$M_A = M_B = 1.36 M_\odot$$
$$\mathcal{C}_A = \frac{M_A}{R_A} = 0.12$$

$$M_A = M_B = 1.51 M_\odot$$
$$\mathcal{C}_A = \frac{M_A}{R_A} = 0.14$$

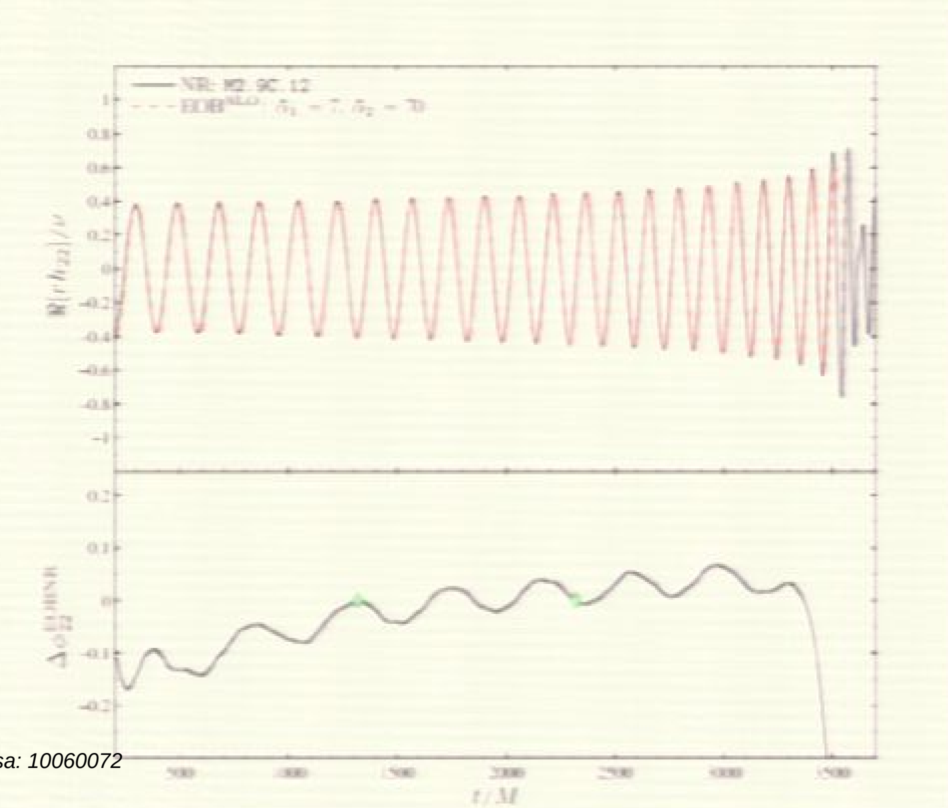

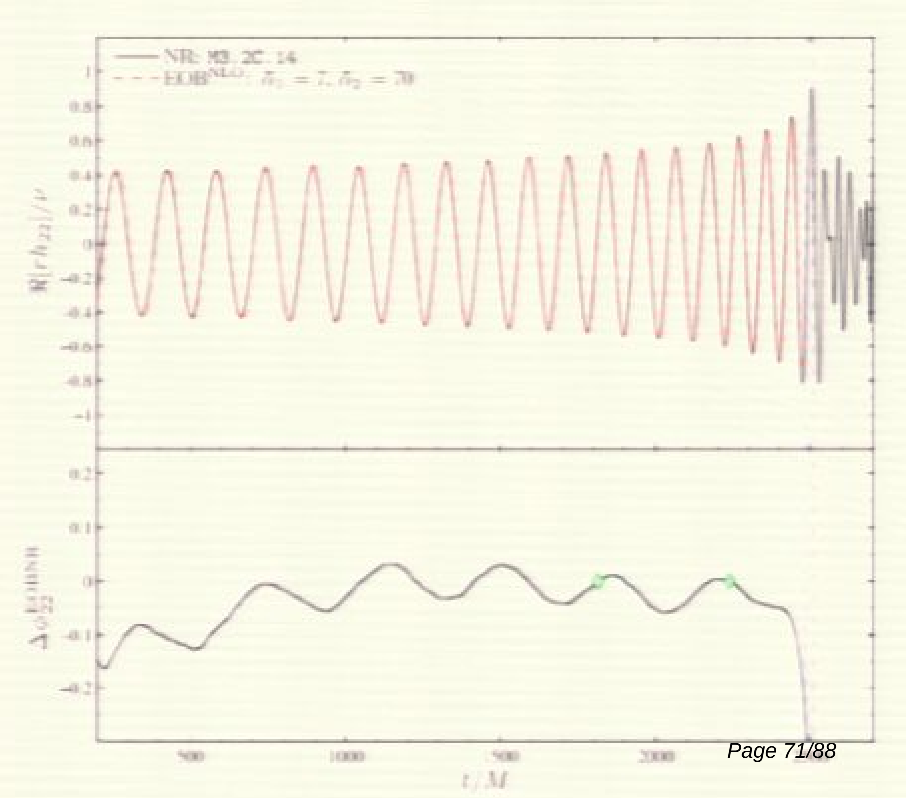

3) Linking regions

Two measurability estimates

Modified PN waveform	Numerical simulation
realistic EOS indistinguishble at 100 Mpc in AdLIGO	realistic EOS distinguishable at 100 Mpc in AdLIGO

Spectra

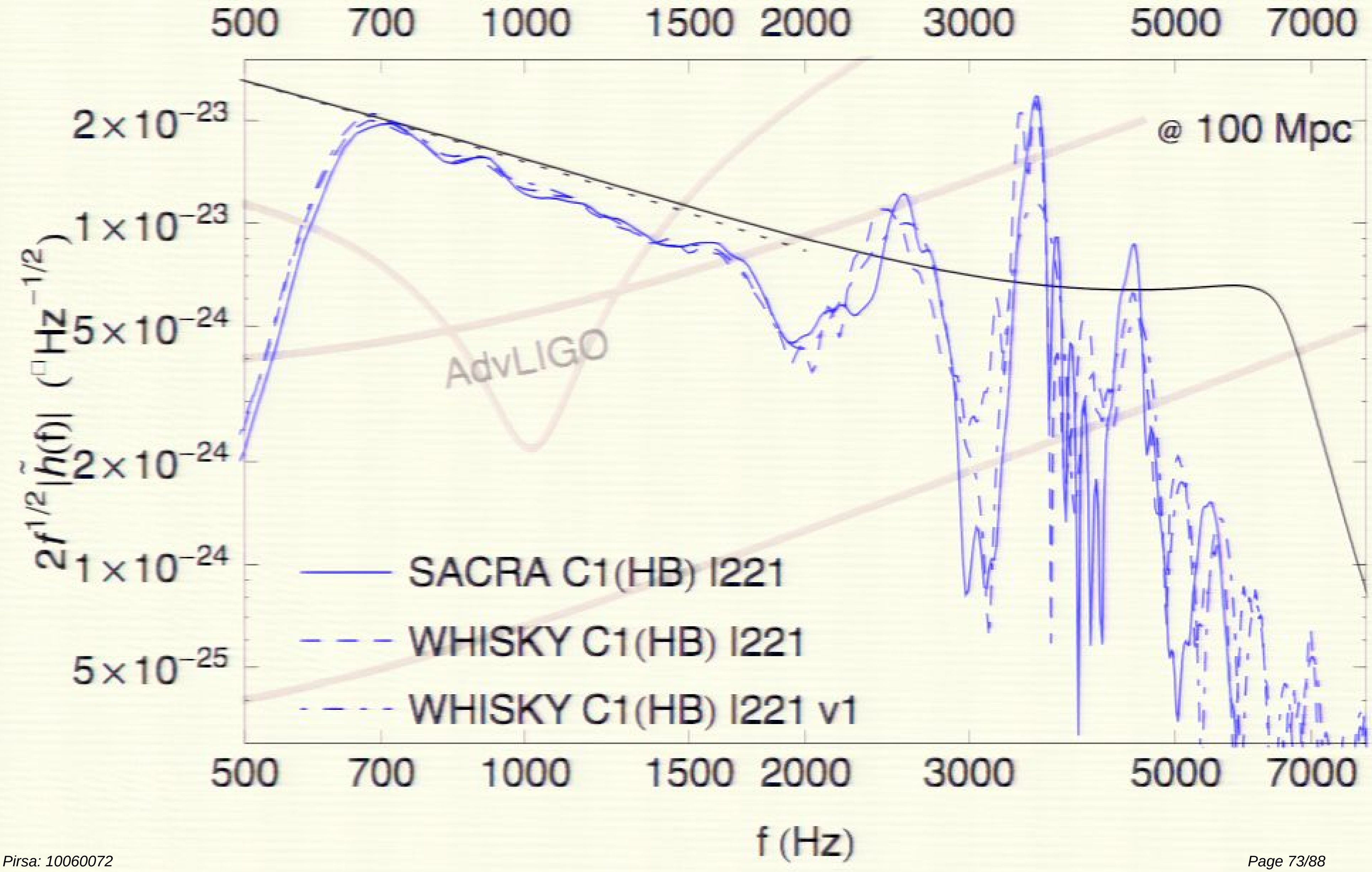

500
700
1000
1500
2000
3000
5000
7000
@ 100 Mpc
2×10^{-23}
1×10^{-23}
5×10^{-24}
2×10^{-24}
1×10^{-24}
5×10^{-25}
$2f^{1/2}|\tilde{h}(f)|$ ($\mathrm{Hz}^{-1/2}$)
AdvLIGO
SACRA C1(HB) I221
WHISKY C1(HB) I221
WHISKY C1(HB) I221 v1
f (Hz)

Spectra

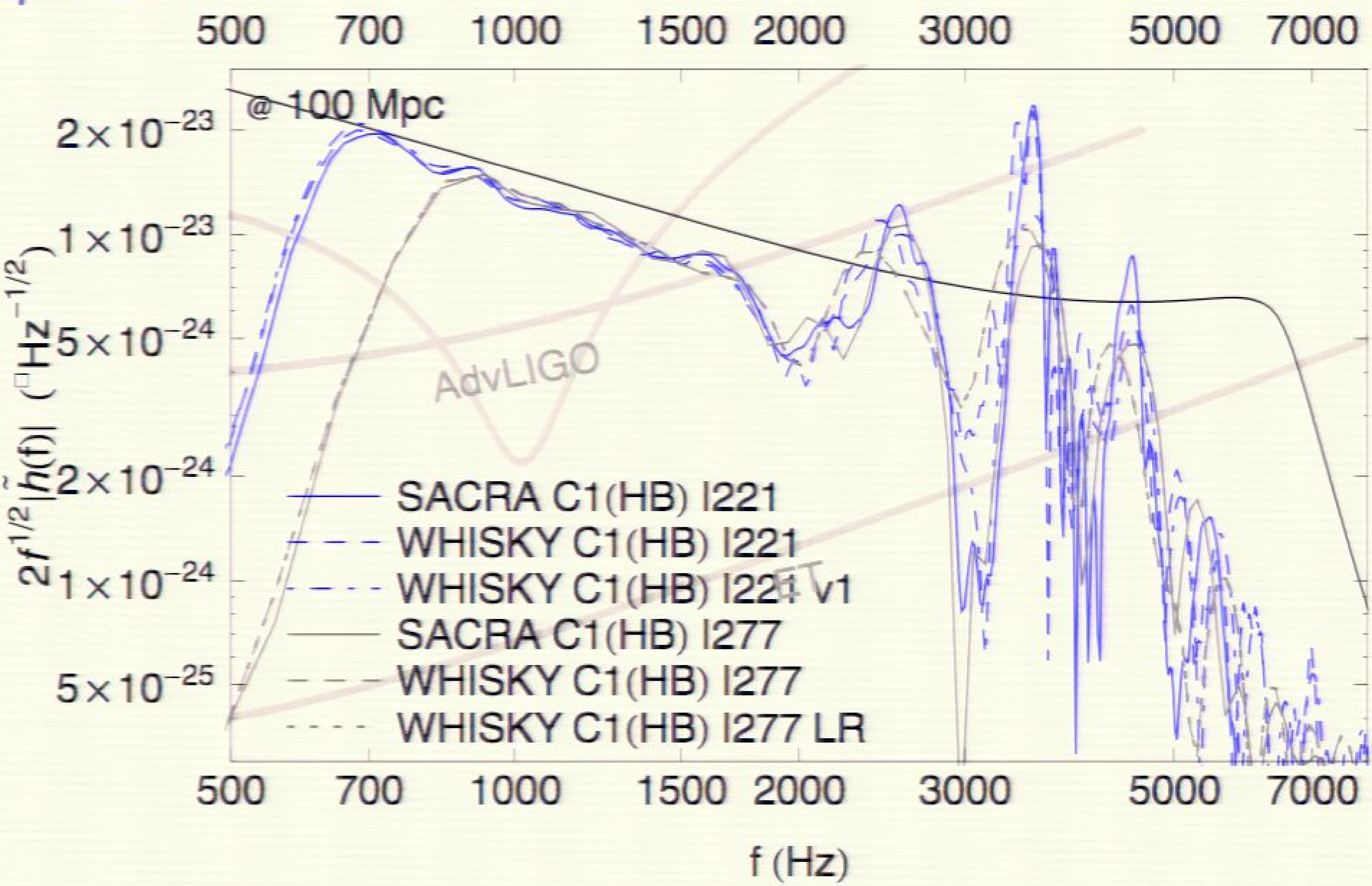

500
700
1000
1500
2000
3000
5000
7000
@ 100 Mpc
2×10^{-23}
1×10^{-23}
5×10^{-24}
2×10^{-24}
1×10^{-24}
5×10^{-25}
$2f^{1/2}|\tilde{h}(f)|$ ($\mathrm{Hz}^{-1/2}$)
AdvLIGO
ET
SACRA C1(HB) I221
WHISKY C1(HB) I221
WHISKY C1(HB) I221 v1
SACRA C1(HB) I277
WHISKY C1(HB) I277
WHISKY C1(HB) I277 LR
f (Hz)

Spectra

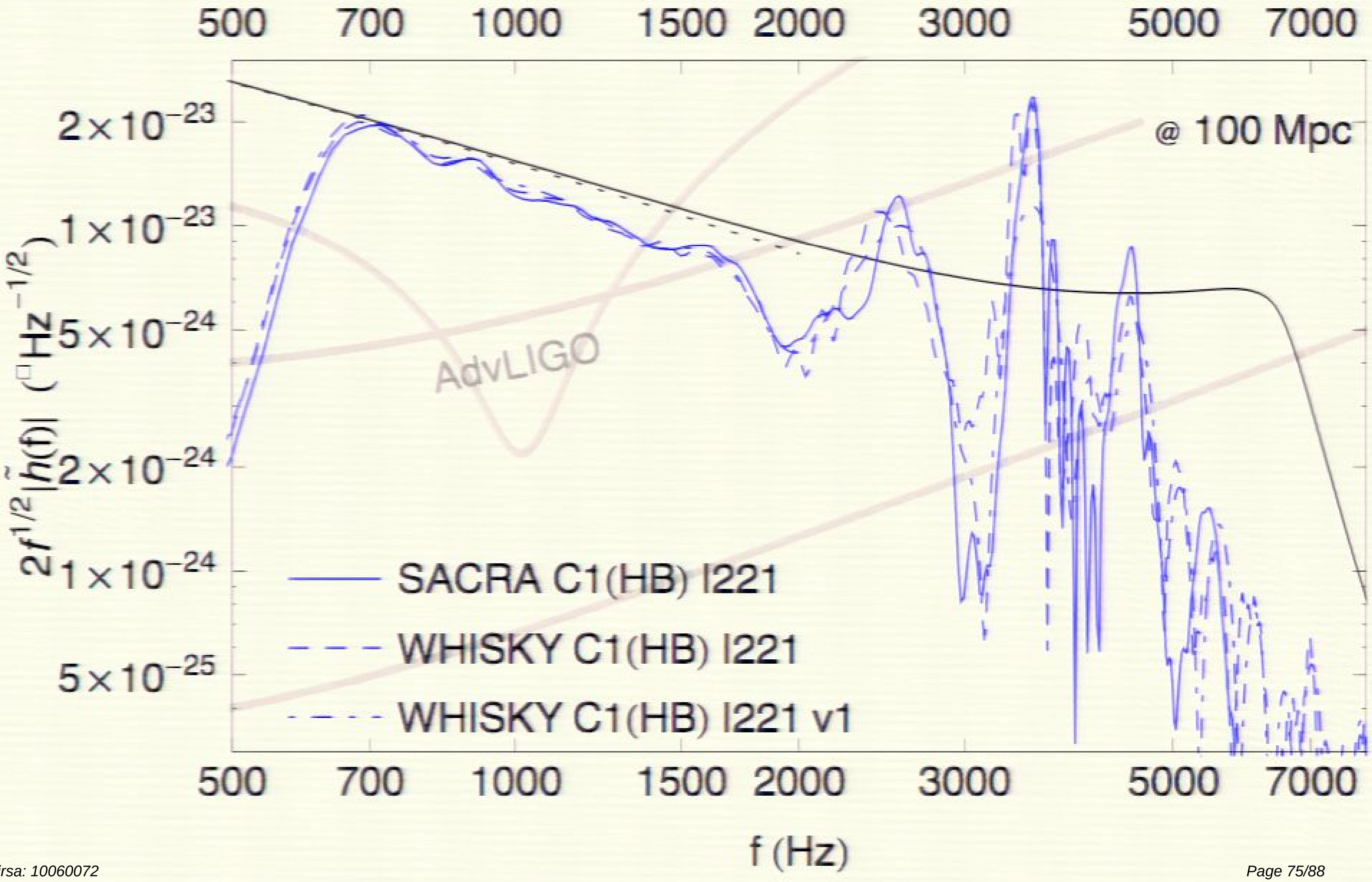

500
700
1000
1500
2000
3000
5000
7000
2×10^{-23}
1×10^{-23}
5×10^{-24}
2×10^{-24}
1×10^{-24}
5×10^{-25}
@ 100 Mpc
AdvLIGO
SACRA C1(HB) I221
WHISKY C1(HB) I221
WHISKY C1(HB) I221 v1
$2f^{1/2}|\tilde{h}(f)|$ ($\text{Hz}^{-1/2}$)
f (Hz)

Spectra

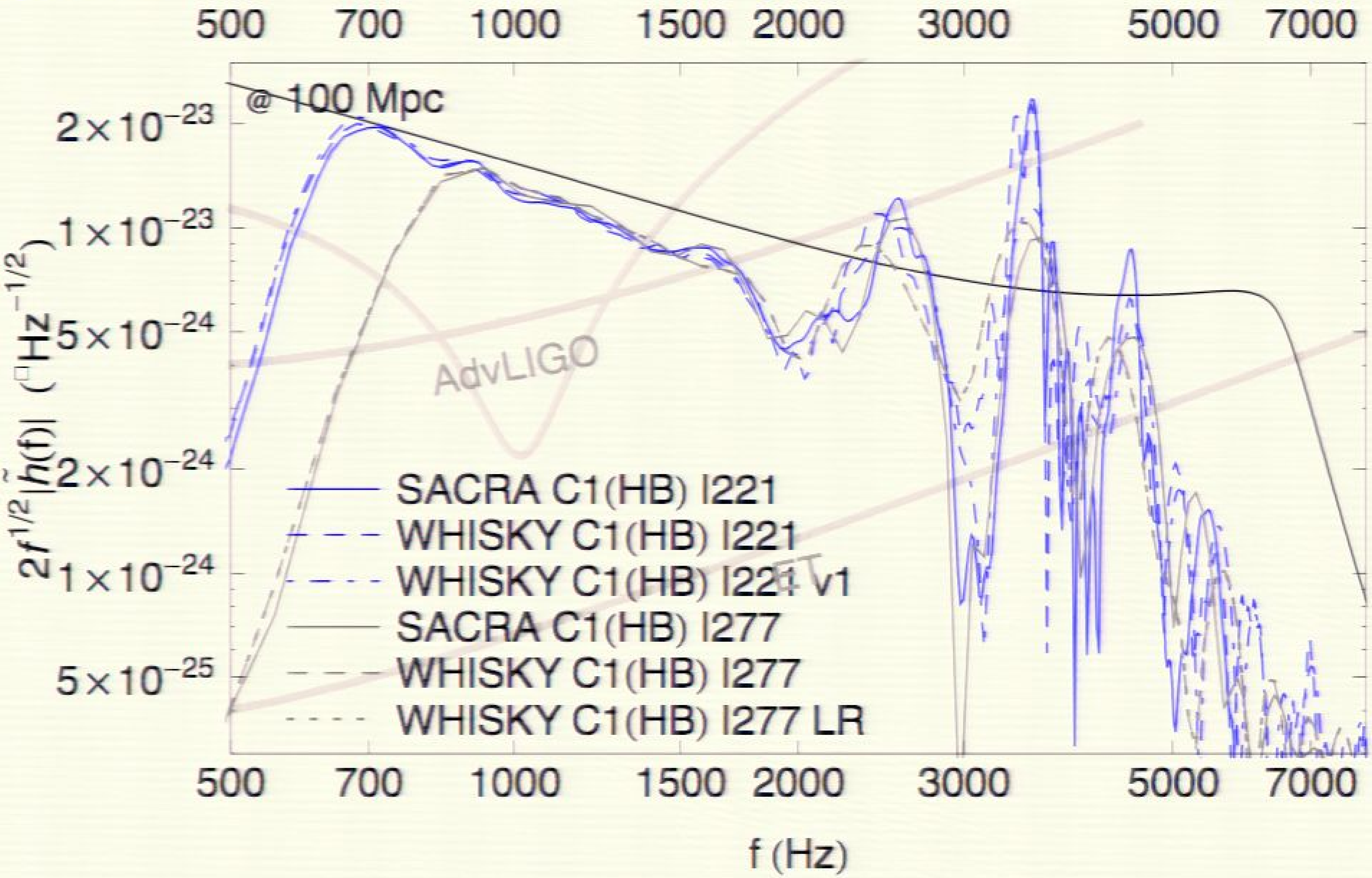

500
700
1000
1500
2000
3000
5000
7000
@ 100 Mpc
2×10^{-23}
1×10^{-23}
5×10^{-24}
2×10^{-24}
1×10^{-24}
5×10^{-25}
$2f^{1/2}|\tilde{h}(f)|$ ($\mathrm{Hz}^{-1/2}$)
AdvLIGO
ET
SACRA C1(HB) I221
WHISKY C1(HB) I221
WHISKY C1(HB) I221 v1
SACRA C1(HB) I277
WHISKY C1(HB) I277
WHISKY C1(HB) I277 LR
f (Hz)

Merger agreement

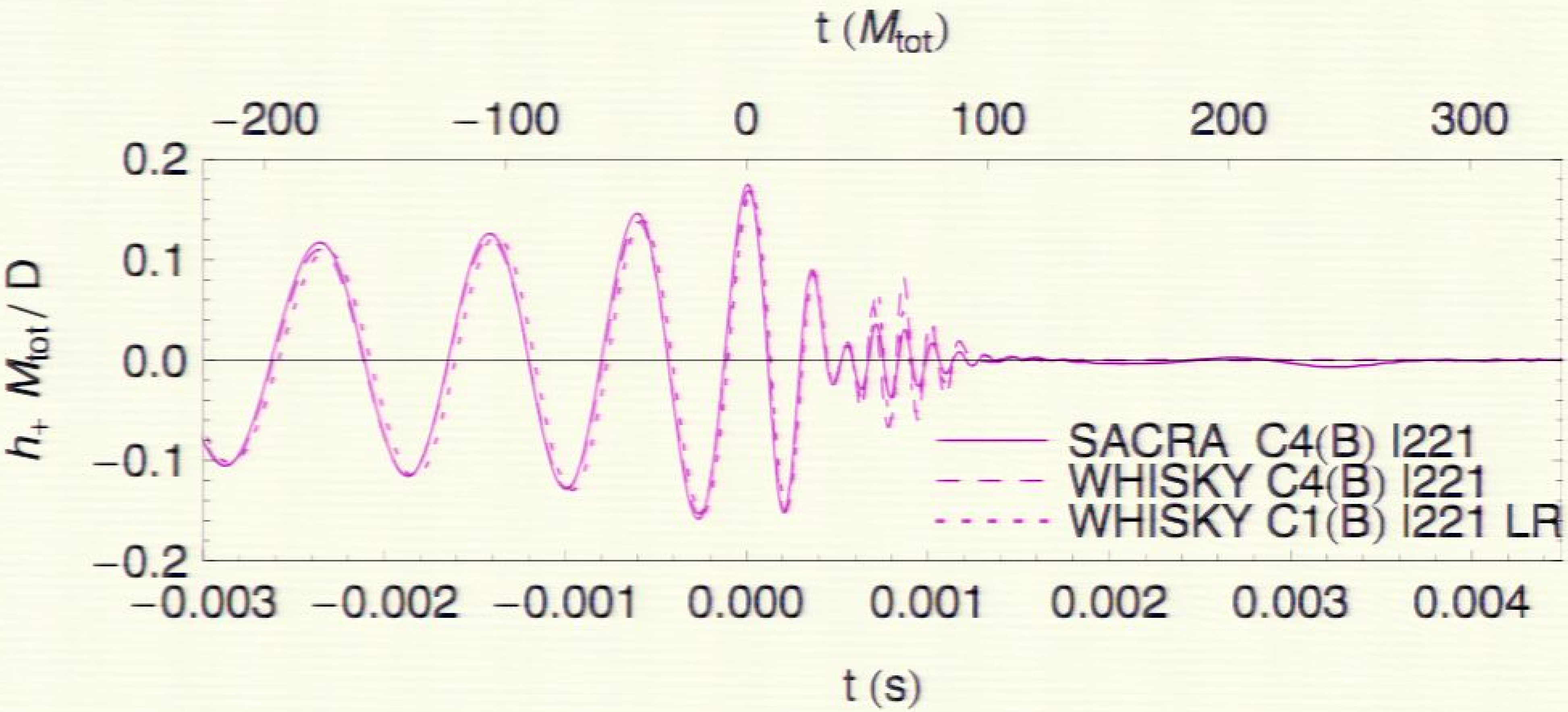

Inspiral agreement

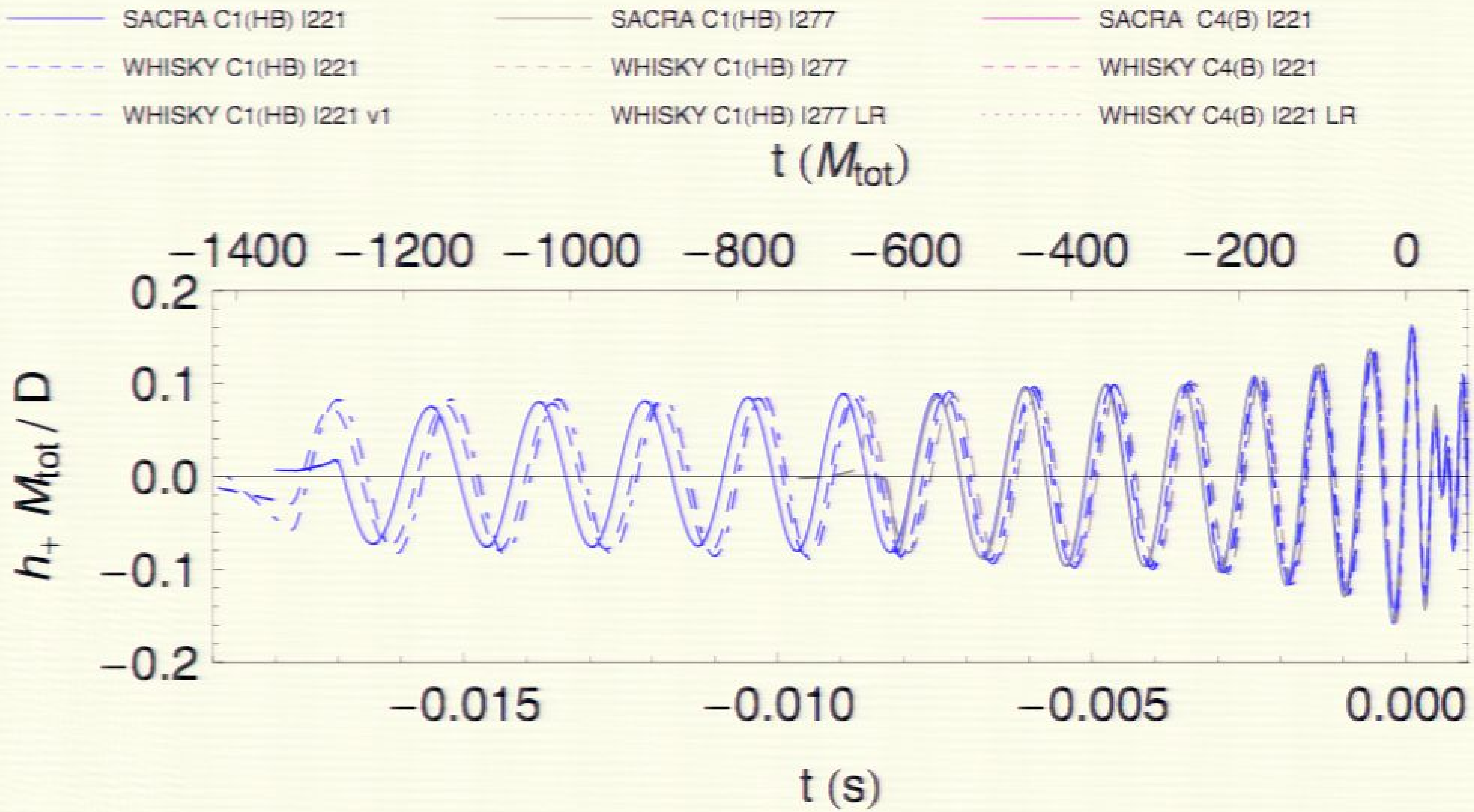

Sampling of results

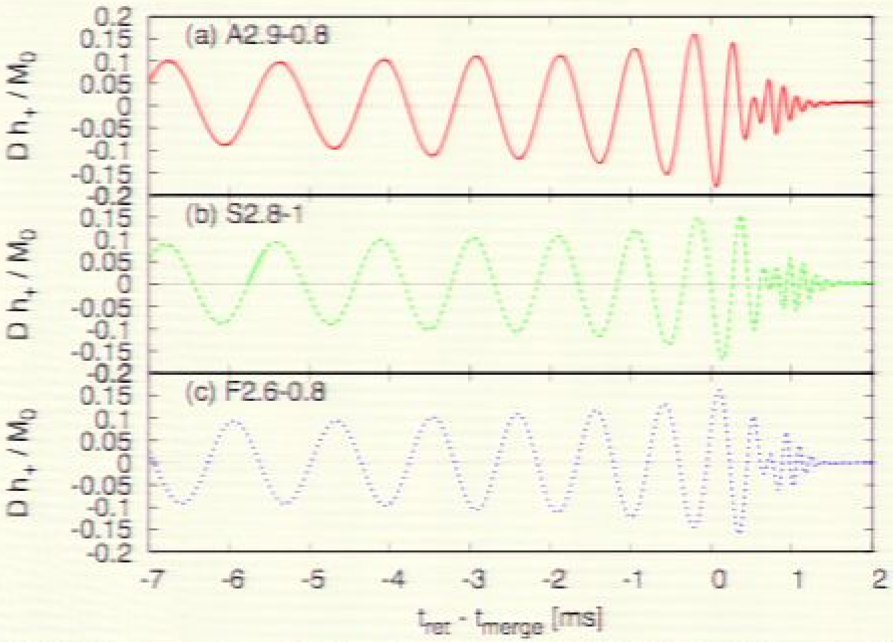

FIG. 1: + modes of GWs for (a) A2.9-0.8, (b) S2.8-1, and (c) F2.6-0.8. D is the distance from the source to the observer, who is located along the axis perpendicular to the orbital plane. $t_{\rm merge}$ denotes approximate time at the onset of the merger.

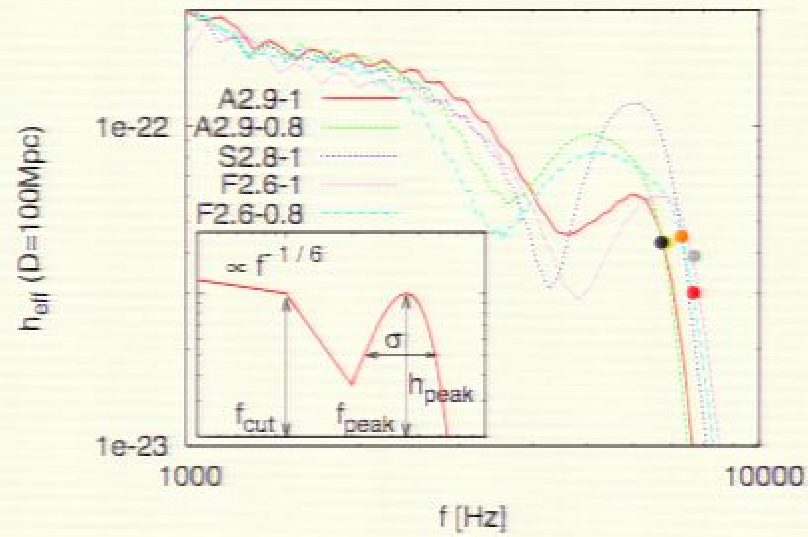

FIG. 2: Effective amplitude for models A2.9-1, A2.9-0.8, S2.8-1, F2.6-1, and F2.6-0.8. The filled circles denote the QNM frequency of the formed BHs. The small panel shows a schematic figure of the GW spectrum.

Kiuchi et al 1002.2689

Sampling of results

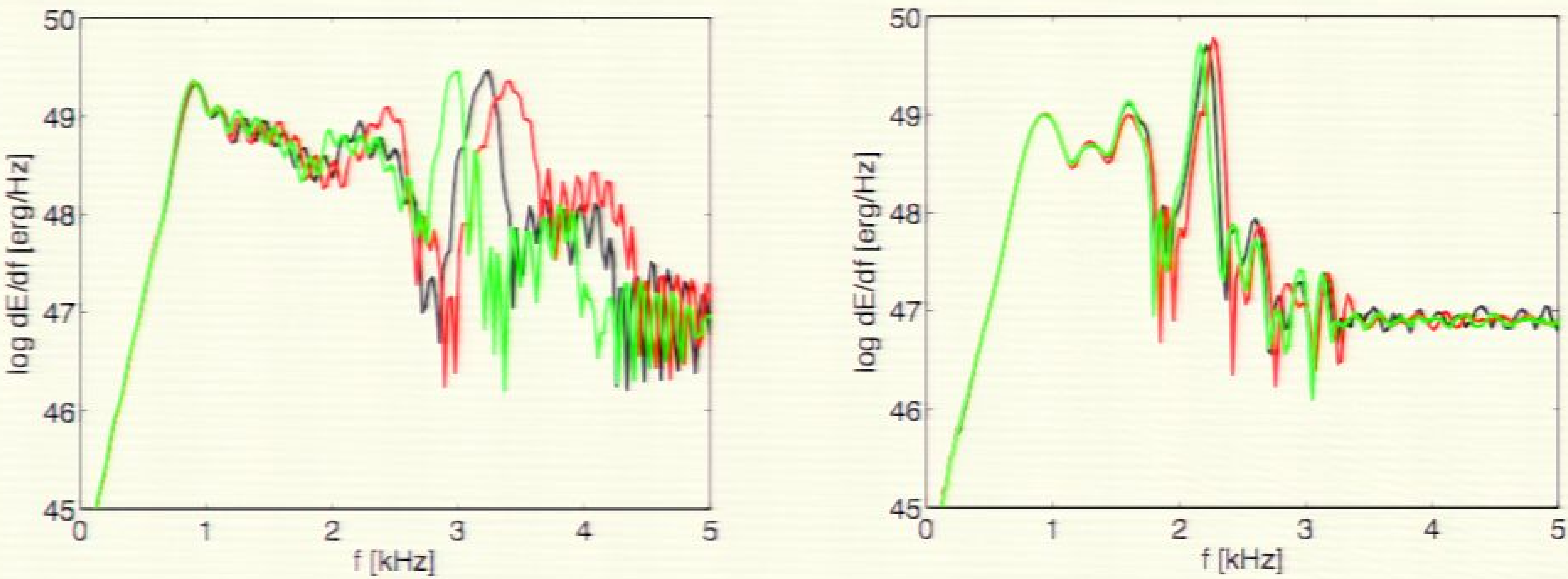

Cold+thermal approximations vs. full thermal (black line) for two EOS.
Bauswein et al 1006.3315

Merger agreement

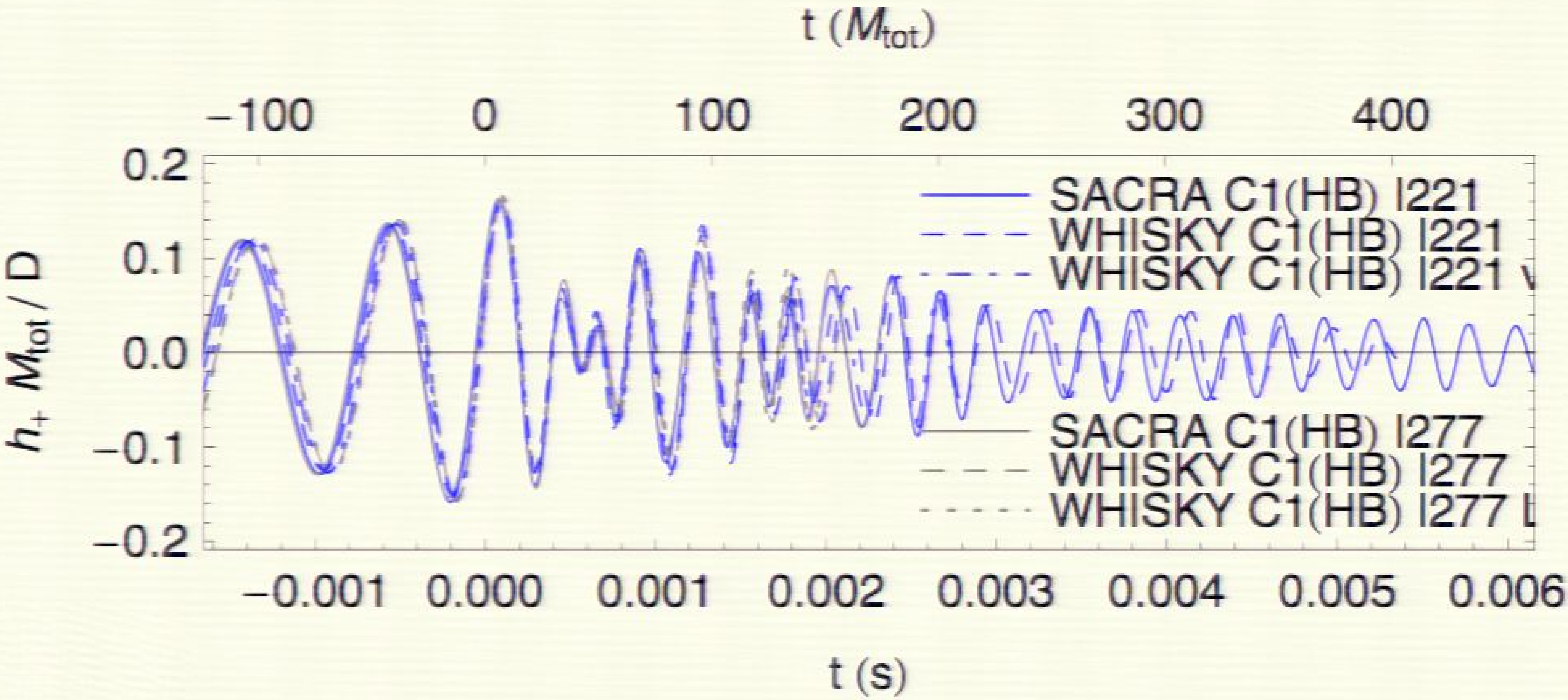

Spectra

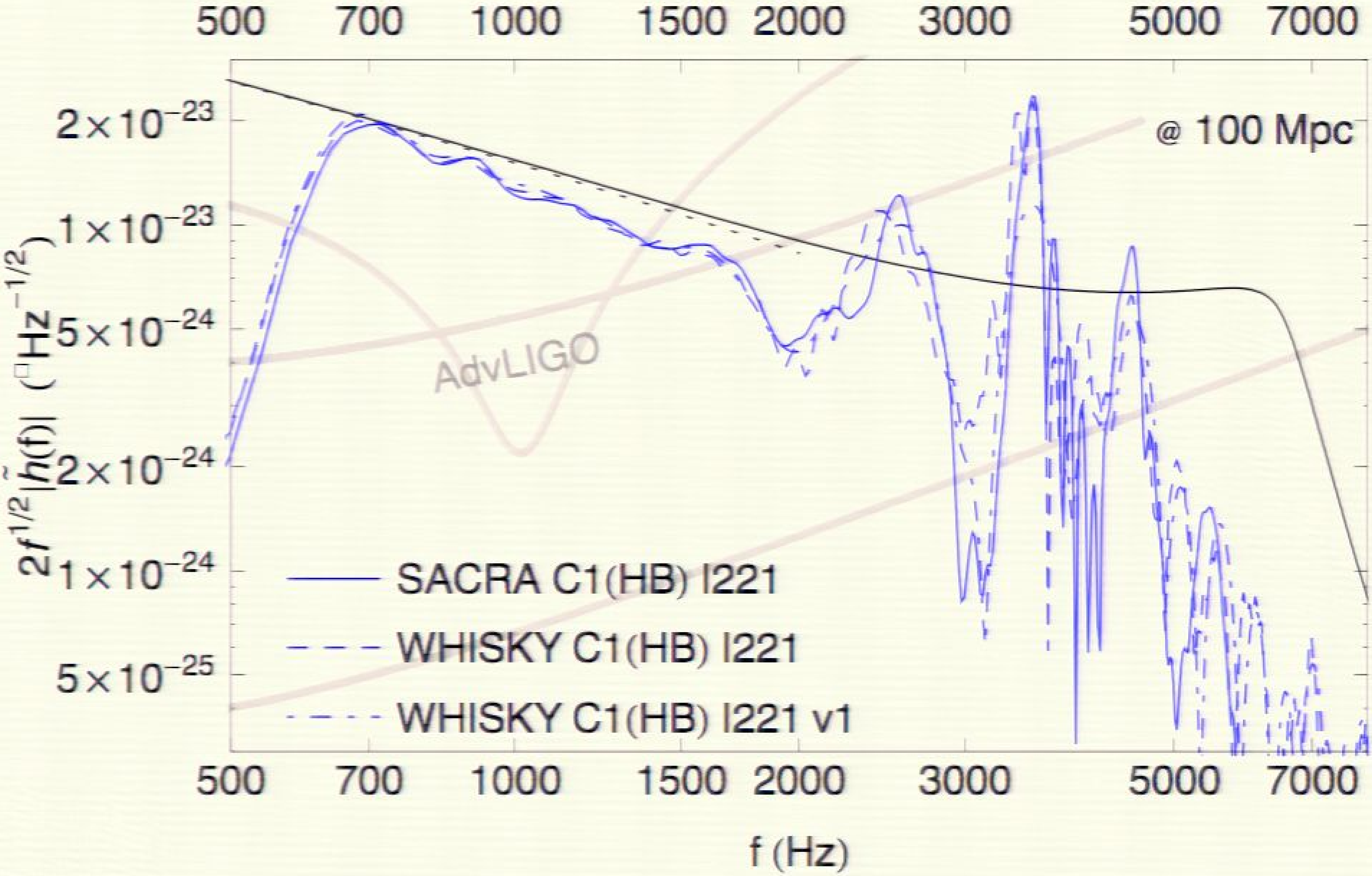

500
700
1000
1500
2000
3000
5000
7000
@ 100 Mpc
2×10⁻²³
1×10⁻²³
5×10⁻²⁴
2×10⁻²⁴
1×10⁻²⁴
5×10⁻²⁵
AdvLIGO
SACRA C1(HB) I221
WHISKY C1(HB) I221
WHISKY C1(HB) I221 v1
f (Hz)

Sampling of results

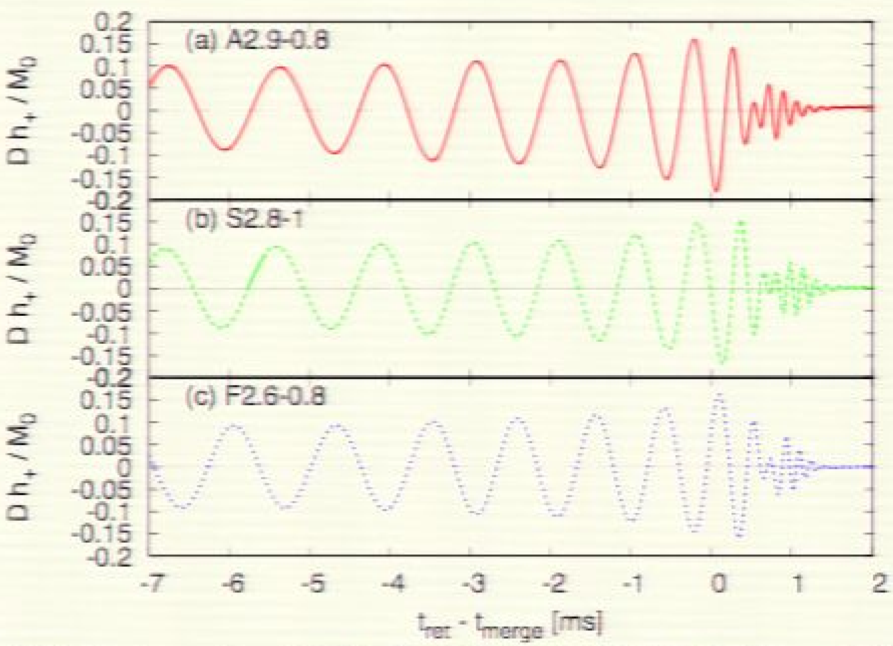

FIG. 1: + modes of GWs for (a) A2.9-0.8, (b) S2.8-1, and (c) F2.6-0.8. D is the distance from the source to the observer, who is located along the axis perpendicular to the orbital plane. $t_{\rm merge}$ denotes approximate time at the onset of the merger.

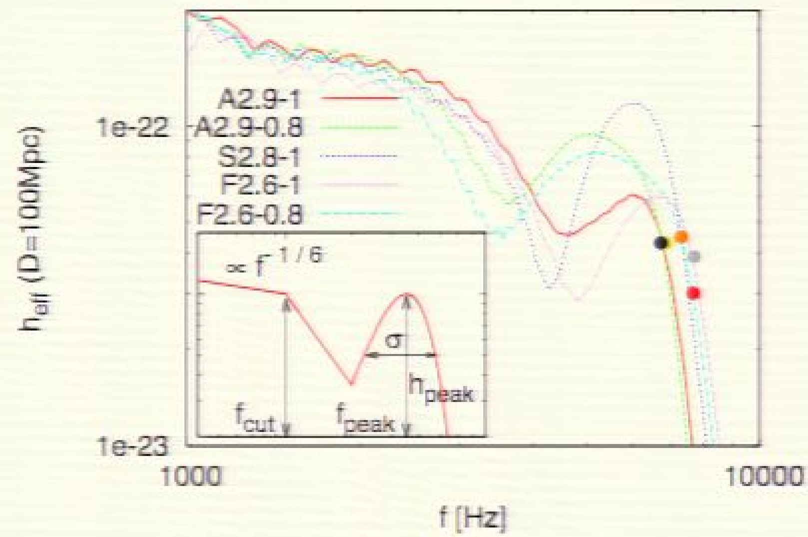

FIG. 2: Effective amplitude for models A2.9-1, A2.9-0.8, S2.8-1, F2.6-1, and F2.6-0.8. The filled circles denote the QNM frequency of the formed BHs. The small panel shows a schematic figure of the GW spectrum.

Kiuchi et al 1002.2689

2) Numerical simulations

Current Status

Waveforms: up to 20 cycles inspiral, realistic mass ratios, GR, shock-capturing hydrodynamics, "realistic" cold EOS, thermal EOS, ideal MHD

Sample of recent results:

- Longer waveforms, increased accuracy, unequal massses, torus formation
  - Kiuchi et al 0904.4551 & 1002.2689, SACRA
  - Rezzolla et al 1001.3074, WHISKY
- Improvements to quasiequilibrium sequences and initial data:
  - Uryu et al 2009 0908.0579
  - Taniguchi and Shibata 2010 1005.0958
- Effect of magnetic field on waveform
  - Giacomazzo et al 2009 0901.2722, WHISKY
- Measurability of EOS in late inspiral
  - JR et al 0901.3258
- Effect of fully thermal EOS on waveform
  - Bauswein et al 2010 1006.3315 CF-SPH

Sampling of results

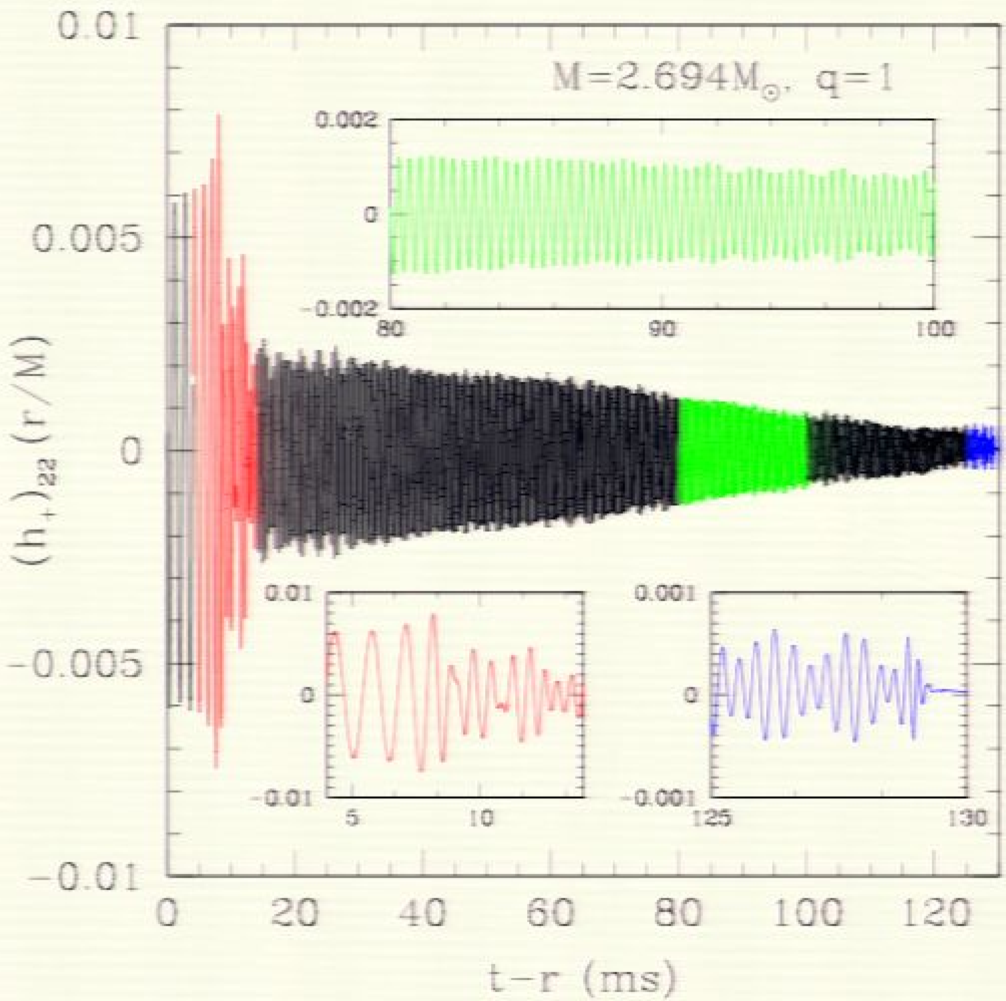

Rezzolla et al 1001.3074

2) Numerical simulations

Current Status

Waveforms: up to 20 cycles inspiral, realistic mass ratios, GR, shock-capturing hydrodynamics, "realistic" cold EOS, thermal EOS, ideal MHD

Sample of recent results:

- Longer waveforms, increased accuracy, unequal massses, torus formation
  - Kiuchi et al 0904.4551 & 1002.2689, SACRA
  - Rezzolla et al 1001.3074, WHISKY
- Improvements to quasiequilibrium sequences and initial data:
  - Uryu et al 2009 0908.0579
  - Taniguchi and Shibata 2010 1005.0958
- Effect of magnetic field on waveform
  - Giacomazzo et al 2009 0901.2722, WHISKY
- Measurability of EOS in late inspiral
  - JR et al 0901.3258
- Effect of fully thermal EOS on waveform
  - Bauswein et al 2010 1006.3315 CF-SPH

Measuring tidal deformability λ

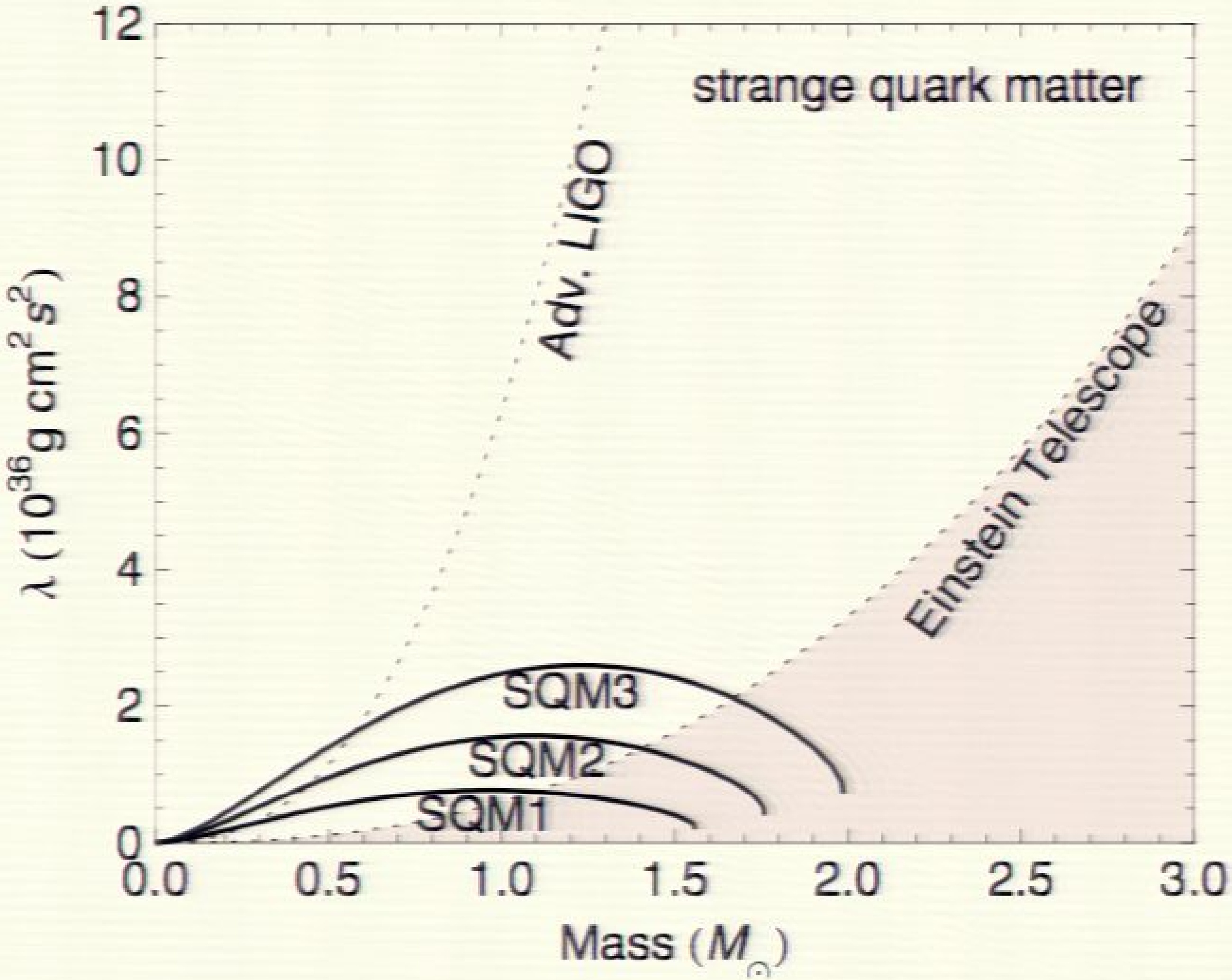

Each thick line: a candidate equation of state gives λ as function of mass.

shaded: Uncertainty in estimating λ for Advanced LIGO and ET using "clean" waveform: below 450 Hz only

Spin and η considered

Advanced LIGO

M ($M_\odot$)	m_2/m_1	$\Delta\mathcal{M}/\mathcal{M}$	$\Delta\eta/\eta$	$\Delta\tilde{\lambda}(10^{36}\,\mathrm{g\,cm^2\,s^2})$	ρ
2.0	1.0	0.00028	0.073	8.4	27
2.8	1.0	0.00037	0.055	19.3	35
3.4	1.0	0.00046	0.047	31.3	41
2.0	0.7	0.00026	0.058	8.2	26
2.8	0.7	0.00027	0.058	18.9	35
3.4	0.7	0.00028	0.055	30.5	41
2.8	0.5	0.00037	0.06	17.8	33